

QUANTUM EFFECTS ON $t \rightarrow H^+ b$ IN THE MSSM : A WINDOW TO "VIRTUAL" SUPERSYMMETRY?

J.A. COARASA, David GARCIA, Jaume GUASCH,
Ricardo A. JIMENEZ, Joan SOLA

Grup de Física Teòrica
and
Institut de Física d'Altes Energies
Universitat Autònoma de Barcelona
08193 Bellaterra (Barcelona), Catalonia, Spain

ABSTRACT

We analyze the one-loop effects (strong and electroweak) on the unconventional top quark decay mode $t \rightarrow H^+ b$ within the MSSM. The results are presented in the on-shell renormalization scheme with a physically well motivated definition of $\tan \beta$. The study of this process at the quantum level is useful to unravel the potential supersymmetric nature of the charged Higgs emerging from that decay. As compared with the standard mode $t \rightarrow W^+ b$, the corrections to $t \rightarrow H^+ b$ are large, slowly decoupling and persist at a sizeable level even for all particle masses well above the LEP 200 discovery range. As a matter of fact, the potential size of the SUSY effects, which amount to corrections of several ten percent, could counterbalance the standard QCD corrections and even make them to appear with the "wrong" sign. Therefore, if the charged Higgs decay of the top quark is kinematically allowed (a possibility which is not excluded by the recent measurements of the branching ratio $BR(t \rightarrow W^+ b)$ at the Tevatron) it could be an invaluable laboratory to search for "virtual" supersymmetry. While a first significant test of these effects could possibly be performed at the upgraded Tevatron, a more precise verification would most likely be carried out in future experiments at the LHC.

1. Introduction

Recently, the Standard Model (SM) of the strong and electroweak interactions has been crowned with the discovery of the penultimate building block of its theoretical structure: the top quark, t [1]. At present the best determination of the top-quark mass at the Tevatron reads as follows [2]:

$$m_t = 175 \pm 6 \text{ GeV} : \quad (1)$$

While the SM has been a most successful framework to describe the phenomenology of the strong and electroweak interactions for the last thirty years, the top quark itself stood, at a purely theoretical level (namely, on the grounds of requiring internal consistency, such as gauge invariance and renormalizability) as a *prediction* of the SM since the very confirmation of the existence of the bottom quark and the measurement of its weak isospin quantum numbers [3]. With the finding of the top quark, the matter content of the SM has been fully accounted for by experiment. Still, the last building block of the SM, viz. the fundamental Higgs scalar, has not been found yet, which means that in spite of the great significance of the top quark discovery the theoretical mechanism by which all particles acquire their masses in the SM remains experimentally unconfirmed. Thus, it is not clear at present whether the SM will remain as the last word in the phenomenology of the strong and electroweak interactions around the Fermi's scale or whether it will be eventually subsumed within a larger and more fundamental theory. The search for physics beyond the SM, therefore, far from been accomplished, must continue with redoubled efforts. Fortunately, the peculiar nature of the top quark (in particular its large mass (in fact, perhaps the heaviest particle in the SM!) and its characteristic interactions with the scalar particles) may help decisively to unearth any vestige of physics beyond the SM.

We envisage at least four wide avenues of interesting new physics potentially conveyed by top quark dynamics and which could offer us the clue to solving the nature of the spontaneous symmetry breaking (SSB) mechanism, to wit: i) The "Top Mode" realization(s) of the SSB mechanism, i.e. SSB without fundamental Higgs scalars, but rather through the existence of tt condensates [4]; ii) The extended Technicolour Models; also without Higgs particles, and giving rise to residual non-oblique interactions of the top quark with the weak gauge bosons [5]; iii) The non-linear (chiral Lagrangian) realization of the $SU(2)_L \times U(1)_Y$ gauge symmetry [6], which may either accommodate or dispense with the Higgs scalars. It can also generate additional (i.e. non-standard) non-oblique interactions of the top quark with the weak gauge bosons [7]; and iv) The supersymmetric (SUSY) realization of the SM, such as the Minimal Supersymmetric Standard Model (MSSM) [8], where also a lot of potential new phenomenology spurred by top and Higgs physics might be creeping in here and there. Hints of this new phenomenology may show

up either in the form of direct or virtual effects from supersymmetric Higgs particles or from the "sparticles" themselves (i.e. the R-odd [8] partners of the SM particles), in particular from the top-squark ("stop") which is the SUSY counterpart of the top quark. Due to the huge mass of the latter, one expects that the top-stop system is one of the most preferential chiral supermultiplets to which the Higgs sector should couple. Therefore, top quark dynamics is deemed to be an ideal environment for Higgs phenomenology and a most suitable SUSY trigger, if SUSY is there at all.

In this paper, we shall focus our attention on the fourth large avenue of hypothetical physics beyond the SM, namely on the (minimal) SUSY extension of the SM, the MSSM, which is at present the most predictive framework for physics beyond the SM and, in contradistinction to all other approaches, it has the virtue of being a fully-edged Quantum Field Theory. Most important, on the experimental side the global analyses to all indirect precision data within the MSSM are at least as good as in the SM; in particular, the MSSM analysis implies that $m_t = 172 \pm 5$ [9, 10], a result which is compatible with the above mentioned experimental determinations of m_t .

In the MSSM the spectrum of Higgs-like particles and of Yukawa couplings is far and away richer than in the SM. In this respect, a crucial fact affecting the results of our work is that in such a framework the bottom-quark Yukawa coupling may counterbalance the smallness of the bottom mass, $m_b \sim 5$ GeV, at the expense of a large value of $\tan \beta$ { the ratio of the vacuum expectation values (VEV's) of the two Higgs doublets (Cf. Section 2) { the upshot being that the top-quark and bottom-quark Yukawa couplings (normalized with respect to the SU(2) gauge coupling) as they stand in the superpotential, take on the form

$$g_t = \frac{h_t}{g} = \frac{m_t}{2M_W \sin \beta} \quad ; \quad g_b = \frac{h_b}{g} = \frac{m_b}{2M_W \cos \beta} \quad (2)$$

Thus, depending on the actual value of $\tan \beta$, g_b and g_t can be of the same order of magnitude, perhaps even showing up in "inverse hierarchy": $g_b > g_t$ for $\tan \beta > m_t/m_b$. Notice that due to the perturbative bound $\tan \beta < 70$ one never reaches a situation where $g_t \ll g_b$. In a sense, $g_b \sim g_t$ could be judged as a natural relation in the MSSM; it can even be a necessary relation in specific SUSY-GUT models, e.g. those based on tb and

Yukawa coupling unification [11], at least at the unification point. Furthermore, one expects that if such a relation holds, then it is not just the top-stop system, but also the bottom-sbottom chiral supermultiplet that could play a momentous role in the quantum physics of the top and bottom quarks. Indeed, since the Higgs sector of the MSSM doubles that of the SM, and it comes associated with the fermionic SUSY partners {the so-called higgsinos}, one expects that in the limit $g_b > g_t$ there should occur a very stimulating dynamics triggered by the presence of a rich variety of potentially large Yukawa-like

interactions formed out of the top/stop-bottom /sbottom-Higgs/higgsino fields.

A particularly brilliant form of this dynamics, on which we shall focus our attention, is revealed through the study of the quantum effects on the non-standard top quark decay into a charged Higgs: $t \rightarrow H^+ b$. This decay, which has already deserved some attention in the early literature on the subject [12, 13], is not at all excluded by the recent measurements (at the Tevatron) of the branching ratio of the standard top quark decay, $t \rightarrow W^+ b$, as will be discussed in more detail in Section 2. The quantum effects on $t \rightarrow H^+ b$, which we wish to compute in the framework of the MSSM at one-loop, can be both strong and electroweak like. Of these the conventional strong corrections (QCD) mediated by gluons have already been treated in detail [14]. Also the subset of strong supersymmetric corrections mediated by gluinos, stop and sbottom squarks, i.e. the SUSY-QCD corrections, has been discussed in Ref.[15]. Here, therefore, we will come to grips with the remaining part (as a matter of fact, the largest and most difficult part) of the MSSM corrections: namely, the multifarious electroweak supersymmetric corrections produced by squarks, sleptons, charginos, neutralinos and supersymmetric Higgs bosons, which we shall combine with the total strong (QCD + SUSY-QCD) corrections to obtain the MSSM correction.

In the present study¹, we will closely follow the systematic pathway adopted in our previous treatment of the supersymmetric quantum corrections to the canonical decay $t \rightarrow W^+ b$ [17, 18]. However, because of the Higgs particle in the final state, we have to incorporate the details of the renormalization of the Higgs sector of the MSSM, which substantially alter the analytical counterterm structure of the tbH -vertex as compared to the conventional tbW -vertex. This also has dramatical consequences on the quantitative side, as we shall see. Moreover, we have to include the quantum corrections from the supersymmetric Higgs bosons themselves. In spite of their negligible effect on the width of the standard decay $t \rightarrow W^+ b$ [19] (a fact which was not obvious a priori since there are potentially large non-oblique Higgs interactions originating from the Yukawa couplings (2)) their impact on the alternative decay $t \rightarrow H^+ b$ must also be carefully evaluated. In certain circumstances, they can be comparable to the virtual effects from the genuine supersymmetric particles (sparticles).

It is worth mentioning that the one-loop analysis of the unconventional top quark decay $t \rightarrow H^+ b$ is motivated not only by its obvious interest on its own as a laboratory to test the spontaneous symmetry breaking mechanism beyond the SM, but also as a way to characterize the SUSY nature of the charged Higgs emerging from that decay. In fact, we shall see that important ($\sim 50\%$) SUSY radiative corrections can be obtained in certain regions of the MSSM parameter space. In one of these regions, $\tan \beta = m_t/m_b$ is large

¹A preliminary presentation of these results was given in Ref.[16].

enough such that $\tan\beta \gg m_t$. Incidentally, we note that these are typical values of $\tan\beta$ characterizing one of the possible regions of the MSSM parameter space highlighted in the literature [20] (other regions have also been exploited [21]) in order to alleviate some formerly claimed "anomalies" observed in the hadronic decay ratios R_b and R_c of the Z -boson into $b\bar{b}$ and $c\bar{c}$, and in general to try to improve the global fits analyses of the MSSM to electroweak precision data. However, most of the fuss about the Z -boson "anomalies" seems to have declined; at present, R_c is fully understood within the SM, and there only remains a marginal 1.8% discrepancy in R_b with respect to the SM prediction [22]. It should, nevertheless, be clear that the situation with the MSSM is not bad at all. As mentioned above, both the SM and the MSSM can comfortably accommodate the present high precision data with basically the same level of statistical significance [10].

Thus the MSSM is at present in very good shape and we are perfectly entitled to deal with the decay $t \rightarrow H^+ b$ from the SUSY point of view. In particular, we wish to quest for generic regions of the MSSM parameter space where the decay rate of $t \rightarrow H^+ b$ is competitive with the SM decay $t \rightarrow W^+ b$ and at the same time to look for regions where it is as much sensitive as possible to virtual supersymmetric effects. For definiteness, in this paper we take the point of view that the study of the decay $t \rightarrow H^+ b$ is worthwhile provided that its branching ratio is operative at a level $\text{BR}(t \rightarrow H^+ b) > 10\%$, a condition which is not excluded by present Tevatron data (see Section 2). From the theoretical point of view, this is fully guaranteed provided that $\tan\beta$ is large enough ($\gtrsim 30$). In these conditions, the SUSY-QCD one-loop corrections can typically be in the 50% range and the electroweak effects induced by the supersymmetric Yukawa couplings κ_t and κ_b can be rather large (typically 20%) and so all of them are liable to being measured in future experiments at the Tevatron and/or at the LHC. We shall see that there are scenarios where these electroweak supersymmetric corrections could basically constitute the total quantum effect from the MSSM, i.e. the net effect after including the complete (standard plus supersymmetric) QCD corrections.

The paper is organized as follows. In Section 2 the lowest order relations concerning the Higgs sector and the top quark decay are given. We also discuss the status of the charged Higgs decay of the top quark in the light of the recent data from Tevatron, and the prospects for its detection. Section 3 discusses the renormalization of the $t b H^+$ -vertex in the on-shell scheme with a physically well motivated definition of $\tan\beta$. In Section 4 we present the full analytical formulae for the one-loop corrected partial width $\Gamma(t \rightarrow H^+ b)$ in the MSSM. The numerical analysis and discussion, as well as the conclusions, are delivered in Section 5, where we also comment on the feasibility of measuring the computed quantum effects in hadron colliders. Finally, we devote three appendices, respectively on SUSY Lagrangians, renormalization details and one-loop functions, in order to make the

paper as self-contained as possible.

2. Lowest order relations and determination of $BR(t \rightarrow H^\pm b)$ from experiment

In this paper we wish to emphasize the possibility that a charged pseudoscalar, H^\pm , involved in a possible unconventional decay of the top-quark, $t \rightarrow H^\pm b$, be the charged Higgs of the MSSM². A charged Higgs is necessary in the MSSM since Supersymmetry requires the existence of at least two Higgs $SU(2)_L$ -doublets with opposite weak-hypercharges to give masses to matter and gauge fields (Cf. Appendix A):

$$H_1 = \begin{pmatrix} H_1^0 \\ H_1^- \end{pmatrix} \quad (Y = -1); \quad H_2 = \begin{pmatrix} H_2^+ \\ H_2^0 \end{pmatrix} \quad (Y = +1); \quad (3)$$

Because of the SUSY constraints, the structure of the Higgs potential of the MSSM constructed out of the two doublets (3) takes on the form [24]:

$$V = m_1^2 H_1^\dagger H_1 + m_2^2 H_2^\dagger H_2 - m_{12}^2 H_1^\dagger H_2 + h.c. + \frac{1}{8}(g^2 + g'^2) (H_1^\dagger H_1 - H_2^\dagger H_2)^2 + \frac{1}{2}g^2 H_1^\dagger H_2 H_2^\dagger H_1; \quad (4)$$

where m_1^2, m_2^2, m_{12}^2 are soft SUSY-breaking masses and g, g' are the $SU(2)_L \times U(1)_Y$ gauge coupling constants. After SSB, the physical content of the Higgs sector of the MSSM consists of one CP-odd ("pseudoscalar") neutral Higgs, A^0 , two CP-even neutral Higgs bosons, h^0, H^0 , and a charged Higgs boson, H^\pm . Upon due account of the physical gauge sector, the masses of the various spinless bosons are determined in terms of just three parameters, which can be chosen to be the two vacuum expectation values (VEV's) $\langle H_2^0 \rangle = v_2, \langle H_1^0 \rangle = v_1$, giving masses to the top and bottom quarks respectively, and one physical Higgs mass. However, due to the SSB constraint

$$v^2 = v_1^2 + v_2^2 = 2M_W^2/g^2 = 2^{3/2}G_F^{-1/2}, \quad (174 \text{ GeV})^2; \quad (5)$$

where G_F is Fermi's constant in β -decay, in the end only two parameters suffice to completely specify the MSSM Higgs masses at the tree-level. Moreover, since we are interested in the decay process $t \rightarrow H^\pm b$, it is natural to take M_H as the physical input mass rather than M_{A^0} , as frequently done in other contexts. As the second independent parameter, one can take the ratio of the two VEV's: $\tan\beta = v_2/v_1$. Then, in lowest order, we have the relations [24]

$$\begin{aligned} M_{A^0}^2 &= M_H^2 - M_W^2; \\ M_{H^0, h^0}^2 &= \frac{1}{2} (M_{A^0}^2 + M_Z^2) \mp \frac{1}{2} \sqrt{(M_{A^0}^2 + M_Z^2)^2 - 4M_Z^2 M_{A^0}^2 \cos^2 2\beta}; \end{aligned} \quad (6)$$

²In the MSSM there are several additional, more exotic, 2-body decays of the top quark and also a host of 3-body final states worth studying [23].

where $M_{H^0} < M_{H^\pm}$. It is well-known that these formulas become modified at one-loop [25]. In our case, once M_H is fixed, the other Higgs masses enter the decay rate of $t \rightarrow H^+ b$ only through virtual corrections. Moreover, the renormalization of the masses also induces a renormalization of the CP-even mixing angle [25]. Although these one-loop effects are necessary to guarantee a neutral Higgs spectrum fully compatible with the phenomenological bounds near the $\tan \beta \simeq 1$ region, one expects that in practice a one-loop shift in the masses and couplings just entails a small (two-loop order) correction to the decay rate. We have explicitly checked this fact (Section 5). As for the supersymmetric charged Higgs, the present LEP 1.5 bound $M_{A^0} > 60 \text{ GeV}$ [26] on the CP-odd state translates into a lower limit $M_H > 100 \text{ GeV}$, which is not significantly modified by the radiative corrections (when M_{A^0} is taken as an input) [25].

The charged Higgs can be, as noted above, very sensitive to bottom-quark interactions. Specially, after expressing the two-doublet Higgs fields of the MSSM in terms of the corresponding mass-eigenstates, the interaction Lagrangian describing the tbH -vertex reads as follows [24]:

$$\mathcal{L}_{Hbt} = \frac{gV_{tb}}{2M_W} H^\pm b [m_t \cot \beta P_R + m_b \tan \beta P_L] t + \text{h.c.}; \quad (7)$$

where V_{tb} is the corresponding Cabibbo-Kobayashi-Maskawa matrix element, and $P_{L,R} = (1 \mp \gamma_5)/2$ are the projection operators on LH and RH fermions. On the phenomenological side, one should not dismiss the possibility that the bottom-quark Yukawa coupling could play a prominent role in the physics of the top quark, to the extent of drastically changing standard expectations on top-quark observables, particularly on the top-quark width. Of course, this is possible because of the potential $\tan \beta$ -enhancement of that Yukawa coupling.

In the " \sqrt{s} -parametrization", where the input parameters are $(\sqrt{s}; M_W; M_Z; M_H; m_f; \dots)$, the coupling g on eq.(7) stands for $e s_W$, where $e m : (q^2 = 0) = e^2 = 4$ and $s_W^2 = 1 - c_W^2 = 1 - M_W^2/M_Z^2$. An alternative framework (" G_F -parametrization") based on the set of inputs $(G_F; M_W; M_Z; M_H; m_f; \dots)$ is also useful, especially at higher orders in perturbation theory (Cf. Section 3). At the tree-level, the relation between the two parametrizations is trivial:

$$\frac{G_F}{\sqrt{2}} = \frac{e^2}{2M_W^2 s_W^2}; \quad (8)$$

From the Lagrangian (7), the tree-level width of the unconventional top quark decay into a charged Higgs boson in the G_F -parametrization reads:

$$\Gamma(t \rightarrow H^+ b) = \frac{G_F}{\sqrt{2}} \frac{|V_{tb}|^2}{m_t} \frac{1}{2} \left(1 + \frac{m_b^2}{m_t^2} + \frac{M_H^2}{m_t^2} \right) [(m_t^2 + m_b^2 - M_H^2)(m_t^2 \cot^2 \beta + m_b^2 \tan^2 \beta) + 4m_t^2 m_b^2]; \quad (9)$$

where

$$^{1=2} (1; x^2; y^2) = \frac{q}{[1 - (x + y)^2][1 - (x - y)^2]} : \quad (10)$$

It is useful to compare eq.(9) with the tree-level width of the canonical top quark decay in the SM :

$$\begin{aligned} \Gamma^{(0)}(t \rightarrow W^+ b) &= \frac{G_F^2}{8} \frac{|V_{tb}|^2}{m_t} \left[1 + \frac{m_b^2}{m_t^2} + \frac{M_W^2}{m_t^2} \right] \\ &= \frac{G_F^2}{8} \frac{|V_{tb}|^2}{m_t} \left[1 + \frac{m_b^2}{m_t^2} + \frac{M_W^2}{m_t^2} \right] : \end{aligned} \quad (11)$$

The ratio between the two partial widths becomes more transparent upon neglecting the kinematical bottom mass contributions, while retaining all the Yukawa couplings:

$$\frac{\Gamma^{(0)}(t \rightarrow H^+ b)}{\Gamma^{(0)}(t \rightarrow W^+ b)} = \frac{1 + \frac{M_H^2}{m_t^2} + \frac{m_b^2}{m_t^2} \tan^2 + \cot^2}{1 + \frac{M_W^2}{m_t^2} + 1 + 2 \frac{M_W^2}{m_t^2}} : \quad (12)$$

We see from it that if M_H is not much heavier than M_W , then there are two regimes, namely a low and a high $\tan \beta$ regime, where the decay rate of the unconventional top quark decay becomes sizeable as compared to the conventional decay. They can be defined approximately as follows: i) Low $\tan \beta$ regime: $\tan \beta < 2$, and ii) High $\tan \beta$ regime: $\tan \beta \gg 35$. The critical regime of the decay $t \rightarrow H^+ b$ occurs at the intermediate value $\tan \beta = m_t/m_b \approx 6$, where the partial width has a pronounced dip. Around this value, the canonical decay $t \rightarrow W^+ b$ is dominant over the charged Higgs decay; more specifically, for $3 < \tan \beta < 15$ the decay rate of the mode $t \rightarrow H^+ b$ is basically irrelevant as compared to the standard mode: $BR(t \rightarrow H^+ b) < 10\%$. Therefore, a detailed study of the quantum effects within that interval is of no practical interest.

Even though the approximate perturbative regime for $\tan \beta$ extends over the wide range

$$0.5 < \tan \beta < 70 ; \quad (13)$$

we shall emphasize the results obtained in the phenomenologically interesting high $\tan \beta$ region (typically $\tan \beta > 30$). As for the low $\tan \beta$ range, while $BR(t \rightarrow H^+ b)$ can also be sizeable it turns out that the corresponding quantum effects are generally much smaller than in the high $\tan \beta$ case (Cf. Section 5). Still, we find that in the very low $\tan \beta$ segment $0.5 < \tan \beta < 1$ these effects can be of some phenomenological interest and we shall also report on them. As mentioned in Section 1, we do have some theoretical motivation to contend that at least one of the two regimes i) or ii) may apply. Therefore, it is justified to focus our attention on $t \rightarrow H^+ b$, not only as a possibility on its own, but also because there may be realistic situations where it could have a non-negligible branching ratio.

As a matter of fact, and despite naive expectations, the non-SM branching ratio $BR(t \rightarrow H^+ b)$ is not as severely constrained as apparently dictated by the recent measurements of the standard branching ratio at the Tevatron, namely, $BR(t \rightarrow W^+ b) > 70\%$ [27]. To assess this fact, notice that the former result strictly applies only under the assumption that the sole source of top quarks in pp collisions is the standard Drell-Yan pair production mechanism $qq \rightarrow t\bar{t}$ [28]. Now, the observed cross-section is equal to the Drell-Yan production cross-section convoluted over the parton distributions times the squared branching ratio. Schematically,

$$\sigma_{obs} = \int d\hat{q}d\hat{q}' (qq \rightarrow t\bar{t}) BR(t \rightarrow W^+ b)^2 : \quad (14)$$

However, in the framework of the MSSM, we rather expect a generalization of this formula in the following way:

$$\begin{aligned} \sigma_{obs} = & \int d\hat{q}d\hat{q}' (qq \rightarrow t\bar{t}) BR(t \rightarrow W^+ b)^2 \\ & + \int d\hat{q}d\hat{q}' (qq \rightarrow g\bar{g}) BR(g \rightarrow t\bar{t}_1)^2 BR(t \rightarrow W^+ b)^2 \\ & + \int d\hat{q}d\hat{q}' (qq \rightarrow \tilde{b}_a \bar{\tilde{b}}_a) BR(\tilde{b}_a \rightarrow t\bar{t}_1)^2 BR(t \rightarrow W^+ b)^2 + \dots; \end{aligned} \quad (15)$$

where g stand for the gluinos, \tilde{t}_1 for the lightest stop and \tilde{b}_a ($a = 1, 2$) for the sbottom quarks. One should also include electroweak and QCD radiative corrections to all these production cross-sections within the MSSM. For some of these processes calculations already exist in the literature showing that one-loop effects can be important [29, 30].

It should be clear that the observed cross-section on eq.(15) refers not only to the standard $b\bar{W} \rightarrow bW$ events, but to all kind of final states that can simulate them. Thus, effectively, we should substitute $BR(t \rightarrow W^+ b)$ in that formula by $BR(t \rightarrow X b)$, and then sum the cross-section over X , where X is any state that leads to an observed pattern of leptons and jets similar to those resulting from W -decay. In particular, $X = H$ would contribute (see below) to the τ -lepton signature, if $\tan\beta$ is large enough. Similarly, there can be direct top quark decays into SUSY particles that could mimic the SM decay of the top quark [23]. Notwithstanding, even in the absence of the X contributions, eq.(15) shows that if there are alternative (non-SM) sources of top quarks subsequently decaying into the SM final state, $W^+ b$, one cannot rigorously place any stringent upper bound on $BR(t \rightarrow W^+ b)$ from the present data. The only restriction being an approximate lower bound $BR(t \rightarrow W^+ b) > 40 - 50\%$ in order to guarantee the purported standard top quark events at the Tevatron [1]. Thus, from these considerations it is not excluded that the non-SM branching ratio of the top quark, $BR(t \rightarrow \text{"new"})$, could be as big as the SM one, i.e. $\sim 50\%$.

Notice that at present one cannot exclude eq.(15) since the observed form of the conventional $t \rightarrow W^+ b$ final state involves missing energy, as it is also the case for the

decays comprising supersymmetric particles. A first step to improve this situation would be to compute some of the additional top quark production cross-sections in the MSSM under given hypotheses on the SUSY spectrum. Recently, the inclusion of the $qq \rightarrow g g$ mechanism followed by the $g \rightarrow t \bar{t}_1$ decay has been considered in Ref.[31], where it is claimed that $BR(t \rightarrow \bar{t}_1 \gamma) \sim 50\%$. By the same token, one cannot place any compelling restriction on $BR(t \rightarrow H^+ b)$ from the present FNAL data. In particular, if $\tan \beta$ is large and there exists a relatively light chargino with a non-negligible higgsino component, the third mechanism suggested on eq.(15), namely $qq \rightarrow \tilde{h}_a \tilde{h}_a$ followed by $\tilde{h}_a \rightarrow t \bar{t}_1$, could also be a rather efficient non-SM source of top quarks. Moreover, if $100 \text{ GeV} < M_{H^\pm} < 150 \text{ GeV}$, then a sizeable portion of the top quarks will decay into a charged Higgs. Thus, if either $m_t + m_{\tilde{t}_1} < m_g < 300 \text{ GeV}$ and/or $m_t + m_{\tilde{t}_1} < m_{\tilde{h}_a} < 300 \text{ GeV}$, so that at least one of the alternative SUSY sources of top quark final states contributing to eq.(15) is available (and $m_g, m_{\tilde{h}_a}$ are not too heavy so that the production cross-section is not too phase-space suppressed), then one may equally argue that a large branching ratio $BR(t \rightarrow H^+ b) \sim 50\%$ is not incompatible with the present measurement of the top quark cross-sections [1]. This could be most likely the case if the frequently advocated SUSY decay $t \rightarrow \bar{t}_1 \gamma$ is kinematically forbidden. Nonetheless, even if it is allowed, it is non-enhanced in our preferential large $\tan \beta$ region, in contrast to $t \rightarrow H^+ b$.

Furthermore, it is worth mentioning that the decay mode $t \rightarrow H^+ b$ has a distinctive signature which could greatly help in its detection, viz. the fact that at large $\tan \beta$ the emergent charged Higgs would seldom decay into a pair of quark jets, but rather into a τ -lepton and associated neutrino. This follows from inspecting the ratio

$$\frac{BR(t \rightarrow H^+ \tau^+ \nu_\tau)}{BR(t \rightarrow H^+ c s)} = \frac{1}{3} \frac{m_c^2}{m_s^2} \frac{\tan^2 \beta}{(m_s^2 = m_c^2) \tan^2 \beta + \cot^2 \beta} \quad (16)$$

$$\sim \frac{1}{3} \frac{m_c^2}{m_s^2} > 10 \quad (\text{for } \tan \beta > \frac{m_c}{m_s} > 2);$$

where we see that the identification of the charged Higgs decay of the top quark could be a matter of measuring a departure from the universality prediction for all lepton channels. In practice, identification is possible at the Tevatron [32, 33]; and the feasibility of tagging the excess of events with one isolated τ -lepton as compared to events with an additional lepton has also been substantiated by studies of the LHC collaborations [34]. The experimental signature for $tt \rightarrow H^+ H^- b \bar{b}$ would differ from $tt \rightarrow W^+ W^- b \bar{b}$ by an excess of final states with two τ -leptons and two b -quarks and large missing transverse energy.

A preliminary study in this direction by the CDF collaboration at the Tevatron [35] has been able to exclude a large portion of the $(\tan \beta; M_{H^\pm})$ -plane characterized by $\tan \beta > 60$ and M_{H^\pm} below a given value which varies with $\tan \beta$. For extremely high $\tan \beta > 100$,

the uppermost excluded mass region is $M_H < 140 \text{ GeV}$. However, within the interval $\tan\beta = 60 \dots 80$, the allowed upper limit on M_H varies very fast with $\tan\beta$. In particular, the MSSM permissible values $M_H > 100 \text{ GeV}$ (compatible with $M_{A^0} > 60 \text{ GeV}$) are not manifestly excluded for $\tan\beta$ equal or below the perturbative bound $\tan\beta = 70$, eq.(13). We shall nevertheless err on the conservative side and assume that $\tan\beta \geq 60$ throughout our analysis. Thus, as far as the high $\tan\beta$ regime is concerned, we will for definiteness optimize our results in the safe, and phenomenologically interesting, high $\tan\beta$ segment

$$30 \leq \tan\beta \leq 60 : \quad (17)$$

To round off the τ -lepton business, it has recently been shown that it should be fairly easy to discriminate between the W -daughter τ 's and the H -daughter τ 's by just taking advantage of the opposite states of polarization resulting from the W and H decays; the two polarization states can be distinguished by measuring the charged and neutral contributions to the 1-prong τ -jet energy (even without identifying the individual meson states) [36, 37].

In short, there are good prospects for detecting the decay $t \rightarrow H^+ b$, if it is kinematically accessible. Unfortunately, on the sole basis of computing tree-level effects we cannot find out whether the charged Higgs emerging from that decay is supersymmetric or not. Quantum effects, however, can.

3. Renormalization of the tbH^+ -vertex

Proceeding closely in parallel with our supersymmetric approach to the conventional decay $t \rightarrow W^+ b$ [17, 18], we shall address the calculation of the one-loop corrections to the partial width of $t \rightarrow H^+ b$ in the MSSM within the context of the on-shell renormalization framework [38]³. Again we may use both the $\overline{\text{MS}}$ or the G_F parametrizations. At one-loop order, we shall call the former the " $\overline{\text{MS}}$ -scheme" and the latter the " G_F -scheme". In the " $\overline{\text{MS}}$ -scheme", the structure constant $\alpha_{\text{em}} (q^2 = 0)$ and the masses of the gauge bosons, fermions and scalars are the renormalized parameters: $(\alpha; M_W; M_Z; M_H; m_f; M_{\text{SUSY}}; \dots)$ (M_{SUSY} standing for the collection of renormalized sparticle masses). Similarly, the " G_F -scheme" is characterized by the set of inputs $(G_F; M_W; M_Z; M_H; m_f; M_{\text{SUSY}}; \dots)$. Beyond lowest order, the relation between the two on-shell schemes is no longer given by eq.(8) but by

$$\frac{G_F}{\sqrt{2}} = \frac{1}{2M_W^2 S_W^2} (1 + r^{\text{MSSM}}); \quad (18)$$

³For a comprehensive exposition, see e.g. Refs.[39]–[41].

where r^{MSSM} is the prediction of the parameter r [39] in the $MSSM$ ⁴.

Let us sketch the renormalization procedure affecting the parameters and fields related to the tbH -vertex, whose interaction Lagrangian was given on eq.(7). In general, the renormalized $MSSM$ Lagrangian $L = L + \delta L$ is obtained following a similar pattern as in the SM, i.e. by attaching multiplicative renormalization constants to each free parameter and field: $g_i \rightarrow (1 + \delta g_i)g_i$, $\psi_i \rightarrow Z_i^{1/2} \psi_i$. As a matter of fact, field renormalization (and so Green's functions renormalization) is unessential and can be either omitted or be carried out in many different ways without altering physical (S-matrix) amplitudes. In our case, in the line of Refs.[17, 18] we shall use minimal field renormalization, i.e. one renormalization constant per gauge symmetry multiplet [40]. In this way the counterterm Lagrangian, δL , as well as the various Green's functions are automatically gauge-invariant. Specifically, for the quark fields under consideration, we have

$$\begin{aligned} t_L &\rightarrow Z_L^{1/2} t_L, & t_R &\rightarrow Z_R^{1/2} t_R, \\ b_L &\rightarrow Z_L^{1/2} b_L, & b_R &\rightarrow Z_R^{1/2} b_R, \end{aligned} \quad (19)$$

Here $Z_i = 1 + \delta Z_i$ are the doublet (Z_L) and singlet (Z_R^{tb}) field renormalization constants for the top and bottom quarks. Although in the minimal field renormalization scheme there is only one fundamental constant, Z_L , per matter doublet, it is useful to work with $Z_L^b = Z_L$ and Z_L^t , where the latter differs from the former by a finite renormalization effect [40]. To fix all these constants one starts from the usual on-shell mass renormalization condition for fermions, f , together with the "residue = 1" condition on the renormalized propagator. These are completely standard procedures, and in this way one obtains⁵

$$\frac{m_f}{m_f} = \frac{1}{2} \left[\frac{f_L^2(m_f^2)}{m_f^2} + \frac{f_R^2(m_f^2)}{m_f^2} \right] + \frac{f_S^2(m_f^2)}{m_f^2}; \quad (20)$$

and

$$Z_{L,R}^f = \frac{f_{L,R}^2(m_f^2)}{m_f^2} + m_f^2 \left[\frac{f_L^0(m_f^2)}{m_f^2} + \frac{f_R^0(m_f^2)}{m_f^2} + 2 \frac{f_S^0(m_f^2)}{m_f^2} \right]; \quad (21)$$

where we have decomposed the fermion self-energy according to

$$\Sigma^f(p) = \frac{f_L^2(p^2)}{p^2} \not{p} P_L + \frac{f_R^2(p^2)}{p^2} \not{p} P_R + m_f \frac{f_S^2(p^2)}{p^2}; \quad (22)$$

and used the notation $\Sigma^0(p) = \Sigma(p) - \not{p}$.

⁴A dedicated study of r^{MSSM} has been presented in Ref[42].

⁵We follow the notation of Ref.[17], which is close enough to that of Ref.[40], but differs from it in several respects, in particular in the sign conventions for the self-energy functions. Moreover, we understand that in all formulas defining counterterms we are taking the real part of the corresponding functions.

One also assigns doublet renormalization constants to the two Higgs doublets (3) of the MSSM :

$$\begin{aligned} \frac{H_1^0}{H_1} &\rightarrow Z_{H_1}^{1=2} \frac{H_1^0}{H_1} ; & \frac{H_2^+}{H_2^0} &\rightarrow Z_{H_2}^{1=2} \frac{H_2^+}{H_2^0} ; \end{aligned} \quad (23)$$

The renormalization of the gauge sector is related to that of the Higgs sector. In particular, we point out the presence in our decay process $t \rightarrow H^+ b$ of the (one-loop induced) mixing term $H^\pm W^\mp$ for the bare fields (Cf. Appendix B), which must be renormalized away for the physical fields H^\pm and W^\pm . In order to generate the corresponding Lagrangian counterterm we write

$$W^\pm \rightarrow (Z_2^W)^{1=2} W^\pm + i \frac{Z_{HW}}{M_W} @ H^\pm ; \quad (24)$$

Therefore, from

$$L_{Wtb} = \frac{g}{2} W^\pm b \not{P}_L t + h.c. \quad (25)$$

we obtain

$$\begin{aligned} L_{HW} &= i Z_{HW} \frac{g}{2M_W} @ H^\pm b \not{P}_L t + h.c. \\ &\rightarrow Z_{HW} \frac{g}{2M_W} H^\pm m_t b \not{P}_R t - m_b b \not{P}_L t + h.c.; \end{aligned} \quad (26)$$

and in this way it adopts the form of the original vertex (7). In the above expression (24), $Z_2^W = 1 + Z_2^W$ is the usual $SU(2)_L$ gauge triplet renormalization constant given by the formula

$$Z_2^W = \frac{(k^2)}{k^2} \Big|_{k^2=0} = \frac{2C_W}{S_W} \frac{Z(0)}{M_Z^2} + \frac{C_W^2}{S_W^2} \frac{M_Z^2}{M_Z^2} - \frac{M_W^2}{M_W^2} ; \quad (27)$$

and

$$M_W^2 = M_W^2(k^2 = M_W^2) ; \quad M_Z^2 = M_Z^2(k^2 = M_Z^2) ; \quad (28)$$

are the gauge boson mass counterterms enforced by the usual on-shell mass renormalization conditions. Furthermore, Z_{HW} on eqs.(24)-(26) is a dimensionless constant associated to the wave-function renormalization mixing among the bare H^\pm and W^\pm fields. Its relation with the doublet renormalization constants, $Z_{H_i} = 1 + \delta Z_{H_i}$, is the following (see Appendix B):

$$Z_{HW} = \sin \theta_W \cos \theta_W \left[\frac{1}{2} (Z_{H_2} - Z_{H_1}) + \frac{\tan \theta_W}{\tan \theta_W} \right] ; \quad (29)$$

where $\tan \theta_W$ is a counterterm associated to the renormalization of $\tan \theta_W$ (see below).

In practice, the most straightforward way to compute Z_{HW} is from the unrenormalized mixed self-energy $\Pi_{HW}(k^2)$ in the unitary gauge, where it takes on the simplest form :

$$Z_{HW} = \frac{\Pi_{HW}(M_H^2)}{M_W^2} ; \quad (30)$$

However, since we shall perform the rest of the calculation in the Feynman gauge [40], it is worth considering the computation of Z_{HW} in that gauge (see Appendix B), where the discussion is slightly more complicated due to the presence of Goldstone bosons (G) leading to additional ($H-G$) mixing terms among the bare fields. The corresponding expression for Z_{HW} is, however, formally identical in both gauges.

For the $SU(2)_L$ gauge coupling constant, we have

$$g = (1 + \frac{g}{g})g = (Z_1^W)^{-1} (Z_2^W)^{-3/2} g; \quad (31)$$

where Z_1^W refers to the renormalization constant associated to the triple vector boson vertex. Therefore, from charge renormalization,

$$1 = \frac{(k^2)}{k^2} \Big|_{k^2=0} = \frac{2}{G_W} \frac{S_W}{M_Z^2} \frac{Z(0)}{M_Z^2}; \quad (32)$$

and the bare relation $g^2 S_W^2 = 4$ and $g^2 = (g^2 + g^2)(S_W^2 + S_W^2) = 4$, one gets for the counterterm to g :

$$\frac{g^2}{g^2} = 1 - \frac{G_W^2}{S_W^2} \frac{M_Z^2}{M_W^2} \frac{M_W^2}{M_Z^2}; \quad (33)$$

and as a by-product

$$Z_1^W = \frac{1}{2} \frac{g^2}{g^2} + \frac{3}{2} Z_2^W; \quad (34)$$

Let us now outline the renormalization of the Higgs sector of the MSSM [25, 43]. Depending on the particular problem at hand, the renormalization procedure may adopt the CP-odd state A^0 as the basic field on which to set the mass and wave-function renormalization conditions. In the present work, however, since the external Higgs particle is charged, we rather take H as the basic field. Its mass and field renormalization constants are defined by

$$M_H^2 = M_H^2 + M_H^2; \quad H = Z_H^{1/2} H; \quad (35)$$

The charged Higgs field renormalization constant, $Z_H = 1 + Z_H$, is of course related to the fundamental doublet renormalization constants introduced on eq.(23), as follows (Cf. Appendix B):

$$Z_H = \sin^2 \theta Z_{H_1} + \cos^2 \theta Z_{H_2}; \quad (36)$$

The structure of the renormalized self-energy is

$$\hat{\Sigma}_H(k^2) = \Sigma_H(k^2) + M_H^2 (k^2 - M_H^2) Z_H; \quad (37)$$

where $\Sigma_H(k^2)$ is the corresponding unrenormalized self-energy.

In order to determine the counterterms, we impose the following renormalization conditions:

i) On-shell mass renormalization condition:

$$\hat{\mathcal{M}}_H^2 = 0; \quad (38)$$

ii) \Residue = 1" condition for the renormalized propagator at the pole mass:

$$\frac{\partial \hat{\mathcal{M}}_H^2(k^2)}{\partial k^2} \Big|_{k^2 = M_H^2} = 0; \quad (39)$$

From these conditions one derives

$$\begin{aligned} M_H^2 &= \mathcal{M}_H^2; \\ Z_H &= 1 + \frac{\partial \mathcal{M}_H^2}{\partial k^2} \Big|_{k^2 = M_H^2}; \end{aligned} \quad (40)$$

Although not needed in our calculation, it is clear that with these settings the neutral Higgs fields will undergo an additional finite wave function renormalization.

Consider next the renormalization of the Higgs potential in the MSSM, eq.(4) [25]. After expanding the neutral components H_1^0 and H_2^0 around their VEV's v_1 and v_2 , the one-point functions of the resulting CP-even fields are required to vanish, i.e. the tadpole counterterms are constrained to exactly cancel the tadpole diagrams, so that the renormalized tadpoles are zero and the quantities $v_{1,2}$ remain as the VEV's of the renormalized Higgs potential. Notwithstanding, at this stage a prescription to renormalize $\tan \beta = v_2/v_1$,

$$\tan \beta \rightarrow \tan \beta + \delta \tan \beta; \quad (41)$$

is still called for. There are many possible strategies. The ambiguity is related to the fact that this parameter is just a Lagrangian parameter and as such it is not a physical observable. Its value beyond the tree-level is renormalization scheme dependent. (The situation is similar to the definition of the weak mixing angle $\sin^2 \theta_W$, or equivalently of $\sin^2 \theta_W$.) However, even within a given scheme, e.g. the on-shell renormalization scheme, there are some ambiguities that must be fixed. For example, we may wish to define $\tan \beta$ in a process-independent ("universal") way as the ratio v_2/v_1 between the true VEV's after renormalization of the Higgs potential [25, 43]. In this case a consistent choice (i.e. a choice capable of renormalizing away the tadpole contributions) is to simultaneously shift the VEV's and the mass parameters of the Higgs potential, eq.(4),

$$\begin{aligned} v_i &\rightarrow Z_{H_i}^{1/2} (v_i + \delta v_i); \\ m_i^2 &\rightarrow Z_{H_i}^{1/2} (m_i^2 + \delta m_i^2); \\ m_{12}^2 &\rightarrow Z_{H_1}^{1/2} Z_{H_2}^{1/2} (m_{12}^2 + \delta m_{12}^2); \end{aligned} \quad (42)$$

($i = 1, 2$) in such a way that $v_1 = v_2$. This choice generates the following counterterm for $\tan \beta$ in that scheme (Cf. Appendix B):

$$\frac{\tan \beta}{\tan \beta} = \frac{1}{2} (Z_{H_2} - Z_{H_1}) : \quad (43)$$

Nevertheless, this procedure looks very formal and one may eventually like to fix the on-shell renormalization condition on $\tan \beta$ in a more physical way, i.e. by relating it to some concrete physical observable, so that it is the measured value of this observable that is taken as an input rather than the VEV's of the Higgs potential. Following this practical attitude, we choose as a physical observable the decay width of the charged Higgs boson into τ -lepton and associated neutrino: $H^\pm \rightarrow \tau^\pm \nu_\tau$. As it has been argued in Section 2, this should be a good choice, because: i) When $t \rightarrow H^\pm b$ is allowed, the decay $H^\pm \rightarrow \tau^\pm \nu_\tau$ is the dominant decay of H^\pm already for $\tan \beta > 2$; ii) From the experimental point of view there is a well-defined method to separate the final state $\tau^\pm \nu_\tau$'s originating from H^\pm -decay from those coming out of the conventional decay $W^\pm \rightarrow \tau^\pm \nu_\tau$, so that $H^\pm \rightarrow \tau^\pm \nu_\tau$ should be physically accessible; and iii) At high $\tan \beta$, the charged Higgs decay of the top quark can have a sizeable branching ratio.

The interaction Lagrangian describing the decay $H^\pm \rightarrow \tau^\pm \nu_\tau$ is directly proportional to $\tan \beta$,

$$\mathcal{L}_H = \frac{gm_\tau \tan \beta}{2M_W} H^\pm \bar{\nu}_\tau \tau_\pm + \text{h.c.}; \quad (44)$$

and the relevant decay width is proportional to $\tan^2 \beta$. Whether in the $\overline{\text{MS}}$ -scheme or in the G_F -scheme, it reads:

$$\Gamma(H^\pm \rightarrow \tau^\pm \nu_\tau) = \frac{m_\tau^2 M_{H^\pm}}{8M_W^2 s_W^2} \tan^2 \beta = \frac{G_F m_\tau^2 M_{H^\pm}}{4} \tan^2 \beta (1 - r^{SM}); \quad (45)$$

where we have used the relation (18). By measuring this decay width one obtains a physical definition of $\tan \beta$ which can be used beyond the tree-level. A combined measurement of M_{H^\pm} and $\tan \beta$ from charged Higgs decaying into τ -lepton in a hadron collider has been described in the literature [44, 34] by comparing the size of the various signals for charged Higgs boson production, such as the multijet channels accompanied by a τ -jet or a large missing p_T , and the two-jet channel. At the upgraded Tevatron, the conventional mechanisms $gg(qq) \rightarrow t\bar{t}$ followed by $t \rightarrow H^\pm b$ have been studied and compared with the usual $t \rightarrow W^\pm b$, and the result is that for $M_{H^\pm} \gtrsim 100 \text{ GeV}$ the charged Higgs production is at least as large as the W production, apart from a gap around $\tan \beta \approx 6$ [44].

Insofar as the determination of the counterterm $\tan \beta$ in our scheme, it can be fixed unambiguously from our Lagrangian definition of $\tan \beta$ on eq.(44) and the renormalization procedure described above. It is straightforward to find:

$$\frac{\tan \beta}{\tan \beta} = \frac{v}{v} \left(\frac{1}{2} Z_H + \cot \beta Z_{HW} + \dots \right); \quad (46)$$

Notice the appearance of the vacuum counterterm

$$\frac{v}{v} = \frac{1}{2} \frac{v^2}{v^2} = \frac{1}{2} \frac{M_W^2}{M_W^2} - \frac{1}{2} \frac{g^2}{g^2}; \quad (47)$$

which is associated to $v^2 = v_1^2 + v_2^2$, and whose structure is fixed from eq.(5). The last term on eq.(46),

$$= \frac{m}{m} - \frac{1}{2} Z_L - \frac{1}{2} Z_R - F; \quad (48)$$

is the (finite) process-dependent part of the counterterm. Here $m = m$, Z_L and Z_R are obtained from eqs.(20) and (21) (with $m = 0$); they represent the contribution from the mass and wave-function renormalization of the $(\psi; \chi)$ -doublet, including the finite renormalization of the neutrino leg. Finally, F on eq.(48) is the form factor describing the vertex corrections to the amplitude of $H^+ \rightarrow \psi^+ \chi$.

On comparing eqs.(43) and (46) we see that the first definition of $\tan\beta$ appears as though it is free from process-dependent contributions. In practice, however, process-dependent terms are inevitable, irrespective of the definition of $\tan\beta$. In fact, the definition of $\tan\beta$ where $v_1 = v_2 = v$ [45] will also develop process-dependent contributions, as can be seen by trying to relate the "universal" value of $\tan\beta$ in that scheme with a physical quantity directly read off some physical observable. For instance, if M_{A^0} is heavy enough, one may define $\tan\beta$ as follows:

$$\frac{(A^0 \rightarrow b\bar{b})}{(A^0 \rightarrow t\bar{t})} = \tan^4\beta \frac{m_b^2}{m_t^2} \left(1 - \frac{4m_t^2}{M_{A^0}^2} \right)^{1/2} \left(1 + 4 \frac{v_2}{v_1} \frac{v_1}{v_2} \right) + 2 \frac{m_b}{m_t} + \frac{1}{2} Z_L^b + \frac{1}{2} Z_R^b - \frac{m_t}{m_b} \frac{1}{2} Z_L^t - \frac{1}{2} Z_R^t + V; \quad (49)$$

where we have neglected $m_b^2/M_{A^0}^2$, and V stands for the vertex corrections to the decay processes $A^0 \rightarrow b\bar{b}$ and $A^0 \rightarrow t\bar{t}$. Since the sum of the mass and wave-function renormalization terms along with the vertex corrections is UV-finite, one can consistently choose $v_1 = v_2 = v$ leading to eq.(43). Hence, deriving $\tan\beta$ from eq.(49) unavoidably incorporates also some process-dependent contributions.

Any definition of $\tan\beta$ is in principle as good as any other; and in spite of the fact that the corrections themselves may show some dependence on the choice of the particular definition, the physical observables should not depend at all on that choice. However, it can be a practical matter what definition to use in a given situation. For example, our definition of $\tan\beta$ given on eq.(45) should be most adequate for $M_H < m_t - m_b$ and large $\tan\beta$, since then $H^+ \rightarrow \psi^+ \chi$ is the dominant decay of H^+ , whereas the definition based on eq.(49) requires also a large value of $\tan\beta$ (to avoid an impractical suppression of the $b\bar{b}$ mode); moreover, in order to be operative, it also requires a much heavier charged Higgs boson, since $M_H > M_{A^0} > 2m_t$ when the decay $A^0 \rightarrow t\bar{t}$ is kinematically open in

the MSSM. (Use of light quark mass states would, of course, be extremely difficult from the practical point of view.)

Within our context, we use eq.(46) for $\tan\beta = \tan\beta$ in order to compute the one-loop corrections to our decay $t \rightarrow H^+ b$. Putting all the pieces together, the counterterm Lagrangian for the vertex tbH^+ follows right away from the bare Lagrangian (7) after re-expressing everything in terms of renormalized parameters and fields in the on-shell scheme. It takes on the form :

$$\mathcal{L}_{Hbt} = \frac{g}{2M_W} H^+ b [C_R m_t \cot\beta + C_L m_b \tan\beta] t + \text{h.c.}; \quad (50)$$

with

$$\begin{aligned} C_R &= \frac{m_t}{m_t} \left[\frac{v}{v} + \frac{1}{2} Z_{H^+} + \frac{1}{2} Z_L^b + \frac{1}{2} Z_R^t + \frac{\tan\beta}{\tan\beta} + Z_{HW} \tan\beta \right]; \\ C_L &= \frac{m_b}{m_b} \left[\frac{v}{v} + \frac{1}{2} Z_{H^+} + \frac{1}{2} Z_L^t + \frac{1}{2} Z_R^b + \frac{\tan\beta}{\tan\beta} + Z_{HW} \cot\beta \right]; \end{aligned} \quad (51)$$

and where we have set $V_{tb} = 1$ ($V_{tb} = 0.999$ within 0.1%, from unitarity of the CKM-matrix under the assumption of three generations).

4. One-loop Corrected $(t \rightarrow H^+ b)$ in the MSSM

As stated in Section 2, the study of the decay $t \rightarrow H^+ b$ is worthwhile in the small ($\tan\beta < 2$), and most conspicuously in the high ($\tan\beta > 30$) $\tan\beta$ region, where the branching ratio can be comparable to the one of the standard decay $t \rightarrow W^+ b$. These are, therefore, the regions on which we will focus our search for potentially significant (strong and electroweak like) SUSY quantum corrections to $t \rightarrow H^+ b$. As for the strong effects, they can be rather large and have been evaluated in Ref. [15]; here we shall not dwell any longer on their detailed structure apart from including them in our numerical analysis and adding some useful remarks in Section 5.

On the electroweak side, one may also expect sizeable quantum corrections from enhanced Yukawa couplings of the type (2). In the relevant $\tan\beta$ regions mentioned above, the latter yield the leading electroweak contributions and in these conditions we will neglect the pure gauge corrections from transversal gauge bosons in the Feynman gauge. Moreover, as already stressed in Section 2, the branching ratio of the charged Higgs mode in the intermediate $\tan\beta$ region is too small to speak of, so that the detailed structure of the radiative corrections in this range is irrelevant.

In the following we will describe the relevant electroweak one-loop supersymmetric diagrams entering the amplitude of $t \rightarrow H^+ b$ in the MSSM. At the tree-level, the only Feynman diagram is the one in Fig.1. At the one-loop, we have the diagrams exhibited in

Figs 2-6. The computation of the one-loop diagrams requires to use the full structure of the MSSM Lagrangian. The explicit form of the most relevant pieces of this Lagrangian, together with the necessary SUSY notation, is provided in Appendix A.

Specially, Fig. 2 shows the electroweak SUSY vertices involving squarks, charginos and neutralinos. In all these diagrams a sum over all indices is taken for granted. The supersymmetric Higgs particles of the MSSM and Goldstone bosons (in the Feynman gauge) contribute a host of one-loop vertices as well (see Fig. 3). As for the various self-energies, they will be treated as counterterms to the vertices. Their structure is dictated by the Lagrangian (50). Thus, Fig. 4 displays the counterterms $C_{b1} \dots C_{t4}$ generated from the external bottom and top quark lines; they include contributions from supersymmetric particles, Higgs bosons and Goldstone bosons. Similarly, Fig. 5 contains the counterterms $C_{H1} \dots C_{H4}$ associated to the self-energy of the external charged Higgs boson. A variant of the latter contribution is the mixed $W^+ H^+$ self-energy counterterms $C_{M1} \dots C_{M3}$ shown in Fig. 6.

Although we have displayed only the process dependent diagrams, the full analysis should also include the SUSY and Higgs/Goldstone boson contributions to the various universal vacuum polarization effects comprised in our counterterms. However, the calculation of all these pieces has already been discussed in detail long ago in the literature [46, 47] and thus the lengthy formulae accounting for these results will not be explicitly quoted here. Their contribution is not $\tan\beta$ -enhanced, but since we wish to compute the full supersymmetric contribution in the relevant regions of the MSSM parameter space, those effects will be included in our numerical code. Finally, the smaller (though numerically overwhelming) subset of strong supersymmetric one-loop graphs are displayed in Fig. 2 of Ref. [15]. We will use the formulae from the latter reference in the present analysis to produce the total (electroweak+strong) SUSY correction to our process.

Next let us report on the contributions from the various vertex diagrams and counterterms in the on-shell renormalization scheme. The generic structure of any renormalized vertex function, Γ , in Figs 2-3 is composed of two form factors F_L, F_R plus the counterterms. Therefore, on making use of the formulae of Section 3, one immediately finds:

$$\Gamma = \frac{ig}{2M_W} [m_t \cot\beta (1 + \kappa_R) P_R + m_b \tan\beta (1 + \kappa_L) P_L]; \quad (52)$$

where

$$\begin{aligned} \kappa_R &= F_R + \frac{m_t}{m_b} + \frac{1}{2} Z_L^b + \frac{1}{2} Z_R^t \\ &\quad - \frac{v^2}{V^2} + Z_{H^+} + (\tan\beta - \cot\beta) Z_W; \end{aligned}$$

$$F_L = F_L + \frac{m_b}{m_b} + \frac{1}{2} Z_L^t + \frac{1}{2} Z_R^b + \dots : \quad (53)$$

In the following the analytical contributions to the vertex form factors and counterterms will be specified diagram by diagram.

4.1 SUSY vertex diagrams

In this section we will make intensive use of the definitions and formulae of Appendix A. We refer the reader there for questions about notation and conventions. Following the labelling of Feynman graphs in Fig. 2 we write down the terms coming from virtual SUSY particles.

Diagram (Y₁): Making use of the coupling matrices of eqs. (A.18) and (A.23) we introduce the shorthands⁶

$$A_{ai}^{(t)} \text{ and } A_a^{(0)} = A_a^{(t)} ; \quad (54)$$

and define the combinations (omitting indices also for $Q^L_i; Q^R_i$)

$$\begin{aligned} A^{(1)} &= \cos A_+ Q^L A^{(0)} ; & E^{(1)} &= \cos A_- Q^L A^{(0)} ; \\ B^{(1)} &= \cos A_+ Q^L A_+^{(0)} ; & F^{(1)} &= \cos A_- Q^L A_+^{(0)} ; \\ C^{(1)} &= \sin A_+ Q^R A^{(0)} ; & G^{(1)} &= \sin A_- Q^R A^{(0)} ; \\ D^{(1)} &= \sin A_+ Q^R A_+^{(0)} ; & H^{(1)} &= \sin A_- Q^R A_+^{(0)} ; \end{aligned} \quad (55)$$

The contribution from diagram (V_{S1}) to the form factors F_L and F_R is then

$$\begin{aligned} F_L &= M_L^h H^{(1)} C_0 + \\ &+ m_b m_t A^{(1)} + M^0 B^{(1)} + m_b H^{(1)} + M_i D^{(1)} C_{12} \\ &+ m_t m_t H^{(1)} + M^0 G^{(1)} + m_b A^{(1)} + M_i E^{(1)} (C_{11} - C_{12})_i \\ &+ m_t m_b A^{(1)} + m_t M_i E^{(1)} + M^0 m_b B^{(1)} + M_i M^0 F^{(1)} C_0 ; \\ F_R &= M_R^h A^{(1)} C_0 + \\ &+ m_b m_t H^{(1)} + M^0 G^{(1)} + m_b A^{(1)} + M_i E^{(1)} C_{12} \\ &+ m_t m_t A^{(1)} + M^0 B^{(1)} + m_b H^{(1)} + M_i D^{(1)} (C_{11} - C_{12})_i \\ &+ m_t m_b H^{(1)} + m_t M_i D^{(1)} + M^0 m_b G^{(1)} + M_i M^0 C^{(1)} C_0 ; \end{aligned} \quad (56)$$

where the overall coefficients M_L and M_R are the following:

$$M_L = \frac{ig^2 M_W}{m_b \tan \beta} \quad M_R = \frac{ig^2 M_W}{m_t \cot \beta} : \quad (57)$$

⁶Lower indices are summed over, whereas upper indices (some of them within parenthesis) are just for notational convenience.

The notation for the various 3-point functions is summarized in Appendix C. On eq. (56) they must be evaluated with arguments:

$$C = C(p; p^0; m_{t_a}; M^0; M_i) : \quad (58)$$

Diagram (V₂): For this diagram {which in contrast to the others is finite} we also use the matrices on eqs. (A.18) and (A.21), and introduce the shorthands

$$A^{(b)} = A^{(b)}_b \quad \text{and} \quad A^{(t)} = A^{(t)}_a ; \quad (59)$$

to define the products of coupling matrices

$$\begin{aligned} A^{(2)} &= G_{ba} A^{(b)}_+ A^{(t)} ; & C^{(2)} &= G_{ba} A^{(b)} A^{(t)} ; \\ B^{(2)} &= G_{ba} A^{(b)}_+ A^{(t)}_+ ; & D^{(2)} &= G_{ba} A^{(b)} A^{(t)}_+ : \end{aligned} \quad (60)$$

The contribution to the form factors F_L and F_R from this diagram is

$$\begin{aligned} F_L &= \frac{M_L}{2M_W} m_b B^{(2)} C_{12} + m_t C^{(2)} (C_{11} - C_{12}) M^0 D^{(2)} C_0^i ; \\ F_R &= \frac{M_R}{2M_W} m_b C^{(2)} C_{12} + m_t B^{(2)} (C_{11} - C_{12}) M^0 A^{(2)} C_0^i ; \end{aligned} \quad (61)$$

the coefficients M_L, M_R being those of eq. (57) and the scalar 3-point functions now evaluated with arguments

$$C = C(p; p^0; M^0; m_{t_a}; m_{b_b}) : \quad (62)$$

Diagram (V₃): For this diagram we will need

$$A = A^{(b)}_{ai} \quad \text{and} \quad A^{(0)} = A^{(b)}_a ; \quad (63)$$

and again on fitting indices we shall use

$$\begin{aligned} A^{(3)} &= \cos A^{(0)}_+ Q^L A ; & E^{(3)} &= \cos A^{(0)} Q^L A ; \\ B^{(3)} &= \cos A^{(0)}_+ Q^L A_+ ; & F^{(3)} &= \cos A^{(0)} Q^L A_+ ; \\ C^{(3)} &= \sin A^{(0)}_+ Q^R A ; & G^{(3)} &= \sin A^{(0)} Q^R A ; \\ D^{(3)} &= \sin A^{(0)}_+ Q^R A_+ ; & H^{(3)} &= \sin A^{(0)} Q^R A_+ : \end{aligned} \quad (64)$$

From these definitions the contribution of diagram (V_{S3}) to the form factors can be obtained by performing the following changes in that of diagram (V_{S1}), eq. (56):

{ Everywhere on eqs. (56) and (58) replace $M_i \rightarrow M^0$ and $m_{t_a} \rightarrow m_{b_b}$.

{ Replace on eq. (56) couplings from (55) with those of (64).

{ Include a global minus sign.

4.2 Higgs vertex diagrams

Now we consider contributions arising from the exchange of virtual Higgs particles and Goldstone bosons in the Feynman gauge, as shown in Fig.3. We follow the vertex formula for the form factors by the value of the overall coefficient N and by the arguments of the corresponding 3-point functions.

Diagram (Y_1) :

$$\begin{aligned} F_L &= N [m_b^2 (C_{12} - C_0) + m_t^2 \cot^2 (\theta) (C_{11} - C_{12})]; \\ F_R &= N m_b^2 [C_{12} - C_0 + \tan^2 (\theta) (C_{11} - C_{12})]; \\ N &= \frac{ig^2}{2} (1 - \frac{fM_{H^0}^2; M_{h^0}^2 g}{2M_W^2} \frac{f \cos(\theta); \sin(\theta) g}{\cos(\theta)}); \\ C &= C(p; p^0; m_b; M_H; fM_{H^0}; M_{h^0} g) : \end{aligned}$$

Diagram (Y_2) :

$$\begin{aligned} F_L &= N \cot(\theta) [m_t^2 (C_{11} - C_{12}) + m_b^2 (C_0 - C_{12})]; \\ F_R &= N m_b^2 \tan(\theta) (2C_{12} - C_{11} - C_0); \\ N &= \frac{ig^2}{4} \frac{f \cos(\theta); \sin(\theta) g}{\cos(\theta)} f \sin(\theta); \cos(\theta) g \frac{M_H^2}{M_W^2} \frac{fM_{H^0}^2; M_{h^0}^2 g}{M_W^2}; \\ C &= C(p; p^0; m_b; M_W; fM_{H^0}; M_{h^0} g) : \end{aligned}$$

Diagram (Y_3) :

$$\begin{aligned} F_L &= N m_t^2 [\cot^2(\theta) C_{12} + C_{11} - C_{12} - C_0]; \\ F_R &= N [m_b^2 \tan^2(\theta) C_{12} + m_t^2 (C_{11} - C_{12} - C_0)]; \\ N &= \frac{ig^2}{2} \frac{f \sin(\theta); \cos(\theta) g}{\sin(\theta)} f \cos(\theta); \sin(\theta) g (1 - \frac{fM_{H^0}^2; M_{h^0}^2 g}{2M_W^2}); \\ C &= C(p; p^0; m_t; fM_{H^0}; M_{h^0} g; M_H) : \end{aligned}$$

Diagram (Y_4) :

$$\begin{aligned} F_L &= N m_t^2 (2C_{12} - C_{11} + C_0) \cot(\theta); \\ F_R &= N [m_b^2 C_{12} + m_t^2 (C_{11} - C_{12} - C_0)] \tan(\theta); \\ N &= \frac{ig^2}{4} \frac{f \sin(\theta); \cos(\theta) g}{\sin(\theta)} f \sin(\theta); \cos(\theta) g \frac{M_H^2}{M_W^2} \frac{fM_{H^0}^2; M_{h^0}^2 g}{M_W^2}; \\ C &= C(p; p^0; m_t; fM_{H^0}; M_{h^0} g; M_W) : \end{aligned}$$

Diagram (Y₅):

$$\begin{aligned}
F_L &= N [m_b^2 (C_{12} + C_0) + m_t^2 (C_{11} - C_{12})]; \\
F_R &= N m_b^2 \tan^2 \beta (C_{11} + C_0); \\
N &= \frac{ig^2}{4} \frac{M_H^2}{M_W^2} \frac{M_{A^0}^2}{M_W^2}; \\
C &= C(p; p^0; m_b; M_W; M_{A^0}):
\end{aligned}$$

Diagram (Y₆):

$$\begin{aligned}
F_L &= N m_t^2 \cot^2 \beta (C_{11} + C_0); \\
F_R &= N [m_b^2 C_{12} + m_t^2 (C_{11} - C_{12} + C_0)]; \\
N &= \frac{ig^2}{4} \frac{M_H^2}{M_W^2} \frac{M_{A^0}^2}{M_W^2}; \\
C &= C(p; p^0; m_t; M_{A^0}; M_W):
\end{aligned}$$

Diagram (Y₇):

$$\begin{aligned}
F_L &= N [(2m_b^2 C_{11} + C_0 + 2(m_t^2 - m_b^2)(C_{11} - C_{12})) \cot^2 \beta + 2m_b^2 (C_{11} + 2C_0) m_t^2]; \\
F_R &= N [(2m_b^2 C_{11} + C_0 + 2(m_t^2 - m_b^2)(C_{11} - C_{12})) \tan^2 \beta + 2m_t^2 (C_{11} + 2C_0) m_b^2]; \\
N &= \frac{ig^2}{4M_W^2} \frac{\sin \alpha}{\sin \alpha \cos \alpha}; \\
C &= C(p; p^0; M_{H^0}; M_{H^0} g; m_t; m_b):
\end{aligned}$$

Diagram (Y₈):

$$\begin{aligned}
F_L &= N m_t^2 \cot^2 \beta C_0; \\
F_R &= N m_b^2 \tan^2 \beta C_0; \\
N &= \frac{ig^2}{4M_W^2}; \\
C &= C(p; p^0; M_{A^0}; M_Z g; m_t; m_b):
\end{aligned}$$

In the equations above, it is understood that the CP-even mixing angle, α , is renormalized into α_e by the one-loop Higgs mass relations [25].

As for the SUSY and Higgs contributions to the counterterms, they are much simpler since they just involve 2-point functions. Thus we shall present the full electroweak results by adding up the various sparticle and Higgs effects. In the following formulae, we append labels referring to the specific diagrams on Figs.4-6.

4.3 Counterterms

Counterterms Σ_f ; Z_L^f ; Z_R^f : For a given down-like fermion b , and corresponding isospin partner t , the fermionic self-energies receive contributions

$$\begin{aligned}
\Sigma_{fL,R}^b(p^2) &= \Sigma_{fL,R}^b(p^2)_{(C_{b1})+(C_{b2})} \\
&= ig^2 A_{ai}^{(t)} B_1(p; m_i; m_{t_a}) + \frac{1}{2} A_a^{(b)} B_1(p; M_0; m_{\tilde{b}_a}) ; \\
\Sigma_S^b(p^2) &= \Sigma_S^b(p^2)_{(C_{b1})+(C_{b2})} \\
&= ig^2 M_i \text{Re} A_{+ai}^{(t)} A_{-ai}^{(t)} B_0(p; m_i; m_{t_a}) \\
&\quad + \frac{1}{2} M_0 \text{Re} A_a^{(b)} A_{+a}^{(b)} B_0(p; M_0; m_{\tilde{b}_a}) ; \tag{65}
\end{aligned}$$

from SUSY particles, and

$$\begin{aligned}
\Sigma_{fL,R}^b(p^2) &= \Sigma_{fL,R}^b(p^2)_{(C_{b3})+(C_{b4})} \\
&= \frac{g^2}{2iM_W^2} m_{ftbg}^2 \left[\tan^2 \theta B_1(p; m_t; M_{H^\pm}) + B_1(p; m_t; M_{W^\pm}) \right] \\
&\quad + \frac{m_b^2}{2\cos^2 \theta} \left[\cos^2 \theta B_1(p; m_b; M_{H^0}) + \sin^2 \theta B_1(p; m_b; M_{h^0}) \right. \\
&\quad \left. + \sin^2 \theta B_1(p; m_b; M_{A^0}) + \cos^2 \theta B_1(p; m_b; M_{Z^0}) \right] ; \\
\Sigma_S^b(p^2) &= \Sigma_S^b(p^2)_{(C_{b3})+(C_{b4})} \\
&= \frac{g^2}{2iM_W^2} m_t^2 [B_0(p; m_t; M_{H^\pm}) - B_0(p; m_t; M_{W^\pm})] \\
&\quad + \frac{m_b^2}{2\cos^2 \theta} \left[\cos^2 \theta B_0(p; m_b; M_{H^0}) + \sin^2 \theta B_0(p; m_b; M_{h^0}) \right. \\
&\quad \left. + \sin^2 \theta B_0(p; m_b; M_{A^0}) - \cos^2 \theta B_0(p; m_b; M_{Z^0}) \right] ; \tag{66}
\end{aligned}$$

from Higgs and Goldstone bosons in the Feynman gauge. To obtain the corresponding expressions for an up-like fermion, t , just perform the label substitutions $b \rightarrow t$ on eqs. (65)–(66); and on eq. (66) replace $\sin \leftrightarrow \cos$ and $\sin \leftrightarrow \cos$ (which also implies replacing $\tan \leftrightarrow \cot$).

Introducing the above expressions into eqs. (20)–(21) one immediately obtains the SUSY contribution to the counterterms Σ_f ; Z_L^f ; Z_R^f .

Counterterm Z_H :

$$Z_H = Z_H - j_{(C_{H1})+(C_{H2})+(C_{H3})+(C_{H4})} = \frac{0}{H} (M_H^2)$$

$$\begin{aligned}
= & \frac{ig^2 N_C}{M_W^2} (m_b^2 \tan^2 + m_t^2 \cot^2) (B_1 + M_H^2 B_1^0 + m_b^2 B_0^0) \\
& + 2m_b^2 m_t^2 B_0^0 (M_H^2; m_b; m_t) \\
& + \frac{ig^2}{2M_W^2} N_C \sum_{ab} G_{ba}^2 B_0^0 (M_H^2; m_b; m_t) \\
& + 2ig^2 \sum_i Q_i^L \cos^2 + Q_i^R \sin^2 (B_1 + M_H^2 B_1^0 + M^{02} B_0^0) \\
& + 2M_i M^0 \text{Re } Q_i^L Q_i^R \sin \cos B_0^0 (M_H^2; M^0; M_i) : \quad (67)
\end{aligned}$$

Notice that diagram (C_{H3}) gives a vanishing contribution to Z_H .

Counterterm Z_W :

$$\begin{aligned}
Z_{HW} &= Z_{HW} (C_{M1}) + (C_{M2}) + (C_{M3}) = \frac{H_W (M_H^2)}{M_W^2} \\
&= \frac{ig^2 N_C}{M_W^2} m_b^2 \tan (B_0 + B_1) + m_t^2 \cot B_1 (M_H^2; m_b; m_t) \\
&+ \frac{ig^2 N_C}{2M_W^2} \sum_{ab} G_{ba} R_{1a}^{(t)} R_{1b}^{(b)} [2B_1 + B_0] (M_H^2; m_b; m_t) \\
&+ \frac{2ig^2}{M_W} \sum_i M^0 \cos Q_i^L C_i^L + \sin Q_i^R C_i^R (B_0 + B_1) \\
&+ M_i \sin Q_i^R C_i^L + \cos Q_i^L C_i^R B_1 (M_H^2; M^0; M_i) : \quad (68)
\end{aligned}$$

A sum is understood over all generations.

Finally, the evaluation of on eq.(48) yields similar bulky analytical formulae, which follow after computing diagrams akin to those in Figs2-6 for the MSSM corrections to $H^+ \rightarrow b \bar{t}$. We refrain from quoting them explicitly here. The numerical effect, though, will be explicitly given in Section 5.

We are now ready to furnish the corrected width of $t \rightarrow H^+ b$ in the MSSM. It just follows after computing the interference between the tree-level amplitude and the one-loop amplitude. It is convenient to express the result as a relative correction with respect to the tree-level width both in the \overline{MS} -scheme and in the G_F -scheme. In the former we obtain the relative MSSM correction

$$\begin{aligned}
\delta_{MSSM}^{(0)} &= \frac{\delta^{(0)}}{\Gamma^{(0)}} \\
&= \frac{N_L}{D} [2\text{Re}(\delta_L)] + \frac{N_R}{D} [2\text{Re}(\delta_R)] + \frac{N_{LR}}{D} [2\text{Re}(\delta_L + \delta_R)]; \quad (69)
\end{aligned}$$

where the corresponding lowest-order width is

$$\Gamma^{(0)} = \frac{1}{s_W^2} \frac{D}{16M_W^2 m_t} \left(1 + \frac{m_b^2}{m_t^2} + \frac{M_H^2}{m_t^2} \right); \quad (70)$$

with

$$\begin{aligned}
D &= (m_t^2 + m_b^2 - M_H^2) (m_t^2 \cot^2 + m_b^2 \tan^2) + 4m_t^2 m_b^2; \\
N_L &= (m_t^2 + m_b^2 - M_H^2) m_b^2 \tan^2; \\
N_R &= (m_t^2 + m_b^2 - M_H^2) m_t^2 \cot^2; \\
N_{LR} &= 2m_t^2 m_b^2;
\end{aligned} \tag{71}$$

From these equations it is obvious that at low $\tan \beta$ the relevant quantum effects basically come from the contributions to the form factor Γ_R whereas at high $\tan \beta$ they come from Γ_L .

Using eq.(18) we find that the relative MSSM correction in the G_F -parameterization reads

$$\frac{M_{G_F}^{\text{MSSM}}}{G_F} = \frac{G_F^{(0)}}{G_F^{(0)}} = M^{\text{MSSM}} r^{\text{MSSM}}; \tag{72}$$

where the tree-level width in the G_F -scheme, $\Gamma_{G_F}^{(0)}$, is given by eq.(9) and is related to eq.(70) through

$$\Gamma^{(0)} = \Gamma_{G_F}^{(0)} (1 - r^{\text{MSSM}}); \tag{73}$$

5. Numerical Analysis and Discussion

Quantum effects should be able to discriminate whether the charged Higgs emerging from the decay $t \rightarrow H^+ b$ is supersymmetric or not, for the MSSM provides a well defined prediction of the typical size of these effects using the present bounds on sparticle masses. Some work on radiative corrections to the decay width of $t \rightarrow H^+ b$ has already appeared in the literature. In particular, the conventional QCD corrections have been evaluated [14] and found to significantly reduce the partial width. The SUSY-QCD corrections are also substantial and have been analyzed, only in part in Refs.[48, 49], and in more detail in Ref.[15]. Nevertheless, the electroweak corrections produced by the roster of genuine (R-odd) sparticles have not been considered at all yet. As for the virtual effects mediated by the Higgs bosons, a first treatment is given in Refs.[50] and [51]. However, these references disagree in several parts of the calculation, and moreover they are both incomplete calculations on their own, for they fully ignore the Higgs effects associated to the bottom quark Yukawa coupling, which could in principle be significant in the large $\tan \beta$ region. On the other hand, even though the latter kind of Higgs effects have been discussed in the literature in other renormalization schemes based on alternative definitions of $\tan \beta$ [43, 52, 53], a detailed analysis including the genuine SUSY effects themselves has never been attempted. Thus, if only for completeness, we are providing here not only a

dedicated treatment of the R-odd contributions mediated by the sparticles of the MSSM, but also the full coverage of the supersymmetric Higgs effects.

Before presenting the results of the complete numerical analysis, it should be clear that the bulk of the high $\tan\beta$ corrections to the decay rate of $t \rightarrow H^+ b$ in the MSSM is expected to come from SUSY-QCD. This could already be foreseen from what is known in SUSY GUT models [11]; in fact, in this context a non-vanishing sbottom mixing (which we also assume in our analysis) may lead to important SUSY-QCD quantum effects on the bottom mass, $m_b = m_b^{\text{GUT}} + \delta m_b$, where δm_b is proportional to $M_{LR}^b \tan\beta$ at sufficiently high $\tan\beta$. These are finite threshold effects that one has to include when matching the SM and MSSM renormalization group equations (RGE) at the effective supersymmetric threshold scale, T_{SUSY} , above which the RGE evolve according to the MSSM β -functions in the $\overline{\text{MS}}$ scheme [54, 55]. In our case, since the bottom mass is an input parameter for the on-shell scheme, these effects obviously have a different physical meaning, but are formally the same; they are just fed into the mass counterterm $\delta m_b = m_b$ on eq.(53) and contribute to it with opposite sign ($\delta m_b = m_b = -m_b + \dots$)⁷.

Explicitly, when viewed in terms of diagrams of the electroweak-eigenstate basis, the relevant finite corrections from the bottom mass counterterm are generated by mixed LR-sbottoms and gluino loops (Cf. Fig.7a):

$$\frac{\delta m_b}{m_b} \Big|_{\text{SUSY-QCD}} = \frac{2}{3} \frac{m_t}{m_b} m_g M_{LR}^b I(m_{b_1}; m_{b_2}; m_g) + \frac{2}{3} \frac{m_t}{m_b} m_g \tan\beta I(m_{b_1}; m_{b_2}; m_g); \quad (74)$$

where the last result holds for sufficiently large $\tan\beta$ and for not too small m_b as compared to A_b . We have introduced the positive-definite function (Cf. Appendix C)

$$I(m_1; m_2; m_3) = 16^{-2} iC_0(0; 0; m_1; m_2; m_3) = \frac{m_1^2 m_2^2 \ln \frac{m_1^2}{m_2^2} + m_2^2 m_3^2 \ln \frac{m_2^2}{m_3^2} + m_1^2 m_3^2 \ln \frac{m_3^2}{m_1^2}}{(m_1^2 - m_2^2)(m_2^2 - m_3^2)(m_1^2 - m_3^2)}; \quad (75)$$

In addition, we could also foresee potentially large (finite) SUSY electroweak effects from $\delta m_b = m_b$. They are induced by $\tan\beta$ -enhanced Yukawa couplings of the type (2). Of course, these effects have already been fully included in the calculation presented in Section 3 that we have performed in the mass-eigenstate basis, but it is illustrative of the origin

⁷In the alternative framework of Ref.[15], the SUSY-QCD corrections have been computed assuming no mixing in the sbottom mass matrix. Nonetheless, the typical size of the SUSY-QCD corrections does not change as compared to the present approach (in which we do assume a non-diagonal sbottom matrix) the reason being that in the absence of sbottom mixing, i.e. $M_{LR}^b = 0$, the contribution $\delta m_b = m_b / \tan\beta$ at large $\tan\beta$ is no longer possible but, in contrast, the vertex correction does precisely inherit this dependence and compensates for it (Cf. Appendix A). The drawback of an scenario based on $M_{LR}^b = 0$, however, is that when it is combined with a large value of $\tan\beta$ it may lead to a value of A_b which overshoots the natural range expected for this parameter.

of the leading contributions to pick them up again directly from the diagrams in the electroweak-eigenstate basis. In this case, from loops involving mixed LR-stops and mixed charged higgsinos (Cf. Fig.7b), one finds:

$$\frac{\delta m_b}{m_b} \Big|_{\text{SUSY Yukawa}} = \frac{h_t h_b}{16\pi^2} \frac{m_t}{m_b} M_{LR}^t I(m_{\tilde{t}_1}; m_{\tilde{t}_2}; \mu) + \frac{h_t^2}{16\pi^2} \tan\beta A_t I(m_{\tilde{t}_1}; m_{\tilde{t}_2}; \mu); \quad (76)$$

where again the last expression holds for large enough $\tan\beta$.

Notice that, at variance with eq.(74), the Yukawa coupling correction (76) dies away with increasing μ . Setting $h_t \rightarrow 1$ at high $\tan\beta$, and assuming that there is no large hierarchy between the sparticle masses, the ratio between (74) and (76) is given, in good approximation, by $4m_g/A_t$ times a slowly varying function of the masses of order 1, where the (approximate) proportionality to the gluino mass reflects the very slow decoupling rate of the latter [15].

In view of the present bounds on the gluino mass, and since A_t (as well as A_b) cannot increase arbitrarily (Cf. Appendix A), we expect that the SUSY-QCD effects can be dominant and even overwhelming for sufficiently heavy gluinos. Unfortunately, in contradistinction to the SUSY-QCD case, there are also plenty of additional vertex contributions both from the Higgs sector and from the stop-bottom /gaugino-higgsino sector where those Yukawa couplings enter once again the game. So if one wishes to trace the origin of the leading contributions in the electroweak-eigenstate basis, a similar though somewhat more involved exercise has to be carried out also for vertex functions. Of course, all of these effects are automatically included in our calculation of Section 3 within the framework of the mass-eigenstate basis⁸.

We may now pass on to the numerical analysis of the over-all quantum effects. After explicit computation of the various loop diagrams, the results are conveniently cast in terms of the relative correction with respect to the tree-level width:

$$\delta \Gamma_H^{(0)} = \frac{\delta \Gamma_H^{(0)}}{\Gamma_H^{(0)}} = \frac{(t \rightarrow H^+ b) - (t \rightarrow H^+ b)^{(0)}}{(t \rightarrow H^+ b)^{(0)}}; \quad (77)$$

In what follows we understand that $\delta \Gamma_H^{(0)}$ defined by eq.(77) is $\delta \Gamma_H^{(0)} / \Gamma_H^{(0)}$ { Cf. eq.(69) } i.e. we shall always give our corrections with respect to the tree-level width $\Gamma_H^{(0)}$ in the $\overline{\text{MS}}$ -scheme. The corresponding correction with respect to the tree-level width in the G_F -scheme is simply given by eq.(72), where $\Gamma_H^{(0)}$ was object of a particular study [42] and therefore it

⁸The mass-eigenstate basis is extremely convenient to carry out the numerical analysis, but it does not immediately provide a "physical interpretation" of the results. The electroweak-eigenstate basis, in contrast, is a better bookkeeping device to trace the origin of the most relevant effects, but as a drawback the intricacies of the full analytical calculation can be (in general) abhorrent.

can be easily incorporated, if necessary. Notice, however, that r^{MSSM} is already tightly bound by the experimental data on $M_Z = 91.1863 \pm 0.0020 \text{ GeV}$ at LEP [56] and the ratio $M_W = M_Z$ in pp, which lead to $M_W = 80.356 \pm 0.125 \text{ GeV}$. Therefore, even without doing the exact theoretical calculation of r within the MSSM, we already know from

$$r = 1 - \frac{1}{2G_F M_W^2 (1 - M_W^2/M_Z^2)}; \quad (78)$$

that r^{MSSM} must lie in the experimental interval $r^{\text{exp}} \in [0.040, 0.018]$.

Now, since the corrections computed in Section 3 can typically be about one order of magnitude larger than r^{MSSM} , the bulk of the quantum effects on $t \rightarrow H^+ b$ is already comprised in the relative correction (77) in the $\overline{\text{MS}}$ -scheme⁹. Furthermore, in the conditions under study, only a small fraction of r^{MSSM} is supersymmetric [42], and we should not be dependent on isolating this universal, relatively small, part of the total SUSY correction to r . To put in a nutshell: if there is to be any hope to measure supersymmetric quantum effects on the charged Higgs decay of the top quark, they should better come from the potentially large, non-oblique, corrections computed in Section 3. The SUSY effects contained in r^{MSSM} [42], instead, will be measured in a much more efficient way from a high precision ($M_W^{\text{exp}} = 80.356 \pm 0.125 \text{ GeV}$) determination of M_W at LEP 200.

Another useful quantity is the branching ratio

$$B_H = \text{BR}(t \rightarrow H^+ b) = \frac{\Gamma_H}{\Gamma_W + \Gamma_H + \Gamma_{\text{SUSY}}}; \quad (79)$$

where $\Gamma_W = \Gamma(t \rightarrow W^+ b)$ and Γ_{SUSY} stands for decays of the top quark into SUSY particles. In particular, the potentially important SUSY-QCD mode $t \rightarrow \tilde{t}_1 g$ is kinematically forbidden in most part of our analysis where we usually assume $m_g = 0$ (300 GeV). There may also be the competing electroweak SUSY decays $t \rightarrow \tilde{t}_1^0$ and $t \rightarrow \tilde{b}_1^+$ for some $i = 1, \dots, 4$ and some $j = 1, 2$. The latter, however, is also phase space obstructed in most of our explored parameter space, since we typically assume $m_{\tilde{b}_1} = 150 \text{ GeV}$. The decay $t \rightarrow \tilde{t}_1^0$, instead, is almost always open, but it is not $\tan\beta$ -enhanced in our favourite segment (17). However, when studying the branching ratio (79) as a function of the squark and gluino masses, we do include the effects from all these supersymmetric channels whenever they are kinematically open. Thus in general Γ_{SUSY} on eq.(79) is given by

$$\Gamma_{\text{SUSY}} = \Gamma(t \rightarrow \tilde{t}_1 g) + \sum_i \Gamma(t \rightarrow \tilde{t}_1^0) + \sum_i \Gamma(t \rightarrow \tilde{b}_1^+): \quad (80)$$

⁹For the standard decay $t \rightarrow W^+ b$, the situation is quite different since the SM electroweak corrections [57] and the maximal SUSY electroweak corrections [17] in the $\overline{\text{MS}}$ -scheme are much smaller than for the decay $t \rightarrow H^+ b$, namely they are of the order of r . Therefore, for the standard decay $t \rightarrow W^+ b$ there is a significant cancellation between the corrections in the $\overline{\text{MS}}$ -scheme and r in most of the $\tan\beta$ range resulting in a substantially diminished correction in the G_F -scheme.

The various terms contributing to this equation are computed at the tree-level. Recently, the SUSY-QCD corrections to some of these supersymmetric modes have been evaluated and in some cases may be important [58]. Similarly, we treat the computation of the partial width of the standard mode $t \rightarrow W^+ b$ at the tree-level. This is justified since, as shown in Refs.[17, 18, 19, 59], this decay cannot in general develop large supersymmetric radiative corrections, or at least as large as to be comparable to those affecting the charged Higgs mode (for the same value of the input parameters). The reason for it stems from the very different structure of the counterterms for both decays; in particular, the standard decay mode of the top quark does not involve the mass renormalization counterterms for the external fermion lines, and as a consequence the aforementioned large quantum effects associated to the bottom quark self-energy at high $\tan\beta$ are not possible.

Figures 8-20 and 22-23 display a clear-cut resume of our numerical results. We wish to point out that they have been thoroughly checked. Scale independence of Γ , eq.(77), and cancellation of UV-divergences have been explicitly verified. Most of the analytical and numerical calculations have been doubled. In particular, we have constructed two independent numerical codes and checked that the two approaches perfectly agree at different stages. In all our numerical evaluations we have imposed the following restriction on the non-SM contributions to the μ -parameter [9]:

$$\mu_{\text{new}} < 0.003 : \quad (81)$$

To start with, we concentrate on the case $\mu < 0$, which we study in Figs.8-20. (The case $\mu > 0$ is studied apart in Figs.22-23 and will be commented later on.) We observe that, for negative μ , the leading SUSY-QCD effects on Γ are positive. This means that in these circumstances the potentially large strong supersymmetric effects are in frank competition with the conventional QCD corrections, which are also very large and stay always negative as will be discussed later on.

Needless to say, a crucial parameter to be investigated is $\tan\beta$. In Fig.8 we plot the tree-level width, $\Gamma_0(t \rightarrow H^+ b)$, and the total partial width, $\Gamma_{\text{MSSM}}(t \rightarrow H^+ b)$, comprising all the MSSM effects, as a function of $\tan\beta$. A typical set of parameters is chosen well within canonical expectations (see below); the individual influence of each one of them is tested in Figs.10 to 20. Also shown in Fig.8 is the (tree-level) partial width of the standard top quark decay $t \rightarrow W^+ b$, which is (as noted above) far less sensitive to quantum corrections. For convenience, we have included in Fig.8 a plot of $\Gamma_{\text{QCD}}(t \rightarrow H^+ b)$, i.e. the partial width that would be obtained in the presence of only the standard QCD corrections. In practice, this is tantamount to saying that $\Gamma_{\text{QCD}}(t \rightarrow H^+ b)$ is the partial width that would be expected in the absence of SUSY effects, for the electroweak non-supersymmetric corrections turn out to be negligible versus the ordinary

QCD effects.

From eq.(69) it is clear that, for large (resp. small) $\tan\beta$, the renormalized form factor yielding the bulk of the SUSY contribution is Δ_L (resp. Δ_R). To appraise the relative importance of the various types of MSSM effects on $t \rightarrow H^+ b$, in Figs.9a-9b we provide plots for the correction to the partial width, eq.(77), and to the branching ratio, eq.(79), as a function of $\tan\beta$, reflecting the various individual contributions. Specifically, we show in Fig.9a:

(i) The supersymmetric electroweak contribution from genuine (R-odd) sparticles (denoted $\Delta_{\text{SUSY EW}}$), i.e. from sfermions (squarks and sleptons), charginos and neutralinos;

(ii) The electroweak contribution from non-supersymmetric (R-even) particles (Δ_{EW}). It is composed of two distinct types of effects, namely, those from Higgs and Goldstone bosons (collectively called "Higgs" contribution, and denoted Δ_{Higgs}) plus the leading SM effects [40] from conventional fermions (Δ_{SM}):

$$\Delta_{\text{EW}} = \Delta_{\text{Higgs}} + \Delta_{\text{SM}}; \quad (82)$$

The remaining non-supersymmetric electroweak effects are subleading and are neglected.

(iii) The strong supersymmetric contribution (denoted by $\Delta_{\text{SUSY QCD}}$) from squarks and gluinos;

(iv) The strong contribution from conventional quarks and gluons (labelled Δ_{QCD}); and

(v) The total MSSM contribution, Δ_{MSSM} , namely, the net sum of all the previous contributions:

$$\Delta_{\text{MSSM}} = \Delta_{\text{SUSY EW}} + \Delta_{\text{EW}} + \Delta_{\text{SUSY QCD}} + \Delta_{\text{QCD}}; \quad (83)$$

In Fig.9b we reflect the impact of the MSSM on the branching ratio, as a function of $\tan\beta$; also shown are the tree-level value of the branching ratio and the latter quantity after including the (non-supersymmetric) QCD corrections. A typical common set of inputs has been chosen in Figs.9a-9b such that the supersymmetric electroweak corrections reinforce the strong supersymmetric effects ($\Delta_{\text{SUSY QCD}}$). For this set of inputs, the total MSSM correction to the partial width of $t \rightarrow H^+ b$ is positive for $\tan\beta > 20$ (approx.). Remarkably enough, this is so in spite of the huge negative effects induced by QCD. In fact, we see that the gluon effects are overridden by the gluino effects provided $\tan\beta$ is

sufficiently large, to be concrete for $\tan \beta = 30$. Beyond this value, the strenght of the supersymmetric loops becomes rapidly overwhelming; e.g. at the representative value $\tan \beta = m_t = m_b = 35$ we find $\delta_{MSSM} \approx +27\%$; and at $\tan \beta = 50$, which is the preferred value claimed by SO (10) Yukawa coupling unification models [11], the correction is already $\delta_{MSSM} \approx +55\%$. Quite in contrast, at that $\tan \beta$ one would expect, in the absence of SUSY effects, a (QCD) correction of about -57% , i.e. virtually of the same size but opposite in sign!.

Coming back to Fig.8, we see that, after including the SUSY effects, the partial width of $t \rightarrow H^+ b$ equals the partial width of the standard decay $t \rightarrow W^+ b$ near the "SO (10)" point $\tan \beta = 50$. (The meeting point is actually a bit earlier in $\tan \beta$, after taking into account the known [17, 18], negative, SUSY corrections to $t \rightarrow W^+ b$, but this effect is not shown in the figure since it is relatively small.) Now, for the typical set of parameter values introduced in Fig.8, the top quark decay width into SUSY particles, eq.(80), is rather tiny. Thus it is not surprising that in these conditions the branching ratio of the charged Higgs mode can be remarkably high: $BR(t \rightarrow H^+ b) \approx 50\%$, i.e. basically $50\% \rightarrow 50\%$ versus the standard decay mode. In contrast, the branching ratio without SUSY effects (i.e. essentially the QCD-corrected branching ratio) is much smaller: at the characteristic SO (10) value, $\tan \beta = 50$, it barely reaches 20% . Clearly, if the SUSY quantum effects are there, they could hardly be missed!.

As noted before, even though the dominant MSSM effects are, by far, the QCD and SUSY-QCD ones, they have opposite signs. Therefore, there is a crossover point of the two strongly interacting dynamics, where the conventional QCD loops are fully counterbalanced by the SUSY-QCD loops. This leads to a funny situation, namely, that at the vicinity of that point the total MSSM correction is given by just the subleading, albeit non-negligible, electroweak supersymmetric contribution: $\delta_{MSSM} \approx \delta_{SUSY EW}$. The crossover point occurs at $\tan \beta > 32 \approx m_t = m_b$, where $\delta_{SUSY EW} > 20$. For larger and larger $\tan \beta$ beyond $m_t = m_b$, the total (and positive) MSSM correction grows very fast, as we have said, since the SUSY-QCD loops largely overcompensate the standard QCD corrections. As a result, the net effect on the partial width appears to be opposite in sign to what might naively be "expected" (i.e. the QCD sign). Of course, this is not a general result since it depends on the actual values of the MSSM parameters. In the following we wish to explore the various parameter dependences and in particular we want to assess whether a favourable situation as the one just described is likely to happen in an ample portion of the MSSM parameter space. In particular, the value $\tan \beta = m_t = m_b = 35$ will be chosen in all our plots where that parameter must be fixed. We consider it as representative of the low end of the high $\tan \beta$ segment, eq.(17). Thus $\tan \beta = m_t = m_b = 35$ behaves as a sort of threshold point beyond which the MSSM quantum effects on $t \rightarrow H^+ b$ take over so

fast that they should have indelible experimental consequences on top quark physics.

As regards to the non-supersymmetric electroweak corrections, δ_{EW} , it is apparent from Fig.9a that they are very small, especially in the high $\tan\beta$ segment. Also in the very low $\tan\beta$ segment, $0.5 < \tan\beta < 1$, δ_{EW} is relatively small; and this is so not only because both δ_{Higgs} and δ_{SM} become never too large in absolute value, but also because in that region there is a cancellation between $\delta_{Higgs} < 0$ and $\delta_{SM} > 0$. As it happens, we end up with the fact that the complicated Higgs effects result in a very tiny contribution, except in the very low $\tan\beta$ end, where e.g. they can reach 15% at $\tan\beta \approx 0.5$. In this corner of the parameter space, δ_{Higgs} becomes the dominant part of δ_{MSSM} , being even larger than the QCD effects, which stay at the level of 8%, and also larger than the SUSY-QCD and SUSY-EW corrections, which remain below +4% and 1%, respectively.

We have treated in detail the very low $\tan\beta$ segment by including the one-loop renormalization of the Higgs masses [25]. This is necessary in order to avoid that the lightest CP-even Higgs mass either vanishes at $\tan\beta = 1$ or becomes lighter than the phenomenological bounds near that value. In passing, we have checked that the one-loop shift of the masses, as well as of the CP-even mixing angle, α , has little impact on the partial width of $t \rightarrow H^+ b$ in the entire range of $\tan\beta$, eq.(13). They entail at most an additional 5% negative shift of δ_{MSSM} in the very low $\tan\beta$ region¹⁰. It is precisely in this region where the Higgs effects could be expected of some relevance, and thus where the renormalization of the CP-even mixing angle could have introduced some noticeable change in the neutral Higgs couplings. Quite on the contrary, at high $\tan\beta$ the corresponding effect is found to be of order one per mil and is thus negligibly small. On the other hand, a simple inspection of Figs.8 and 9b shows that even in the very low $\tan\beta$ ballpark, where there may be some ten percent effect from the Higgs sector, the rising of the tree-level width is so fast that it becomes very hard to isolate these corrections. We conclude that, despite the rather large number of diagrams involved, the over-all yield from the Higgs sector of the MSSM on $t \rightarrow H^+ b$ is rather meagre in the whole $\tan\beta$ range (13). This fact is somewhat surprising and was not obvious a priori, due to the presence of enhanced Yukawa couplings (2) in the whole plethora of Higgs diagrams. The cancellations involved are reminiscent of the scanty SUSY Higgs effects obtained for the standard top quark decay $t \rightarrow W^+ b$ [19].

We come now to briefly discuss the standard QCD effects up to $O(\alpha_s^2)$, which involve one-loop gluon corrections and gluon bremsstrahlung [14]. As it is plain from Fig.9a, δ_{QCD} is negative-definite and very important in the high $\tan\beta$ segment. It quickly saturates

¹⁰To perform that check, we have included both the stop and sbottom contributions to the one-loop Higgs mass relations. A set of 7 independent parameters has been used to fully characterize these effects, viz. $(M_H; \mu; \tan\beta; m_{B_1}; m_{t_1}; A_B; A_t)$. We refrain from writing out the cumbersome formulae [25].

for $\tan \beta > 10$ at a large value of order 60%. Therefore, the QCD effects need to be considered in order to isolate the virtual SUSY signature [14]. The leading behaviour of the standard QCD component in the relative correction (77) can be easily assessed by considering the following asymptotic formula

$$Q_{CD} = \frac{2}{3} s \frac{\frac{8}{12} (m_b^2 \tan^2 + m_t^2 \cot^2) + 3(4 + \tan^2 \frac{M_{H^\pm}^2}{m_t^2} \cot^2) m_b^2 \ln \frac{m_t^2}{m_b^2}}{m_b^2 \tan^2 + m_t^2 \cot^2}; \quad (84)$$

which we have obtained by expanding the exact one-loop formula up to $O(m_b^2/m_t^2; M_{H^\pm}^2/m_t^2)$. Here $s = s(m_t^2)$, normalized as $s(M_Z^2) = 0.12$. The big log factor $\ln(m_t^2/m_b^2)$ originates from the running b-quark mass evaluated at the top quark scale. The correction is seen to be always negative. We point out that while we have used the exact $O(s)$ formula for the numerical evaluation, the approximate expression given above is sufficiently accurate to convey the general features to be expected both at low and at high $\tan \beta$. In particular, for $m_b \neq 0$ and $\tan \beta$ in the relevant high segment (17), the QCD correction becomes very large and saturates at the value

$$Q_{CD} = \frac{2}{3} s \frac{8}{36} + \ln \frac{m_t^2}{m_b^2} \approx 62\% \quad (\tan \beta \gg \frac{M_{H^\pm}}{m_b} \approx 6); \quad (85)$$

(The exact $O(s)$ formula gives slightly below 60%.) At low values of $\tan \beta$, the corrections are much smaller, as it follows from the approximate expression $Q_{CD} \approx (s=1)(\frac{8}{36} - 15) = 18 \approx 12\%$. We remark that for $m_b = 0$ the dependence on $\tan \beta$ totally disappears from eq.(84), so that one would never be able to suspect the large contribution (85) in the high $\tan \beta$ regime. The limit $m_b = 0$, nevertheless, has been considered for the standard QCD corrections in some places of the literature [60, 61] but, as we have seen, it is untenable unless one concentrates on values of $\tan \beta$ of order 1, in which case the relevance of our decay for SUSY is doomed to oblivion. This situation is similar to the one mentioned above concerning the SUSY-QCD corrections in the limit $m_b = 0$, which leads to an scenario totally blind to the outstanding supersymmetric quantum effects obtained for $m_b \neq 0$ at high $\tan \beta$ [15]. We stress that in spite of the respectable size of the standard QCD effects, they become fast stuck at the saturation value (85), which is independent of $\tan \beta$. On the contrary, the SUSY-QCD effects grow endlessly with $\tan \beta$ and thus rapidly overtake the standard QCD prediction.

Worth noticing is the evolution of the quantities (77) and (79) as a function of the gluino mass (Cf. Figs.10a-10b). Of course, only the SUSY-QCD component is sensitive to m_g . Although the SUSY-QCD effects have been object of a particular study in Ref.[15], we find it convenient, to ease comparison, to display the corresponding results in the very same conditions in which the electroweak supersymmetric corrections are presented. The

steep falls in Fig.10a are associated to the presence of threshold effects occurring at points satisfying $m_{\tilde{g}} + m_{\tilde{t}_1} = m_t$. An analogous situation was observed in Ref.[17, 18] for the SUSY corrections to the standard top-quark decay. Away from the threshold points, the behaviour of $\delta_{\text{SUSY-QCD}}$ is smooth and perfectly consistent with perturbation theory. In Fig.10b, where the branching ratio (79) is plotted, the steep falls at the threshold points are no longer present since they are compensated for by the simultaneous opening of the two-body supersymmetric mode $t \rightarrow \tilde{t}_1 \tilde{g}$, for $m_{\tilde{g}} < m_t - m_{\tilde{t}_1}$.

We emphasize that the relevant gluino mass region for the decay $t \rightarrow H^+ b$ is not the light gluino region, but the heavy one, the reason being that the important self-energy correction mentioned above, eq.(74), involves a gluino mass insertion. As a consequence, virtually for any set of MSSM parameters, there is a well sustained SUSY correction for any gluino mass above a certain value, in our case $m_{\tilde{g}} > 250 - 300 \text{ GeV}$. The correction raises with the gluino mass up to a long plateau before bending (very gently) into the decoupling regime (far beyond 1 TeV). The fact that the decoupling rate of the gluinos appears to be so slow has an obvious phenomenological interest.

Next we consider in detail the sensitivity of our decay on the higgsino-gaugino parameters $(\mu; M)$ characterizing the chargino-neutralino mass matrices (Cf. Appendix A). We start with the supersymmetric Higgs mixing mass, μ . As already stated above, we will largely concentrate on the $\mu < 0$ case. Together with $A_t > 0$ this yields $A_t < 0$, which is a sufficient condition [62] for the MSSM prediction on $\text{BR}(b \rightarrow s)$ to be compatible with experiment in the presence of a relatively light charged Higgs boson (as the one participating in the top decay under study). In fact, it is known that charged Higgs bosons of $O(100) \text{ GeV}$ interfere constructively with the SM amplitude and would render a μ value of $\text{BR}(b \rightarrow s)$ exceedingly high. Fortunately, this situation can be remedied in the MSSM since the alternative contribution from charginos and stops tends to cancel the Higgs contribution provided that $A_t < 0$. Furthermore, one must also require relatively light values for the masses of the lightest representatives of these particles, as well as high values of $\tan \beta$ [62]; hence one is led to a set of conditions which fit in nicely to build up a favourable scenario for the decay $t \rightarrow H^+ b$.

The evolution of the individual contributions (83), together with the total MSSM yield, as a function of $\mu < 0$, is shown in Figs.11a-11b for given values of the other parameters. We immediately gather from these figures that the SUSY-QCD correction is extremely sensitive to μ . In fact, $\delta_{\text{SUSY-QCD}}$ grows rather fast with $|\mu|$. This is already patent at the level of the leading $m_b = m_b$ effect given by eq.(74). In all figures where a definite $\mu < 0$ is to be chosen, we have taken the moderate value $\mu = -150 \text{ GeV}$. In this way, for $M = |\mu| = 150 \text{ GeV}$, we guarantee that the lightest chargino mass is above the LEP 1.5 phenomenological bound: $m_{\tilde{\chi}_1^\pm} > 65 \text{ GeV}$ [26]. Concerning the electroweak

contribution, we noted above that the component $m_b = m_b$, eq.(76), actually decreases with $\tan\beta$. However, the dependences in the full $\Delta_{\text{SUSY EW}}$ are more complicated than in $\Delta_{\text{SUSY QCD}}$ and cannot be read off eq.(76). This is evident from Fig.11a where the total $\Delta_{\text{SUSY EW}}$ is fairly insensitive to $\tan\beta$; Δ_{MSSM} , therefore, inherits its marked $\tan\beta$ -dependence basically from the $\Delta_{\text{SUSY QCD}}$ component. As for the sensitivity of the corrections on the $SU(2)_L$ -gaugino soft SUSY-breaking parameter, M_2 , Fig.12 conveys immediately that it is virtually non-existent. We point out that the choice of M_2 and $\tan\beta$ is always made in a range where the chargino masses are above 65 GeV.

There is some slight evolution of the corrections with A_b (Fig.13a), mainly on the $\Delta_{\text{SUSY QCD}}$ side. We realize that $\Delta_{\text{SUSY QCD}}$ is not perfectly symmetric with respect to the sign of A_b . Once the sign $\tan\beta < 0$ is chosen, the correction is larger for negative values of A_b than for positive values. We have erred on the conservative side by choosing $A_b = +300$ GeV wherever this parameter is fixed. As far as A_t is concerned, $\Delta_{\text{SUSY QCD}}$ can only evolve as a function of that parameter through vertex corrections, which are proportional to $A_t \cot\beta$ (Cf. Appendix A); however, at large $\tan\beta$ these are very depressed. The electroweak correction $\Delta_{\text{SUSY EW}}$, instead, is very much dependent on A_t ; indeed, a typical component exhibiting this behaviour is given by eq.(76), which is linear in A_t . The full dependence, however, is not linear and is recorded in Fig.13b. We realize that $\Delta_{\text{SUSY EW}}$ and Δ_{MSSM} change sign with A_t . The shaded vertical band in Fig.13b is excluded by our choice of parameters in Fig.8.

Another very crucial parameter to be investigated is the value of $m_{\tilde{b}_1}$. This is because the $\Delta_{\text{SUSY QCD}}$ correction hinges a great deal on the value of the sbottom masses, as it is plain from eq.(74). As a matter of fact, a too large a value of $m_{\tilde{b}_1}$ may upside down the leadership of the $\Delta_{\text{SUSY QCD}}$ effects. As a phenomenological lower bound for all the squark masses we take the absolute LEP 1.5 bound $m_{\tilde{q}} \geq 65$ GeV [26]. However, as a typical mass value for all squarks other than the stop we use $m_{\tilde{q}} = 150 - 200$ GeV (q6t). From Fig.14a we see that provided $m_{\tilde{b}_1} < 300$ GeV the $\Delta_{\text{SUSY QCD}}$ effects remain dominant, but they steadily go down the larger is $m_{\tilde{b}_1}$. The electroweak correction $\Delta_{\text{SUSY EW}}$, on the other hand, is quite sustained with increasing $m_{\tilde{b}_1}$ and there are parameter configurations where for sufficiently heavy sbottoms the supersymmetric electroweak effects are larger than the $\Delta_{\text{SUSY QCD}}$ effects. However, this is not the most likely situation. The behaviour of the branching ratio is plotted in Fig.14b.

Obviously, the evolution of the $\Delta_{\text{SUSY QCD}}$ corrections with the stop masses is basically flat (Fig.15) since the leading contribution is independent of $m_{\tilde{t}_1}$. Therefore, it is of little help to use the strict lower mass bound $m_{\tilde{t}_1} \geq 65$ GeV in our calculation instead of, say, the more conservative $m_{\tilde{t}_1} \geq 100$ GeV. Nonetheless, if we wish to keep $\Delta_{\text{MSSM}} > 0$, we cannot go too far with $m_{\tilde{t}_1}$, for the electroweak correction is also seen to decrease with $m_{\tilde{t}_1}$.

Indeed, whereas for $m_{\tilde{t}_1} = 65 - 100 \text{ GeV}$ one has $\delta_{\text{SUSY EW}} > 20\%$, for $m_{\tilde{t}_1} > 250 \text{ GeV}$ one finds $\delta_{\text{SUSY EW}} < 10\%$. For heavier stop masses, δ_{MSSM} becomes zero or slightly negative. In this situation, the imprint of SUSY lies in the fact that the total quantum effect is not as negative as predicted by standard QCD, eq.(85).

The influence from the sleptons and the other squarks is practically irrelevant as it is borne out by Figs.16a-16b. They enter the correction through oblique (universal) quantum corrections. The only exception are the τ -sleptons $\tilde{\nu}_\tau$ ("staus"), since they are involved in the process-dependent (non-oblique) contribution eq.(48), where the τ -lepton Yukawa coupling becomes enhanced at large $\tan\beta$. For this reason, $\delta_{\text{SUSY EW}}$ in Fig.16b is somewhat larger the smaller is the τ -sneutrino mass (assumed to be degenerate with the other sneutrinos). In all our calculation we have fixed the common sneutrino mass at 200 GeV .

We have also tested the variation of our results as a function of the external particle masses, namely the masses of the top quark, bottom quark and charged Higgs. As for the external fermion masses, the corrections themselves are not very sensitive (see Figs.17a and 18a). Among the SUSY corrections, the most sensitive one on m_t (respectively on m_b) is $\delta_{\text{SUSY EW}}$ (resp. $\delta_{\text{SUSY QCD}}$). The branching ratios also show some dependence (Figs.17b and 18b), especially on m_b . This effect is mainly due to the variation of the tree-level partial widths as a function of m_t and m_b . As for the charged Higgs mass, M_{H^\pm} , up to now it has been fixed at $M_{H^\pm} = 120 \text{ GeV}$. We confirm from Fig.19a that there is nothing special in the chosen value for that parameter since the sensitivity of the correction is generally low, except near the uninteresting boundary of the phase space where the branching ratio (Fig.19b) boils down to zero.

We close our study of the corrections in the $\tan\beta < 0$ case by plotting δ_{MSSM} as a function of $\tan\beta$ (see Fig.20). By definition, δ_{MSSM} is that part of δ_{MSSM} originating from the full process-dependent term δ_{MSSM} , eq.(48), which stems from our definition of $\tan\beta$ on eq.(45). This piece of information is relevant enough. In fact, it should be recalled that the quantum corrections described in the previous figures are scheme dependent. In particular, they rely on our definition of $\tan\beta$ given on eq.(45). What is not scheme dependent, of course, is the predicted value of the width and branching ratio (Figs.8 and 9b) after including all the radiative corrections. Now, from Fig.20 it is clear that the δ_{MSSM} -term is not negligible, and so there is a process-dependence in our definition of $\tan\beta$, as it was announced in Section 3. At first sight, the effects are not dramatic since they are small as compared to $\delta_{\text{SUSY QCD}}$, but since the latter is cancelled out by standard QCD we end up with being of the order (roughly half the size) of the electroweak correction $\delta_{\text{SUSY EW}}$.

The main source of process-dependent effects lies in the corrections generated by the mass counterterm, $\delta m = m$, and can be easily picked out in the electroweak-eigenstate

basis (see Fig 21) much in the same way as we did for the b -mass counterterm. There are, however, some differences, as can be appraised by comparing the diagrams in Figs. 7 and 21, where we see that in the latter case the effect derives from diagrams involving $\tilde{\text{stop}}$ -sleptons with gauginos or mixed gaugino-higgsinos. An explicit computation of the diagrams (a) + (b) in Fig 21 yields

$$\begin{aligned} \frac{m}{m} &= \frac{g^2}{16\pi^2} M^0 \tan \beta I(m_1; m_2; M^0) \\ &+ \frac{g^2}{16\pi^2} M \tan \beta I(\tilde{m}; m; M); \end{aligned} \quad (86)$$

where $g^0 = g_{SW} = g_W$ and $M^0; M$ (Cf. Appendix A) are the soft SUSY-breaking Majorana masses associated to the bino \tilde{B} and winos \tilde{W} , respectively, and the function $I(m_1; m_2; m_3)$ is again given by eq.(75). In the formula above we have projected, from the bino diagram in Fig 21a, only the leading piece which is proportional to $\tan \beta$. Even so, the contribution from the wino-higgsino diagram in Fig 21b is much larger. Numerical evaluation of the sum of the two contributions on eq.(86) indeed shows that it reproduces to within few percent the full numerical result (Cf. Fig 20) previously obtained in the mass-eigenstate basis, thus confirming that eq.(86) gives the leading contribution. In practice, for a typical choice of parameters as in Fig 8, this contribution is approximately cancelled out by part of the electroweak supersymmetric corrections associated to the original process $t \rightarrow H^+ b$, and one is effectively left with eq.(76) as being the main source of electroweak supersymmetric quantum effects at high $\tan \beta$.

Finally, the corrections corresponding to the case where $\tan \beta > 0$ are studied in Figs 22a and 22b. The problem with $\tan \beta > 0$ is that, then, the large SUSY-QCD corrections have the same (negative) sign as the conventional QCD effects, and as a consequence the total MSSM correction can easily blow up above 100%, the branching ratio becoming negative!. To avoid this disaster (from the point of view of perturbation theory), we enforce the SUSY-QCD correction to be smaller than in the $\tan \beta < 0$ case by assuming an "obese SUSY scenario" characterized by very large values for the sbottom mass ($m_{\tilde{b}_1} = 600 \text{ GeV}$) and the gluino mass ($m_{\tilde{g}} = 1000 \text{ GeV}$). We also choose $A_t < 0$ so that the electroweak SUSY correction becomes opposite in sign to the SUSY-QCD correction (a feature that also applies in the $\tan \beta < 0$ case, see Fig 13b) and in this way the total SUSY correction is further lessened in absolute value. Incidentally, we remark that the simultaneous sign change of both $\tan \beta$ and A_t is also necessary in order to keep $A_t < 0$; as noted above, this is required in order that the MSSM can be compatible with $BR(b \rightarrow s)$ in the presence of a relatively light charged Higgs. In Fig 23 we bring forward the effect of the new situation on the total partial width. In the present instance, the physical signature would be to measure a partial width significantly smaller than the one predicted by QCD. Clearly, the

> 0 ($A_t < 0$) scenario is not as appealing as the < 0 ($A_t < 0$) one.

In the end, from the explicit numerical analysis, we have confirmed our expectations that the SUSY-QCD contribution to $(t \rightarrow H^+ b)$ is generally dominant. This conclusion would not hold only in some (unlikely) cases, e.g. if the gluino is very light and/or the lightest bottom squark is "obese" as compared to lightest top squark, i.e. if the former is unusually much heavier than expected. Furthermore, by restricting ourselves to the case < 0 ($A_t < 0$) we confirm that at large $\tan \beta$ and for typical values of the parameters the total (standard plus supersymmetric) QCD correction largely cancels out, leaving a remainder on the SUSY-QCD side (Figs.8-9). In all circumstances the virtual Higgs effects remain comparatively very small. Around $\tan \beta = m_t/m_b \approx 35$, one is left with basically the electroweak supersymmetric correction, $\delta_{SUSY EW}$, which can be sizeable enough to be pinned down by experiment. However, as stated above, there is in general a strong remainder, $\delta_{SUSY QCD} + \delta_{QCD} > 0$, which grows very fast with $\tan \beta$ and it has the same sign as $\delta_{SUSY EW}$. In this favourable scenario, the virtual SUSY effects could be spectacular. This is true not only because in the relevant window of parameter space the SUSY quantum corrections are by themselves rather large, but also because they push into the opposite direction than the "expected" standard QCD corrections. As a result, the relative deviation between the MSSM prediction and the QCD prediction effectively "doubles" the size of the observable effect, a fact which is definitely welcome from the experimental point of view.

From all the previous discussion there is one fact standing out which can be hardly overemphasized: If the charged Higgs decay mode of the top quark, $t \rightarrow H^+ b$, does show up with a branching ratio of order 10% or above (perhaps even as big as 50%), a fairly rich event statistics will be collected at the Tevatron and especially at the LHC e.g. by making use of the identification methods described in Section 2. If, in addition, it comes out that the dynamics underlying that decay is truly supersymmetric, then the valuable quantum signatures that our calculation has unveiled over an ample portion of the MSSM parameter space should eventually become manifest and, for sure, we could not miss them.

At present all the collected event statistics basically relies on our experimental ability to recognize the top quark decays originating from standard patterns (angular distribution, energy spectrum, jet topology etc.) associated to the usual Drell-Yan production mechanism. Notwithstanding, we wish to point out that it should in principle be possible to clutch at the supersymmetric virtual corrections associated to the vertex tbH also through an accurate measurement of the various inclusive top quark and Higgs boson production cross sections in hadron colliders. As an example, in Fig.24 we sketch a few alternative mechanisms which would generate top quark production patterns heavily hinging on the properties of the interaction tbH -vertex [63]. Thus, while this vertex

could be responsible in part for the decay of the top quark once it is produced, it might as well be at the root of the production process itself at LHC energies, where it could take over from Drell-Yan production [28].

We observe that in some of these mechanisms a Higgs boson is produced in association, but in some others (fusion processes) the Higgs boson enters as a virtual particle. Now, however different these production processes might be, all of them are sensitive to the effective structure of the tbH -vertex. Similar mechanisms can of course be depicted involving the neutral Higgs bosons of the MSSM interacting with tt and bb via enhanced Yukawa couplings [63]. While it goes beyond the scope of this paper to compute the SUSY corrections to the production processes themselves, we have at least faced the detailed analysis of a partial decay width which involves one of the relevant production vertices. In this way, a definite prediction is made on the properties of a physical observable and, moreover, this should suffice both to exhibit the relevance of the SUSY quantum effects and to demonstrate the necessity to incorporate these corrections in a future, truly comprehensive, analysis of the cross-sections, namely, an analysis where one would include the quantum effects on all the relevant production mechanisms within the framework of the MSSM. For this reason we think that in the future a precise measurement of the various (single and double) top quark production cross-sections [64, 65] should be able to detect or to exclude the tbH -vertex as well as the vertices qqA^0 ($h^0; H^0$) involving the neutral Higgs particles of the MSSM and the third generation quarks $q = t; b$.

We conclude our discussion with the following remark. Whereas, on the one hand, one expects that some top quark partial widths will be determined with an accuracy of 10% at the upgraded Tevatron and perhaps better than 10% at LHC [28], on the other hand we believe that from the point of view of an inclusive model-independent measurement of the total top-quark width, Γ_t , the future e^+e^- supercollider should be a better suited machine [66, 67]. For, in an inclusive measurement, all possible non-SM effects will appear on top of the corresponding SM effects already computed in the literature [57]. Moreover, as shown in Ref. [66], one hopes to be able to measure the total top-quark width in e^+e^- supercolliders at an unmatched precision of $\sim 4\%$ on the basis of a detailed analysis of the threshold effects in the cross-section, in particular of the top momentum distribution and the resonance contributions to the forward-backward asymmetry in the tt threshold region. Under the assumption that $\Gamma_H \ll \Gamma_W$, and that the SUSY effects on Γ_t are purely virtual effects, it follows that a large SUSY correction of, say 50%, to $t \rightarrow H^+ b$ translates into a 20% correction to Γ_t . This effect could not escape detection. Thus, the combined information from a future e^+e^- supercollider and from present and medium term hadron machines can be extremely useful to pin down the nature of the observed effects. Our general conclusion is, therefore, extremely encouraging: In view of the potentially large

size and large variety of manifestations, quantum effects on top quark and Higgs boson physics could be the clue to the discovery of "virtual" Supersymmetry.

Acknowledgements:

One of us (JS) is thankful to W. Hollik for useful conversations on the renormalization framework used in our work and its relation to other schemes based on alternative definitions of $\tan\beta$. He is also very grateful to M. Carena and C. Wagner for pointing out interesting connections of our work with SUSY GUT's and for enjoyable discussions. Thanks are extended to G.L. Kane and H. Baer for remarks on SUSY phenomenology at the Tevatron, and to F. Matarras and D.P. Roy for helpful information on physics at the LHC. Private talks on the experimental aspects of present and future top quark physics at the Tevatron and at the LHC with A. Heinson, S. Willenbrock and with the experimental colleagues in our Institute, especially with M. Bosman, M. Cavalli-Sforza and M. Martinez, are gratefully acknowledged. Finally, JS wishes to thank the hospitality and financial support provided by the CERN Theory Division where this work was finished. This work has also been partially supported by CICYT under project No. AEN 93-0474. The work of DG and JG has been financed by grants of the Comissió Interdepartamental de Recerca i Innovació Tecnològica, Generalitat de Catalunya.

Appendix A. Interaction Lagrangian of the MSSM in the mass-eigenstate basis

In this appendix we single out specific pieces of the MSSM Interaction Lagrangian involved in the decay rate of the process $t \rightarrow H^+ b$. Although the Lagrangian of the MSSM is well-known [8], it is always useful to project explicitly the relevant pieces and to cast them in a most suitable form for specific purposes. As a matter of fact, we have produced a complete set of Feynman rules for the MSSM using an algebraic computer code based on MATHEMATICA [68]¹¹. Here we limit ourselves to quote the Lagrangian interactions affecting the process-dependent parts of our decay and omit the interaction pieces needed to compute the universal counterterm structures, whose SM parts are well-known [40] and the corresponding SUSY contributions are also available in the literature since long time ago [46]. All our interactions are expressed in the mass-eigenstate basis.

Within the context of the MSSM we need two Higgs superfield doublets

$$\hat{H}_1 = \begin{pmatrix} \hat{H}_1^0 \\ \hat{H}_1^- \end{pmatrix}; \quad \hat{H}_2 = \begin{pmatrix} \hat{H}_2^+ \\ \hat{H}_2^0 \end{pmatrix}; \quad (\text{A.1})$$

¹¹We have corrected several mistakes in the subset of rules presented in Ref.[24] involving particles and Higgses.

with weak hypercharges $Y_{1,2} = -1$. The (neutral components of the) corresponding scalar Higgs doublets give mass to the down (up)-like quarks through the VEV $\langle H_1^0 \rangle = v_1$ ($\langle H_2^0 \rangle = v_2$). This is seen from the structure of the MSSM superpotential [8]

$$\hat{W} = \sum_{ij} h_b \hat{H}_1^i \hat{Q}^j \hat{D} + h_t \hat{H}_2^j \hat{Q}^i \hat{U} - \hat{H}_1^i \hat{H}_2^j; \quad (A.2)$$

where we have singled out only the Yukawa couplings of the third quark-squark generation, $(t; b) \rightarrow (\tilde{t}; \tilde{b})$, as a general fermion-sfermion generation of chiral matter superfields \hat{Q} , \hat{U} and \hat{D} . Their respective scalar (squark) components are:

$$\hat{Q} = \begin{pmatrix} \tilde{t}_L^0 \\ \tilde{b}_L^0 \end{pmatrix}; \quad \hat{U} = \tilde{t}_R^0; \quad \hat{D} = \tilde{b}_R^0; \quad (A.3)$$

with weak hypercharges $Y_Q = +1/3$, $Y_U = 4/3$ and $Y_D = +2/3$. The primes in (A.3) denote the fact that $\tilde{q}_a^0 = f \tilde{q}_L^0; \tilde{q}_R^0$ are weak-eigenstates, not mass-eigenstates. The ratio

$$\tan \beta = \frac{v_2}{v_1}; \quad (A.4)$$

is a most relevant parameter throughout our analysis.

We briefly describe the necessary SUSY formalism entering our computations:

The fermionic partners of the weak-eigenstate gauge bosons and Higgs bosons, called gauginos, \tilde{B} , \tilde{W} , and higgsinos, \tilde{H} , respectively. From them we construct the fermionic mass-eigenstates, the so-called charginos and neutralinos, by, first, forming the following three sets of two-component Weyl spinors:

$$\begin{pmatrix} \chi_i^+ \\ \psi_i^- \end{pmatrix} = f \begin{pmatrix} \tilde{W}^+ \\ \tilde{H}_2^+ \end{pmatrix} g; \quad \begin{pmatrix} \chi_i^- \\ \psi_i^+ \end{pmatrix} = f \begin{pmatrix} \tilde{W}^- \\ \tilde{H}_1^- \end{pmatrix} g; \quad (A.5)$$

$$\begin{pmatrix} \tilde{\chi}^0 \\ \tilde{\psi}^0 \end{pmatrix} = f \begin{pmatrix} \tilde{B}^0 \\ \tilde{W}_3^0 \end{pmatrix} g; \quad \begin{pmatrix} \tilde{\chi}^0 \\ \tilde{\psi}^0 \end{pmatrix} = f \begin{pmatrix} \tilde{H}_2^0 \\ \tilde{H}_1^0 \end{pmatrix} g; \quad (A.6)$$

which get mixed up when the neutral Higgs fields acquire nonvanishing VEV's and then diagonalizing the resulting "mass Lagrangian

$$\begin{aligned} L_M = & \begin{pmatrix} \chi^+ & \psi^- \end{pmatrix} \begin{pmatrix} M & 0 \\ 0 & M^0 \end{pmatrix} \begin{pmatrix} \chi^- \\ \psi^+ \end{pmatrix} \\ & + \begin{pmatrix} \chi^+ & \psi^- \end{pmatrix} \begin{pmatrix} M_Z s_W & M_Z c_W \\ M_Z c_W & 0 \end{pmatrix} \begin{pmatrix} \chi^- \\ \psi^+ \end{pmatrix} \\ & + \begin{pmatrix} \chi^+ & \psi^- \end{pmatrix} \begin{pmatrix} M_Z s_W & M_Z c_W \\ M_Z c_W & 0 \end{pmatrix} \begin{pmatrix} \chi^- \\ \psi^+ \end{pmatrix} \\ & + \text{h.c.}; \end{aligned} \quad (A.7)$$

where we remark the presence of the parameter introduced above and of the soft SUSY-breaking Majorana masses M and M^0 , usually related as $M^0 = M =$

$(5=3) \tan^2 \theta_w$, and where $c = \cos$ and $s = \sin$. The corresponding mass-eigenstates¹² (charginos and neutralinos) are the following:

$$\chi_i^+ = \begin{pmatrix} U_{ij} & V_{ij} \\ V_{ij} & U_{ij} \end{pmatrix} \begin{pmatrix} j^+ \\ j \end{pmatrix}; \quad \chi_i^0 = C \begin{pmatrix} V_{ij} & U_{ij} \\ U_{ij} & V_{ij} \end{pmatrix}^T \begin{pmatrix} j^+ \\ j \end{pmatrix}; \quad (\text{A.8})$$

and

$$\chi_0^0 = \begin{pmatrix} N & 0 \\ N & 0 \end{pmatrix} = C \begin{pmatrix} 0 & 0 \\ 0 & 0 \end{pmatrix}^T; \quad (\text{A.9})$$

where the matrices $U; V; N$ are defined through

$$U^T M V = \text{diag}(M_1; M_2)g; \quad N^T M^0 N = \text{diag}(M_1^0; \dots; M_4^0)g; \quad (\text{A.10})$$

In practice, we have performed the calculation with real matrices U, V and N , so we have been using unphysical mass-eigenstates (associated to non-positively definite chargino-neutralino masses). The transition from our unphysical mass-eigenstate basis $f g = f_i; {}^0g$ into the physical mass-eigenstate basis $f g = f_i; {}^0g$ can be done by introducing a set of parameters as follows: for every chargino-neutralino whose mass matrix eigenvalue is $M_i; M_i^0$ the proper physical state, χ_i , is given by

$$\chi_i = \begin{cases} \chi_i^+ & \text{if } M_i = 1 \\ \chi_i^0 & \text{if } M_i = 1; \end{cases} \quad (\text{A.11})$$

and the physical masses for charginos and neutralinos are $m_{\chi_i} = M_i$ and $m_{\chi_0} = M_0$, respectively. Needless to say, in this real formalism one is supposed to propagate the parameters accordingly in all the relevant couplings, as shown in detail in Ref. [23]. This procedure is entirely equivalent [69] to use complex diagonalization matrices insuring that physical states are characterized by a set of positive-definite mass eigenvalues; and for this reason we have maintained the complex notation in all our formulae in Section 4. Whereas for computations with real sparticles the distinction matters [23], for virtual sparticles the parameters cancel out, and so one could use either basis $f g$ or $f g$ without the inclusion of the coefficients. We have stressed here the differences between the two bases just to make clear what are the physical chargino-neutralino states, when they are referred to in the text.

Among the gauginos we also have the strongly interacting gluinos, \tilde{g}^r ($r = 1; \dots; 8$), which are the fermionic partners of the gluons.

As for the scalar partners of quarks and leptons, they are called squarks, \tilde{q} , and sleptons, \tilde{l} , respectively. Again we will use the third quark-squark generation ($t; b$) ($\tilde{t}; \tilde{b}$) as a generical fermion-sfermion generation. The squark mass-eigenstates,

¹²We use the following notation: first Latin indices $a, b, \dots = 1, 2$ are reserved for sfermions, middle Latin indices $i, j, \dots = 1, 2$ for charginos, and first Greek indices $\alpha; \beta; \dots = 1; \dots; 4$ for neutralinos.

$\tilde{q}_a = f\tilde{q}_1; g\tilde{q}_2$, if we neglect intergenerational mixing, are obtained from the weak-eigenstate ones $\tilde{q}_a^0 = f\tilde{q}_1^0; g\tilde{q}_2^0$, through

$$\begin{aligned}\tilde{q}_a^0 &= \sum_b R_{ab}^{(q)} \tilde{q}_b; \\ R^{(q)} &= \begin{pmatrix} \cos q & \sin q \\ \sin q & \cos q \end{pmatrix} \quad (q = t; b); \end{aligned} \quad (\text{A.12})$$

The rotation matrices in (A.12) diagonalize the corresponding stop and sbottom mass matrices:

$$M_q^2 = \begin{pmatrix} M_{\tilde{q}_L}^2 + m_q^2 + \cos 2q (T_3^{\tilde{q}_L} - Q_q S_W^2) M_Z^2 & m_q M_{LR}^q \\ m_q M_{LR}^q & M_{\tilde{q}_R}^2 + m_q^2 + \cos 2q (T_3^{\tilde{q}_R} - Q_q S_W^2) M_Z^2 \end{pmatrix}; \quad (\text{A.13})$$

$$R^{(q)Y} M_q^2 R^{(q)} = \text{diag} \{ m_{\tilde{q}_2}^2, m_{\tilde{q}_1}^2 \} \quad (m_{\tilde{q}_2} > m_{\tilde{q}_1}); \quad (\text{A.14})$$

with $T_3^{\tilde{q}_L}$ the third component of weak isospin, Q the electric charge, and $M_{\tilde{q}_{L,R}}$ the soft SUSY-breaking squark masses [8]. (By $SU(2)_L$ -gauge invariance, we must have $M_{\tilde{t}_L} = M_{\tilde{b}_L}$, whereas $M_{\tilde{t}_R}, M_{\tilde{b}_R}$ are in general independent parameters.) The mixing angle on eq.(A.12) is given by

$$\tan 2q = \frac{2m_q M_{LR}^q}{M_{\tilde{q}_L}^2 - M_{\tilde{q}_R}^2 + \cos 2q (T_3^{\tilde{q}_L} - 2Q_q S_W^2) M_Z^2}; \quad (\text{A.15})$$

where

$$M_{LR}^t = A_t \cot \beta; \quad M_{LR}^b = A_b \tan \beta; \quad (\text{A.16})$$

are, respectively, the stop and sbottom off-diagonal mixing terms on eq.(A.13). Furthermore, μ is the SUSY Higgs mass parameter in the superpotential, and $A_{t;b}$ are the trilinear soft SUSY-breaking parameters. We shall assume that $|\tilde{A}_{t;b}| < 3M_{\tilde{g}}$, where $M_{\tilde{g}}$ is the average soft SUSY-breaking mass appearing in the mass matrix (A.13); this relation roughly corresponds to the necessary, though not sufficient, condition for the absence of colour-breaking minima [70].

The charged slepton mass-eigenstates can be obtained in a similar way after straightforward substitutions in the mass matrices, with the only proviso that there is no $\tilde{\nu}_R$, so that $\tilde{\nu}_L$ is itself the sneutrino mass-eigenstate, hence $R_{ab}^{(\tilde{\nu})} = 0$ unless $a = b = 1$ where $R_{11}^{(\tilde{\nu})} = 1$.

Next let us describe the relevant pieces of the MSSM interaction Lagrangian involving the fields defined above.

fermion { sfermion { (chargino or neutralino)

After translating the allowed quark-squark-higgsino/gaugino interactions into the mass-eigenstate basis, one finds

$$\begin{aligned}
L_{\text{qq}} = & g \sum_{a=1,2} \sum_{i=1,2} \bar{\tau}_a^{(t)} [A_{+ai}^{(t)} P_L + A_{ai}^{(t)} P_R] b + \bar{\tau}_a^{(b)} [A_{+ai}^{(b)} P_L + A_{ai}^{(b)} P_R] t \\
& + \frac{g}{2} \sum_{a=1,2} \sum_{i=1,2} \bar{\tau}_a^{(0)} [A_{+a}^{(t)} P_L + A_a^{(t)} P_R] t + \bar{\tau}_a^{(0)} [A_{+a}^{(b)} P_L + A_a^{(b)} P_R] b \\
& + \text{h.c.}
\end{aligned} \tag{A.17}$$

where $A_{ai}^{(t)}$; $A_{ai}^{(b)}$; $A_a^{(t)}$; $A_a^{(b)}$ are

$$\begin{aligned}
A_{+ai}^{(t)} &= R_{1a}^{(t)} U_{i1} - t R_{2a}^{(t)} U_{i2}; \\
A_{ai}^{(t)} &= b R_{1a}^{(t)} V_{i2}; \\
A_{+a}^{(t)} &= R_{1a}^{(t)} (N_2 + Y_L \tan_w N_1) + \frac{p}{2} \bar{t} R_{2a}^{(t)} N_3; \\
A_a^{(t)} &= \frac{p}{2} \bar{t} R_{1a}^{(t)} N_3 - Y_R^t \tan_w R_{2a}^{(t)} N_1; \\
A_{+ai}^{(b)} &= R_{1a}^{(b)} V_{i1} - b R_{2a}^{(b)} V_{i2}; \\
A_{ai}^{(b)} &= t R_{1a}^{(b)} U_{i2}; \\
A_{+a}^{(b)} &= R_{1a}^{(b)} (N_2 - Y_L \tan_w N_1) + \frac{p}{2} \bar{b} R_{2a}^{(b)} N_4; \\
A_a^{(b)} &= \frac{p}{2} \bar{b} R_{1a}^{(b)} N_4 + Y_R^b \tan_w R_{2a}^{(b)} N_1;
\end{aligned} \tag{A.18}$$

with Y_L and $Y_R^{t,b}$ the weak hypercharges of the left-handed $SU(2)_L$ doublet and right-handed singlet fermion, and t and b are {C.f. eq.(2)} the potentially significant Yukawa couplings normalized to the $SU(2)_L$ gauge coupling constant g .

quark {squark {gluino

$$L_{\text{gqq}} = \frac{g_s}{2} \bar{q}_{a,k} g_r^{(r)} R_{1a}^{(q)} P_L - R_{2a}^{(q)} P_R q_k + \text{h.c.} \tag{A.19}$$

where $^{(r)}$ are the Gell-Mann matrices. This is just the SUSY-QCD Lagrangian written in the squark mass-eigenstate basis.

squark {squark {Higgs

$$L_{H\text{qq}} = \frac{g}{2M_W} H \bar{\tau}_a G_{ab} \tau_b + \text{h.c.} \tag{A.20}$$

where we have introduced the coupling matrix

$$\begin{aligned}
G_{ab} &= R_{cb}^{(t)} R_{da}^{(b)} g_{cd} \\
g_{cd} &= \frac{m_b^2 \tan_w + m_t^2 \cot_w}{m_t (1 + A_t \cot_w)} \frac{M_W^2 \sin 2}{m_t m_b (\tan_w + \cot_w)} : \tag{A.21}
\end{aligned}$$

chargino {neutralino {charged Higgs

$$L_{H\text{}} = g H^0 \cos Q^L_i P_L + \sin Q^R_i P_R + \text{h.c.} \tag{A.22}$$

with

$$\begin{aligned}
Q^L_i &= U_{i1} N_3 + \frac{1}{2} (N_2 + \tan_w N_1) U_{i2} \\
Q^R_i &= V_{i1} N_4 - \frac{1}{2} (N_2 + \tan_w N_1) V_{i2};
\end{aligned} \tag{A.23}$$

Gauge interactions

In our calculation we only need the particle interactions with the W^\pm quarks

$$L_{W \text{ qq}} = \frac{g}{2} \bar{q} \gamma^\mu T^a q W^\mu_\pm + \text{h.c.} \quad (\text{A } 24)$$

squarks

$$L_{W \text{ qq}} = \frac{g}{2} \bar{q} \gamma^\mu T^a q W^\mu_\pm + \text{h.c.} \quad (\text{A } 25)$$

charginos and neutralinos

$$L_{W \text{ ch}} = g \bar{\chi}^0 \gamma^\mu C^L_i P_L + C^R_i P_R \chi^\pm W^\mu_\pm + \text{h.c.} \quad (\text{A } 26)$$

$$\begin{aligned} C^L_i &= \frac{1}{2} N_{3i2} - N_{2i1} \\ C^R_i &= \frac{1}{2} N_{4i2} - N_{2i1} \end{aligned} \quad (\text{A } 27)$$

Appendix B . The Counterterm Z_{HW}

We discuss the structure of Z_{HW} both in the unitary gauge and in the Feynman gauge. In order to renormalize the mixed self-energy $\Pi_{HW}(k^2)$, a mixing counterterm must be introduced in the wave function of W :

$$W^\mu = Z_W^{1/2} W^\mu + \frac{Z_{HW}}{M_W} \partial^\mu H \quad (\text{B } 1)$$

B.1 Unitary gauge

If one chooses to work in the unitary gauge, then the renormalization is straightforward:

$$L_{UG} = \frac{1}{4} F^\mu F_\mu + M_W^2 W^\mu W_\mu + L_{ct} = i M_W Z_{HW} (W^\mu \partial_\mu H^\dagger - W^\mu \partial_\mu H) : \quad (\text{B } 2)$$

In this gauge the corresponding renormalized 2-point Green function reads (Fig 25a):

$$\frac{i}{k^2 - M_H^2} k^\mu \frac{i \Pi_{HW}(k^2)}{M_W} + i k^\mu M_W^2 \frac{Z_{HW}}{M_W} \frac{i g}{k^2 - M_W^2} : \quad (\text{B } 3)$$

Thus, a renormalized self-energy can be defined as follows:

$$\hat{\Pi}_{HW}(k^2) = \Pi_{HW}(k^2) - M_W^2 Z_{HW} \quad (\text{B } 4)$$

Now we must impose a renormalization condition on $\hat{\Pi}_{HW}(k^2)$; and we choose it in a way that the physical Higgs does not mix with the physical W :

$$\hat{\Pi}_{HW}(M_H^2) = 0 \Rightarrow Z_{HW} = \frac{\Pi_{HW}(M_H^2)}{M_W^2} : \quad (\text{B } 5)$$

B.2 Feynman gauge

As we carry out our calculation in the Feynman gauge, we would also like to perform the renormalization of the Higgs sector in that gauge. The Lagrangian is sketched as follows [40]:

$$\mathcal{L} = \mathcal{L}_C + \mathcal{L}_{GF} + \mathcal{L}_{FP} : \quad (\text{B.6})$$

where \mathcal{L}_{GF} stands for the gauge-fixing term in that gauge,

$$\mathcal{L}_{GF} = F^\dagger F + \dots \quad (F = \partial W^\pm - iM_W G^\pm) \quad (\text{B.7})$$

and $\mathcal{L}_{FP} = \partial^\mu \bar{F}^a \partial_\mu F^a$ is the Faddeev-Popov ghost Lagrangian constructed from FP and anti-FP Grassmann scalar fields. Since we are interested in the charged gauge-Higgs ($W^\pm H$) and charged Goldstone-Higgs ($G^\pm H$) mixing terms in that gauge, we have singled out just the relevant term on eq.(B.7).

The relationship with the original weak-eigenstate components on eq.(A1) is the following:

$$\begin{pmatrix} H_1^+ \\ H_2^+ \end{pmatrix} = \begin{pmatrix} c & s \\ s & c \end{pmatrix} \begin{pmatrix} G^+ \\ H^+ \end{pmatrix} : \quad (\text{B.8})$$

As is well-known, although the classical Lagrangian, \mathcal{L}_C , also contains a nonvanishing mixing among the weak gauge boson fields, W^\pm , and the Goldstone boson fields, G^\pm , namely

$$\mathcal{L}_{GW} = iM_W W^\pm \partial G^\pm + \text{h.c.}; \quad (\text{B.9})$$

the latter is cancelled (in the action) by a piece contained in \mathcal{L}_{GF} . Now, after substituting the renormalization transformation for the Higgs doublets, eq.(23), on the Higgs boson kinetic term with $SU(2)_L \times U(1)_Y$ gauge covariant derivative, one easily projects out the following relevant counterterms

$$\begin{aligned} \mathcal{L} = & Z_H \partial^\mu H^\dagger \partial_\mu H + Z_G \partial^\mu G^\dagger \partial_\mu G \\ & + Z_{HG} \partial^\mu H^\dagger \partial_\mu G^\dagger + \text{h.c.} + Z_{HW} iM_W W^\pm \partial H^\pm + \text{h.c.} + \dots \end{aligned} \quad (\text{B.10})$$

where

$$\frac{Z_H}{Z_G} = \frac{c^2 - s^2}{s^2 - c^2} \frac{Z_{H_1}}{Z_{H_2}}; \quad (\text{B.11})$$

and

$$\begin{aligned} Z_{HG} &= s c \left(\frac{Z_{H_2}}{Z_{H_1}} \right); \\ Z_{HW} &= s c \left[\frac{1}{2} \left(\frac{Z_{H_2}}{Z_{H_1}} \right) + \frac{\tan \beta}{\tan \beta} \right]; \end{aligned} \quad (\text{B.12})$$

The renormalization transformation for the VEV's of the Higgs potential (4),

$$v_i \neq Z_{H_i}^{1/2} (v_i + \bar{v}_i) = 1 + \frac{\bar{v}_i}{v_i} + \frac{1}{2} Z_{H_i} \bar{v}_i; \quad (\text{B.13})$$

implies that the counterterm to $\tan \beta$ is related to the fundamental counterterms in the Higgs potential by

$$\frac{\tan \beta}{\tan \beta} = \frac{v_2}{v_2} = \frac{v_1}{v_1} + \frac{1}{2} (Z_{H_2} - Z_{H_1}) : \quad (\text{B.14})$$

If one imposes the usual on-shell renormalization conditions for the A^0 -boson, one has

$$Z_{H_2} - Z_{H_1} = \frac{\tan \beta + \cot \beta}{M_Z^2} \text{A Z} (M_{A^0}^2) : \quad (\text{B.15})$$

In addition, there is another mixing term between H and G originating from the mass matrix of the Higgs sector [43]. This one loop mixture is contained in:

$$V^b = H^+ G^+ \left[M_H^{b2} \frac{t_0^b}{2v^b} A + \frac{t_1^b}{2v^b} \right] G^b ; \quad (\text{B.16})$$

where we have attached a superscript b to bare quantities, and t_i are the tadpole counterterms

$$\begin{aligned} t_0 &= \sin(\beta) t_0^+ + \cos(\beta) t_0^- \\ t_1 &= \sin(\beta) t_1^+ + \cos(\beta) t_1^- : \end{aligned} \quad (\text{B.17})$$

We are now ready to find an expression for the mixed 2-point Green functions (Figs 25a and 25b). As the mixing Lagrangian between H and W on eq. (B.2) is the same as on eq. (B.10), the 2-point Green function will have the same expression (B.3) but with the W propagator in the Feynman gauge, namely:

$$\begin{aligned} & \frac{i}{k^2 - M_H^2} k^\mu \frac{i_{HW}(k^2)}{M_W} + ik^\mu M_W^2 \frac{Z_{HW}}{M_W} \frac{ig}{k^2 - M_W^2} \\ &= \frac{i}{k^2 - M_H^2} k^\mu \frac{\hat{1}_{HW}(k^2)}{M_W} \frac{i}{k^2 - M_W^2} : \end{aligned} \quad (\text{B.18})$$

Next we impose $\hat{1}_{HW}(M_{H^0}^2) = 0$ as before, leading to the same formal expression for Z_{HW} as in eq.(B.5). However, as a new ingredient, we now have the mixed $H-G$ self-energy:

$$\frac{i}{k^2 - M_H^2} i_{HG}(k^2) + ik^2 Z_{HG} \frac{t_0^b}{2v^b} \frac{i}{k^2 - M_W^2} : \quad (\text{B.19})$$

This allows us to define renormalized self-energies, (B.4) and

$$\hat{1}_{HG}(k^2) = i_{HG}(k^2) - k^2 Z_{HG} + \frac{t_0^b}{2v^b} : \quad (\text{B.20})$$

The mixed self-energies $\hat{1}_{HW}(k^2)$ and $\hat{1}_{HG}(k^2)$ obey the following Slavnov-Taylor identity:

$$k^2 \hat{1}_{HW}(k^2) - M_W^2 \hat{1}_{HG}(k^2) = 0 : \quad (\text{B.21})$$

This identity is derived from a BRS transformation involving the Green function constructed with an anti-FP field and the charged Higgs field: $\langle 0 | j_{\text{BRS}} (\phi^\dagger H^\dagger) \phi \rangle = 0$. Following the standard procedure [71] one immediately gets:

$$\langle 0 | \phi^\dagger H^\dagger \phi \rangle = \langle 0 | \phi^\dagger W^\dagger + H^\dagger (-M_W G^\dagger H^\dagger) \phi \rangle = 0; \quad (\text{B } 22)$$

which in momentum space reads

$$k^\mu H_W^\mu + M_W H_G = 0 \quad (\text{B } 23)$$

with

$$H_G = \frac{i}{k^2 - M_H^2} h \quad i \hat{H}_G(k^2) \frac{i}{k^2 - M_W^2} : \quad (\text{B } 24)$$

Clearly, eq.(B 23) implies eq.(B 21). The latter identity guarantees that the contribution to our decay $\Gamma(H^\pm \rightarrow b)$ from the two diagrams in Figs. 25a and 25b vanishes since no mixing is generated among the physical boson H and the renormalized fields G and W : $\hat{H}_G(M_H^2) = \hat{H}_W(M_H^2) = 0$. There is of course another Slavnov-Taylor identity, derived in a similar manner, which insures that the renormalized mixing between G and W also vanishes. Thus we have proven that the expression for Z_{HW} is formally the same in both unitary and Feynman gauges, but that in the latter gauge one must take into account the additional renormalization of the mixed selfenergy Π_{HG} .

Appendix C . Vertex functions

In this appendix we briefly collect, for notational convenience, the basic vertex functions frequently referred to in the text. Dimensional regularization is used throughout. The given formulas are exact for arbitrary internal masses and external on-shell momenta. Most of them are an adaptation to the $\epsilon = 4 - n$ metric of the standard formulae of ref.[72]. The basic one, two and three-point scalar functions are:

$$A_0(m) = \int^Z d^n q \frac{1}{[q^2 - m^2]}; \quad (\text{C } 1)$$

$$B_0(p; m_1; m_2) = \int^Z d^n q \frac{1}{[q^2 - m_1^2][(q+p)^2 - m_2^2]}; \quad (\text{C } 2)$$

$$C_0(p; k; m_1; m_2; m_3) = \int^Z d^n q \frac{1}{[q^2 - m_1^2][(q+p)^2 - m_2^2][(q+p+k)^2 - m_3^2]}; \quad (\text{C } 3)$$

using the integration measure

$$d^n q = \frac{(4 - n)}{(2\pi)^n} d^n q : \quad (\text{C } 4)$$

The two and three-point tensor functions needed for our calculation are the following

$$B_{\mu\nu}; B_{\mu\nu\lambda}(p; m_1; m_2) = \int^Z d^n q \frac{[q_\mu q_\nu q_\lambda]}{[q^2 - m_1^2][(q+p)^2 - m_2^2]}; \quad (\text{C } 5)$$

$$\mathbb{C}_0; \mathbb{C}_1; \mathbb{C}_2](p; k; m_1; m_2; m_3) = \int \frac{d^n q}{(2\pi)^n} \frac{[q^2; q; q; q]}{[q^2 - m_1^2][(q+p)^2 - m_2^2][(q+p+k)^2 - m_3^2]} : \quad (\text{C.6})$$

By Lorentz covariance, they can be decomposed in terms of the above basic scalar functions and the external momenta:

$$\begin{aligned} B(p; m_1; m_2) &= p B_1(p; m_1; m_2); \\ B(p; m_1; m_2) &= p p B_{21}(p; m_1; m_2) + g B_{22}(p; m_1; m_2); \\ \mathbb{C}_0(p; k; m_1; m_2; m_3) &= B_0(k; m_2; m_3) + m_1^2 C_0(p; k; m_1; m_2; m_3); \\ \mathbb{C}(p; k; m_1; m_2; m_3) &= p p C_{21} + k k C_{22} + (p k + k p) C_{23} + g C_{24}; \quad (\text{C.7}) \end{aligned}$$

where we have defined the Lorentz invariant functions:

$$B_1(p; m_1; m_2) = \frac{1}{2p^2} [A_0(m_1) - A_0(m_2) - f_1 B_0(p; m_1; m_2)]; \quad (\text{C.8})$$

$$\begin{aligned} B_{21}(p; m_1; m_2) &= \frac{1}{2p^2(n-1)} [(n-2)A_0(m_2) - 2m_1^2 B_0(p; m_1; m_2) \\ &\quad - n f_1 B_1(p; m_1; m_2)]; \quad (\text{C.9}) \end{aligned}$$

$$B_{22}(p; m_1; m_2) = \frac{1}{2(n-1)} [A_0(m_2) + 2m_1^2 B_0(p; m_1; m_2) + f_1 B_1(p; m_1; m_2)]; \quad (\text{C.10})$$

$$\begin{aligned} \begin{pmatrix} C_{11} \\ C_{12} \end{pmatrix} &= Y \begin{pmatrix} B_0(p+k; m_1; m_3) & B_0(k; m_2; m_3) \\ B_0(p; m_1; m_2) & B_0(p+k; m_1; m_3) \end{pmatrix} \begin{pmatrix} f_1 C_0 \\ f_2 C_0 \end{pmatrix}; \quad (\text{C.11}) \end{aligned}$$

$$\begin{aligned} \begin{pmatrix} C_{21} \\ C_{23} \end{pmatrix} &= Y \begin{pmatrix} B_1(p+k; m_1; m_3) + B_0(k; m_2; m_3) & f_1 C_{11} \\ B_1(p; m_1; m_2) & B_1(p+k; m_1; m_3) \end{pmatrix} \begin{pmatrix} 2C_{24} \\ f_2 C_{11} \end{pmatrix}; \quad (\text{C.12}) \end{aligned}$$

$$\begin{aligned} C_{22} &= \frac{1}{2[p^2 k^2 - (pk)^2]} [pk B_1(p+k; m_1; m_3) - B_1(k; m_2; m_3) - f_1 C_{12}] \\ &\quad + p^2 [B_1(p+k; m_1; m_3) - f_2 C_{12} - 2C_{24}]; \quad (\text{C.13}) \end{aligned}$$

$$C_{24} = \frac{1}{2(n-2)} [B_0(k; m_2; m_3) + 2m_1^2 C_0 + f_1 C_{11} + f_2 C_{12}]; \quad (\text{C.14})$$

the factors $f_{1,2}$ and the matrix Y ,

$$\begin{aligned} f_1 &= p^2 + m_1^2 - m_2^2; \\ f_2 &= k^2 + 2pk + m_2^2 - m_3^2; \\ Y &= \frac{1}{2[p^2 k^2 - (pk)^2]} \begin{pmatrix} k^2 & pk \\ pk & p^2 \end{pmatrix}; \quad (\text{C.15}) \end{aligned}$$

The UV divergences for $n \rightarrow 4$ can be parametrized as

$$\begin{aligned} &= \frac{n-4}{2} + \frac{1}{\epsilon} \ln(4); \quad (\text{C.16}) \end{aligned}$$

being γ_E the Euler constant. In the end one is left with the evaluation of the scalar one-loop functions:

$$A_0(m) = \frac{i}{16\pi^2} m^2 \left(1 + \ln \frac{m^2}{2} \right); \quad (C.17)$$

$$B_0(p; m_1, m_2) = \frac{i}{16\pi^2} + \ln \frac{p^2}{2} + \ln[(x_1 - 1)(x_2 - 1)] \\ + x_1 \ln \frac{x_1}{x_1 - 1} + x_2 \ln \frac{x_2}{x_2 - 1}; \quad (C.18)$$

$$C_0(p; k; m_1, m_2, m_3) = \frac{i}{16\pi^2} \frac{1}{2} \frac{1}{pk + p^2} \quad (C.19)$$

with

$$x_{1,2} = x_{1,2}(p; m_1, m_2) = \frac{1}{2} + \frac{m_1^2 - m_2^2}{2p^2} \pm \frac{1}{2p^2} \sqrt{p^4 - 2p^2(m_1^2 + m_2^2) + (m_1^2 - m_2^2)^2}; \quad (C.20)$$

and where \pm is a bookkeeping device for the following alternate sum of twelve (complex) Spence functions:

$$= \text{Sp} \frac{y_1}{y_1 - z} + \text{Sp} \frac{y_1}{y_1 - z} + \text{Sp} \frac{y_1}{y_1 - z} + \text{Sp} \frac{y_1}{y_1 - z} \\ + \text{Sp} \frac{y_2}{y_2 - z} + \text{Sp} \frac{y_2}{y_2 - z} + \text{Sp} \frac{y_2}{y_2 - z} + \text{Sp} \frac{y_2}{y_2 - z} \\ + \text{Sp} \frac{y_3}{y_3 - z} + \text{Sp} \frac{y_3}{y_3 - z} + \text{Sp} \frac{y_3}{y_3 - z} + \text{Sp} \frac{y_3}{y_3 - z}; \quad (C.21)$$

The Spence function is defined as

$$\text{Sp}(z) = - \int_0^z \frac{\ln(1 - tz)}{t} dt; \quad (C.22)$$

and we have set, on one hand:

$$z_{1,2}^i = x_{1,2}(p; m_2, m_1); \\ z_{1,2}^{ii} = x_{1,2}(p + k; m_3, m_1); \\ z_{1,2}^{iii} = x_{1,2}(k; m_3, m_2); \quad (C.23)$$

and on the other:

$$y_1 = y_0 + \frac{h}{2}; \quad y_2 = \frac{y_0}{1}; \quad y_3 = \frac{y_0}{2}; \quad y_0 = \frac{1}{2} \frac{g + h}{pk + p^2}; \quad (C.24)$$

where

$$g = k^2 + m_2^2 - m_3^2; \quad h = p^2 - 2pk - m_2^2 + m_1^2; \quad (C.25)$$

and k is a root (always real for external on-shell momenta) of

$$p^2 - 2pk + k^2 = 0 : \quad (C 26)$$

Derivatives of some 2-point functions are also needed in the calculation of selfenergies, and we use the following notation:

$$\frac{\partial}{\partial p^2} B(p; m_1, m_2) \equiv B^0(p; m_1, m_2) : \quad (C 27)$$

We can obtain all the derivatives from the basic B_0^0 :

$$B_0^0(p; m_1, m_2) = \frac{i}{16\pi^2} \left(\frac{1}{p^2} + \frac{1}{p^2 - m_1^2 - m_2^2} \right. \\ \left. x_1 (x_1 - 1) \ln \frac{x_1 - 1}{x_1} - x_2 (x_2 - 1) \ln \frac{x_2 - 1}{x_2} \right) ; \quad (C 28)$$

which has a threshold for $|p| = m_1 + m_2$ and a pseudo-threshold for $|p| = |m_1 - m_2|$.

References

- [1] F. Abe et al. (CDF Collab.), Phys. Rev. Lett. 74 (1995) 2626; S. Abachi et al. (D0 Collab.), Phys. Rev. Lett. 74 (1995) 2632.
- [2] P. Grannis, talk at the 28th International Conference on High Energy Physics, Warsaw, Poland, July 25-31st 1996.
- [3] D. Shale, P.M. Zerwas, Phys. Rev. D 45 (1992) 3262.
- [4] W.A. Bardeen, C.T. Hill, M. Lindner, Phys. Rev. D 41 (1990) 1647; C.T. Hill, Phys. Lett. B 266 (1991) 419; *ibid.* B 345 (1995) 483.
- [5] R.S. Chikuvula, E.H. Simmons, J. Teming, Phys. Lett. B 331 (1994) 383.
- [6] H. Georgi, Weak Interactions and Modern Particle Theory (The Benjamin/Cummings Publishing Company, 1984).
- [7] R.D. Peccei, X. Zhang, Nucl. Phys. B 337 (1990) 269; C. Hill, X. Zhang Phys. Rev. D 51 (1995) 3563.
- [8] H. Nilles, Phys. Rep. 110 (1984) 1; H. Haber, G. Kane, Phys. Rep. 117 (1985) 75; A. Lahanas, D. Nanopoulos, Phys. Rep. 145 (1987) 1; See also the exhaustive reprint collection Supersymmetry (2 vols.), ed. S. Ferrara (North Holland/World Scientific, Singapore, 1987).

- [9] P. Langacker, in: Tests and status of the Standard Model, talk given at the 4th International Workshop on Supersymmetry (SUSY 96), Univ. of Maryland, College Park, USA, May 29th-June 1st 1996; J. Ellis, G.L. Fogli, E. Lisi, Phys. Lett. B 333 (1994) 118; P. Chankowski, S. Pokorski, preprint IFT-95/6 [hep-ph/9505308];
- [10] W. de Boer, A. Dabelstein, W. Hollik, W. Mösle, U. Schwickerath, Updated global fits of the SM and the MSSM to electroweak precision data, preprint IEK-KA 96-07 [hep-ph/9609209].
- [11] M. Carena, S. Pokorski, C.E.M. Wagner, Nucl. Phys. B 426 (1994) 269; L.J. Hall, R. Rattazzi, U. Sarid, Phys. Rev. D 50 (1994) 7048; V. Barger, M.S. Berger, P. Ohm ann Phys. Rev. D 47 (1993) 1093.
- [12] I. Bigi, Y. Dokshitzer, V. Khoze, J. Kuhn, P. Zerwas, Phys. Lett. B 181 (1986) 157; V. Barger, R.J.N. Phillips, Phys. Rev. D 41 (1990) 884; A.C. Bawa, C.S. Kim, A.D. Martin Z. Phys. C 47 (1990) 95; M. Drees, D.P. Roy, Phys. Lett. B 269 (1991) 155; B.K. Bullock, K. Hagiwara, A.D. Martin, Phys. Rev. Lett. 67 (1991) 3055; W. Bernreuther et al., in Proc. of the Workshop on e^+e^- Collisions at 500 GeV: The Physics Potential, Hamburg, 1991, ed. P.M. Zerwas; preprint DESY 92{123A (1992).
- [13] Z. Kunszt, F. Zwimer, Nucl. Phys. B 385 (1992) 3; D.P. Roy, Phys. Lett. B 283 (1992) 403.
- [14] A. Czamecki, S. Davidson, Phys. Rev. D 48 (1993) 4183; D 47 (1993) 3063, and references therein.
- [15] J. Guasch, R.A. Jimenez, J. Sola, Phys. Lett. B 360 (1995) 47.
- [16] J. Sola, Supersymmetric effects on top quark and Higgs boson decay widths in the MSSM, talk given at the 4th International Workshop on Supersymmetry and Unification (SUSY 96), Univ. of Maryland, College Park, USA, May 29th-June 1st 1996; and talk given at the Cracow International Symposium on Radiative Corrections (CRAD 96), Cracow, Poland, 1-5 August 1996; and talk given at the CERN Theory Division, September 20th, 1996.
- [17] D. Garcia, W. Hollik, R.A. Jimenez, J. Sola, Nucl. Phys. B 427 (1994) 53.
- [18] A. Dabelstein, W. Hollik, R.A. Jimenez, C. Junger, J. Sola, Nucl. Phys. B 456 (1995) 75.

- [19] B.Grzadkowski, W.Hollik, Nucl.Phys.B 384 (1992) 101; A.Denner, A.H.Hoang, Nucl.Phys.B 397 (1993) 483.
- [20] D.Garcia, R.A.Jimenez, J.Sola, Phys.Lett.B 347 (1995) 321; D.Garcia, J.Sola, Phys.Lett.B 354 (1995) 335 and B 357 (1995) 349.
- [21] J.D.Wells, C.Kolda, G.L.Kane, Phys.Lett.B 338 (1994) 219; X.Wang, J.L.Lopez, D.V.Nanopoulos, Phys.Rev.D 52 (1995) 4116 and preprint CERN-TH.7553/95 [hep-ph/9501258]; A.Dabelstein, W.Hollik, W.Mosle, preprint KA-TH-EP-5-1995 [hep-ph/9506251]; P.Chankowski, S.Pokorski, preprint IFT-96/6 [hep-ph/9603310].
- [22] A.Blondel, Plenary talk at the 28th International Conference on High Energy Physics, Warsaw, Poland, July 25-31st 1996; G.Altarelli, summary talk at the Cracow International Symposium on Radiative Corrections (CRAD 96), Cracow, Poland, 1-5 August 1996.
- [23] J.Guasch, J.Sola, preprint UAB-FT-389 [hep-ph/9603441] (Z.Phys.C, in press).
- [24] J.F.Gunion, H.E.Haber, G.L.Kane, S.Dawson, The Higgs Hunters' Guide (Addison-Wesley, Menlo-Park, 1990).
- [25] J.Ellis, G.Ridol, F.Zwimer, Phys.Lett.B 262 (1991) 477; A.Brignole, J.Ellis, G.Ridol, F.Zwimer, Phys.Lett.B 271 (1991) 123; H.E.Haber, R.Hemping, Phys.Rev.Lett. 66 (1991) 1815; Phys.Rev.D 48 (1993) 4280; H.E.Haber, in: Perspectives on Higgs Physics, Advanced Series on Directions in High Energy Physics, Vol.13, ed.by G.L.Kane (World Scientific, Singapore, 1993).
- [26] J.Nachtmann and P.Rebecchi, talks given at the XXXIst Rencontres de Moriond on Electroweak Interactions and Grand Unified Theories, Les Arcs, March 1996, to appear in the Proceedings (eds.Frontieres).
- [27] G.F.Tartarelli, talk given at the XXXIst Rencontres de Moriond on Electroweak Interactions and Grand Unified Theories, Les Arcs, March 1996, to appear in the Proceedings (eds.Frontieres).
- [28] C.-P.Yuan, Top Quark Physics, preprint-M SUHEP-50228 [hep-ph/9503216].
- [29] J.Kim, J.L.Lopez, D.V.Nanopoulos, R.Rangarajan, preprint ACT-05/96 [hep-ph/9605419]; J.M.Yang, C.S.Li, [hep-ph/9603442]; W.Beenakker, R.H.Hopker, [hep-ph/9606290 and 9607345].

- [30] J. Guasch and J. Sola, unpublished; A. Djouadi, W. Hollik, C. Junger, preprint KA-TP-20-96 [hep-ph/9609419].
- [31] G.L. Kane, S. Mrenna, preprint ANL-HEP-PR-96-43 [hep-ph/9605351]; T. Kon, T. Nonaka, Phys. Rev. D 50 (1994) 6005.
- [32] F. Abe et al. (CDF Collab.), Phys. Rev. Lett. 72 (1994) 1977.
- [33] F. Matorras, private communication.
- [34] Atlas Collab., Atlas technical proposal for a general-purpose pp experiment at the Large Hadron Collider at CERN, preprint CERN/LHCC/94-43, December 1994.
- [35] J. Conway, talk given at the 4th International Workshop on Supersymmetry, Univ. of Maryland, College Park, USA, May 29th-June 1st 1996.
- [36] D.P. Roy, private communication.
- [37] S. Raychaudhuri, D.P. Roy, Phys. Rev. D 52 (1995) 1556, and Phys. Rev. D 53 (1996) 4902.
- [38] D.A. Ross, J.C. Taylor, Nucl. Phys. B 51 (1973) 25; A. Sirlin, Phys. Rev. D 22 (1980) 971; W. Marciano, A. Sirlin, Phys. Rev. D 22 (1980) 2695.
- [39] See e.g. M. Consoli, W. Hollik, G. Burgers, F. Jegerlehner, in: Z physics at LEP 1, eds. G. Altarelli, R. Kleiss, C. Verzegnassi, Yellow Report CERN 89-08 (1989).
- [40] M. Bohm, H. Spiesberger, W. Hollik, Fortschr. Phys. 34 (1986) 687; W. Hollik, Fortschr. Phys. 38 (1990) 165; W. Hollik, in: Precision Tests of the Standard Electroweak Model, Advanced Series in Directions in High Energy Physics, ed. by P. Langacker (World Scientific, Singapore, 1995).
- [41] F. Jegerlehner, Renormalizing the Standard Model, lectures given at the Theoretical Advanced Study Institute in Elementary Particle Physics, Boulder, Colorado, June 1990 (TASI 90) p. 476; A. Denner, Fortschr. Phys. 41 (1993) 307.
- [42] D. Garcia, J. Sola, Mod. Phys. Lett. A 9 (1994) 211; P.H. Chankowski, A. Dabelstein, W. Hollik, W. Mosle, S. Pokorski, J. Rosiek, Nucl. Phys. B 417 (1994) 101.
- [43] A. Yamada Z. Phys. C 61 (1994) 247; P.H. Chankowski, S. Pokorski, J. Rosiek, Nucl. Phys. B 423 (1994) 437; A. Dabelstein, Z. Phys. C 67 (1995) 495; Nucl. Phys. B 456 (1995) 25.

- [44] R.M. Barnett, J.F. Gunion, H.E. Haber, I. Hinchli e, B. Hubbard, H.J. Trost, preprint SDC-90-00141; R.M. Godbole, D.P. Roy, Phys. Rev. D 43 (1991) 3640; J.F. Gunion, L.H. Orr, Phys. Rev. D 46 (1992) 2052.
- [45] W. Hollik, private conversation; W. Hollik, talk given at the IFAE, Univ. Autonom a de Barcelona, February 1996.
- [46] J. Grifols, J. Sola, Nucl. Phys. B 253 (1985) 47; Phys. Lett. B 137 (1984) 257; For a detailed review, see: J. Sola, in: Phenomenological Aspects of Supersymmetry, ed. W. Hollik, R. Ruckl and J. Wess (Springer-Verlag, Lecture Notes in Physics 405, 1992) p. 187.
- [47] S. Bertolini, Nucl. Phys. B 272 (1986) 77.
- [48] H. Konig, Phys. Rev. D 50 (1994) 3310.
- [49] C.S. Li, J.M. Yang, B.Q. Hu, Phys. Rev. D 48 (1993) 5425.
- [50] A. Mendez, A. Pomarol, Phys. Lett. B 265 (1991) 177.
- [51] C.S. Li, B.Q. Hu, J.M. Yang, Phys. Rev. D 47 (1993) 2865.
- [52] A. Yamada, Phys. Lett. B 263 (1991) 233; A. Brignole, Phys. Lett. B 281 (1992) 284; H.E. Haber, R. Hemping, Phys. Rev. D 48 (1993) 4280; M.A. Diaz, H.E. Haber, Phys. Rev. D 45 (1992) 4246; M.A. Diaz, Phys. Rev. D 48 (1993) 2152.
- [53] Y. Yamada, preprint MADPH-96-956 [hep-ph/9608382].
- [54] M. Carena, S. Pokorski, C.E.M. Wagner Nucl. Phys. B 406 (1993) 59.
- [55] M. Carena and C. Wagner, private conversation.
- [56] LEP Electroweak Working Group, CERN preprint LEPEW WG/96-02, July 1996.
- [57] M. Jezabek, J.H. Kuhn, Nucl. Phys. B 314 (1989) 1; *ibid* B 320 (1989) 20; C.S. Li, R.J. Oakes, T.C. Yuan, Phys. Rev. D 43 (1991) 3759; G. Eilam, R.R. Mendel, R. Migneron, A. Soni, Phys. Rev. Lett. 66 (1991) 3105; A. Denner, T. Sack, Z. Phys. C 46 (1990) 653; Nucl. Phys. B 358 (1991) 46; B.A. Irwin, B. Magnolis, H.D. Trottier, Phys. Lett. B 256 (1991) 533; T.C. Yuan, C.-P. Yuan, Phys. Rev. D 44 (1991) 3603.
- [58] A. Djouadi, W. Hollik, C. Junger, preprint KA-TP-14-96 [hep-ph/9605340]; C.S. Li, R.J. Oakes, J.M. Yang, preprint NUHEP-TH-96-3 [hep-ph/9606385].

- [59] J.M. Yang, C.S. Li, Phys. Lett. B 320 (1994) 117.
- [60] C.S. Li, T.C. Yuan, Phys. Rev. D 42 (1990) 3088.
- [61] T. Mehen, preprint JHU-TIPAC-96004 [hep-ph/9602410].
- [62] R. Garisto, J.N. Ng, Phys. Lett. B 315 (1993) 372; R. Barbieri, G.F. Giudice, Phys. Lett. B 309 (1993) 86; M. Carena, C.E.M. Wagner, Nucl. Phys. B 452 (1995) 45.
- [63] R.A. Jimenez, J. Sola, preprint UAB-FT-375 [hep-ph/9511292] (Phys. Lett.B, in press); J.A. Coarasa, R.A. Jimenez, J. Sola, preprint UAB-FT-376 [hep-ph/9511402] (Phys. Lett.B, in press).
- [64] S. Willenbrock, Top Quark Physics at Fermilab, talk presented at the International Symposium on Particle Theory and Phenomenology, Iowa State University, May 1995 [hep-ph/9508212], and talk presented in the XXXIst Rencontres de Moriond on Electroweak Interactions and Grand Unified Theories, Les Arcs, March 1996, to appear in the Proceedings (eds. Frontieres); C. Quigg, preprint Fermilab-CONF-95/139-T [hep-ph/9507257].
- [65] A.P. Hinson, Electroweak Top Quark Production at the Fermilab Tevatron, Talk given at the Workshop on Physics of the Top Quark, Ames, Iowa, May 1995; A.P. Hinson, A.S. Belyaev, E.E. Boos, preprint UCR/95-17 [hep-ph/9509274].
- [66] K. Fujii, T. Matsui, Phys. Rev. 50 (1994) 4341.
- [67] R. Frey, preprint OREXP 96-04 [hep-ph/9606201].
- [68] S. Wolfram, Mathematica—A System for doing Mathematics by Computer, Addison-Wesley, Redwood City, CA, 1991).
- [69] J.F. Gunion, H. Haber, Nucl. Phys. B 272 (1986) 1.
- [70] J.M. Frere, D.R.T. Jones, S. Raby, Nucl. Phys. B 222 (1983) 11; M. Claudson, L. Hall, I. Hinchli, Nucl. Phys. B 228 (1983) 501; C. Kounnas, A.B. Lahanas, D.V. Nanopoulos, M. Quiros, Nucl. Phys. B 236 (1984) 438; J.F. Gunion, H.E. Haber, M. Sher, Nucl. Phys. B 306 (1988) 1.
- [71] See e.g. J. Collins, Renormalization (Cambridge University Press, 1984).
- [72] G. 't Hooft, M. Veltman, Nucl. Phys. B 153 (1979) 365; G. Passarino, M. Veltman, Nucl. Phys. B 160 (1979) 151; A. Axelrod, Nucl. Phys. B 209 (1982) 349.

Figure Captions

Fig.1 The lowest-order Feynman diagram for the charged Higgs decay of the top quark.

Fig.2 Feynman diagrams, up to one-loop order, for the electroweak SUSY vertex corrections to the decay process $t \rightarrow H^+ b$. Each one-loop diagram is summed over all possible values of the mass-eigenstate charginos (χ_i ; $i=1;2$), neutralinos ($\tilde{\chi}^0$; $i=1;\dots;4$), stop and sbottom squarks ($\tilde{t}_a; \tilde{b}_a$; $a;b=1;2$).

Fig.3 Feynman diagrams, up to one-loop order, for the Higgs and Goldstone boson vertex corrections to the decay process $t \rightarrow H^+ b$.

Fig.4 Electroweak self-energy corrections to the top and bottom quark external lines from the various supersymmetric particles, Higgs and Goldstone bosons.

Fig.5 Corrections to the charged Higgs self-energy from the various supersymmetric particles and matter fermions. Only the third quark-squark generation is illustrated.

Fig.6 Corrections to the mixed $W^+ H^+$ self-energy from the various supersymmetric particles and matter fermions. Only the third quark-squark generation is illustrated.

Fig.7 (a) Leading SUSY-QCD contributions to $m_b = m_b$ in the electroweak-eigenstate basis; (b) Leading supersymmetric Yukawa coupling contributions to $m_b = m_b$ in the electroweak-eigenstate basis.

Fig.8 The total partial width, $\Gamma_{\text{MSSM}}(t \rightarrow H^+ b)$, including all MSSM effects, versus $\tan \beta$, as compared to the tree-level width and the QCD-corrected width. Also plotted is the tree-level partial width of the standard top quark decay, $t \rightarrow W^+ b$. The masses of the top and bottom quarks are $m_t = 175 \text{ GeV}$ and $m_b = 5 \text{ GeV}$, respectively, and the rest of the inputs are explicitly given. We remark that $A_t = A_b = \dots = A$ is a common value of the trilinear coupling for all squark and slepton generations. Unless explicitly stated otherwise, the inputs staying at fixed values in the remaining figures are common to the values stated here.

Fig.9 (a) The relative corrections δ , eq.(77), as a function of $\tan \beta$. Shown are the SUSY-EW, standard EW (i.e. non-supersymmetric electroweak), SUSY-QCD, standard QCD, and total MSSM contribution, eq.(83); (b) The branching ratio (79), as a function of $\tan \beta$; separately shown are the values of this observable after including standard QCD corrections, full MSSM corrections, and the tree-level value.

Fig.10 (a) The relative corrections δ , eq.(77), as a function of the gluino mass, $m_{\tilde{g}}$, for the SUSY-EW, standard EW, SUSY-QCD, standard QCD contributions, and total MSSM contribution, (b) As in (a), but for the tree-level and full MSSM-corrected branching ratios (79). We have set $\tan\beta = m_t/m_b = 35$. This value is maintained in all figures where $\tan\beta$ is fixed.

Fig.11 (a) The relative corrections δ , eq.(77), as a function of the supersymmetric Higgs mixing parameter, μ , for the various contributions as in Fig.9a; (b) As in (a), but for the same branching ratios as in Fig.10b.

Fig.12 Dependence of δ , eq.(77), on the SU(2)-gaugino soft SUSY-breaking mass, M_2 , assuming that the U(1)_Y gaugino mass, M_1^0 , is related to M_2 through $M_1^0/M_2 = \frac{5}{3} \tan^2\theta_W$. The same individual and total contributions as in Fig.9a are shown.

Fig.13 (a) The relative corrections δ , eq.(77), as a function of the trilinear soft SUSY-breaking parameter A_b in the bottom sector. The other trilinear couplings are kept as in Fig.8; (b) As in (a), but for the trilinear soft SUSY-breaking parameter A_t in the top sector. Shown are the same individual and total contributions as in Fig.9a.

Fig.14 (a) The relative corrections δ , eq.(77), as a function of the lightest sbottom mass, $m_{\tilde{b}_1}$, for the various contributions as in Fig.9a; (b) As in (a), but for the same branching ratios as in Fig.10b.

Fig.15 The relative corrections δ , eq.(77), as a function of the lightest stop mass, $m_{\tilde{t}_1}$, for the various contributions as in Fig.9a.

Fig.16 (a) The relative corrections δ , eq.(77), as a function of the up-squark masses $m_{\tilde{u}_1} = m_{\tilde{u}_2}$. The c-squarks are assumed to be degenerate with the up-squarks; (b) δ as a function of the sneutrino masses, assumed to be degenerate.

Fig.17 (a) The relative corrections δ , eq.(77), as a function of the top quark mass within about 2% of the present experimental range at the Tevatron. (b) As in (a), but for the same branching ratios as in Fig.10b.

Fig.18 (a) The relative correction δ , eq.(77), as a function of the bottom quark mass. (b) As in (a), but for the same branching ratios as in Fig.10b.

Fig.19 (a) The relative corrections δ , eq.(77), as a function of the charged Higgs mass; (b) As in (a), but for the same branching ratios as in Fig.10b.

Fig.20 The supersymmetric ($\delta_{\text{SUSY EW}}$) and non-supersymmetric (δ_{EW}) electroweak contributions to $\delta\Gamma$, eq.(77), from the process-dependent term $\delta\Gamma_{\text{SD}}$, eq.(48), as a function of $\tan\beta$.

Fig.21 Leading supersymmetric electroweak contributions to $\delta\Gamma$ in the electro-weak-eigenstate basis.

Fig.22 (a) The relative corrections $\delta\Gamma/\Gamma$, eq.(77), as a function of the lightest sbottom quark mass, for positive $\mu = +150 \text{ GeV}$, negative A_t and given values of the other parameters. In this case, huge values of $m_{\tilde{b}_1}$ are needed in order to damp the absolute value of the total correction down to 100%; (b) As in (a), but for the same branching ratios as in Fig.10b.

Fig.23 The total partial width, $\Gamma(t \rightarrow H^+ b)$, including all MSSM effects, versus $\tan\beta$, for the same inputs as in Fig.22a, as compared to the tree-level width and the QCD-corrected width. A typical value of $m_{\tilde{b}_1}$ within the range used in Fig.22a is selected. Also plotted is the tree-level partial width of the standard top quark decay $t \rightarrow W^+ b$.

Fig.24 Typical diagrams for top quark and charged Higgs production in hadron colliders involving the relevant tbH -vertex.

Fig.25 The mixed blobs $W^+ H^+$ and $G^+ H^+$ at any order of perturbation theory.

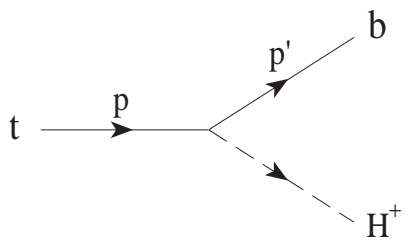


Fig.1

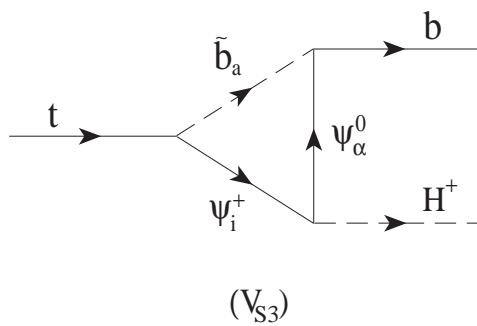
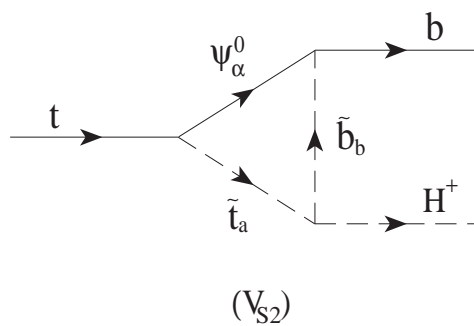
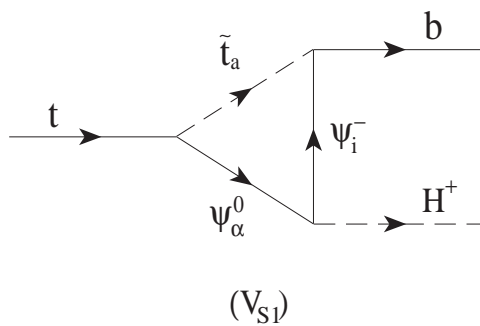


Fig.2

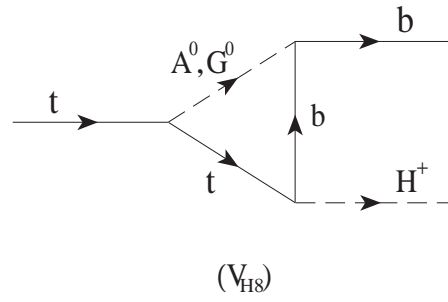
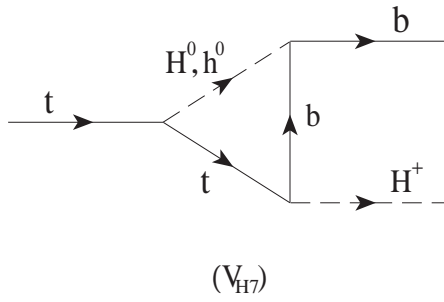
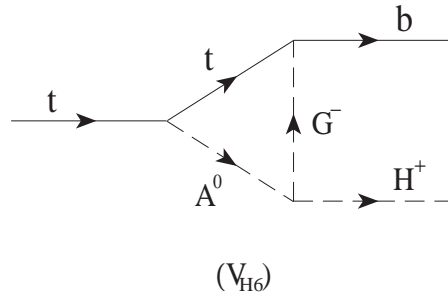
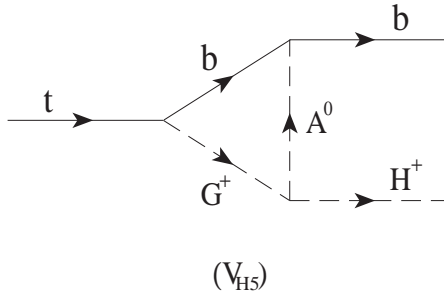
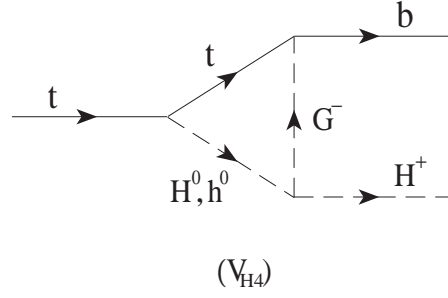
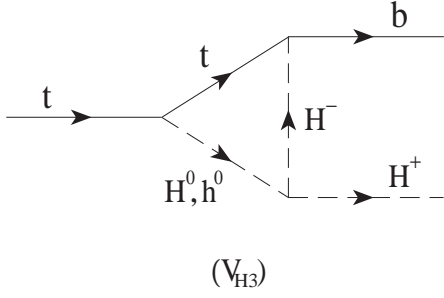
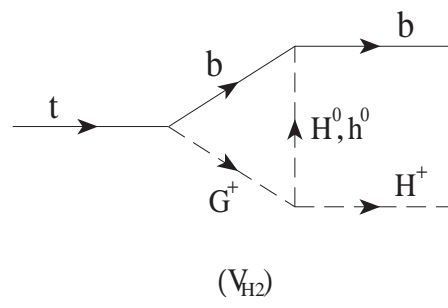
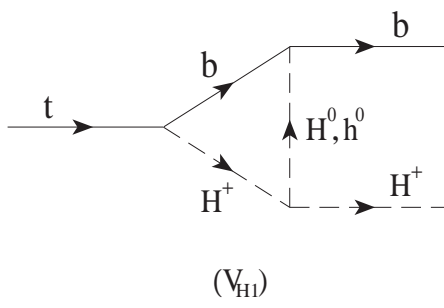


Fig.3

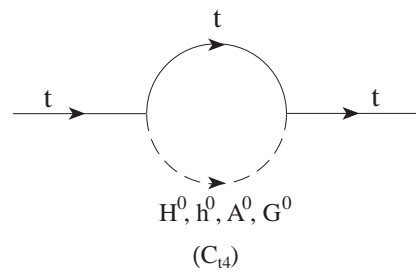
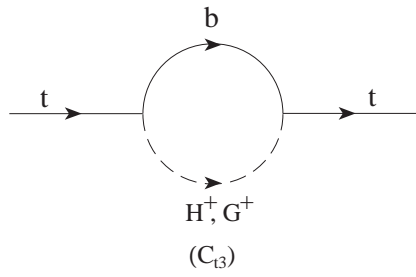
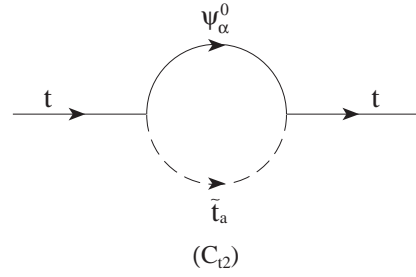
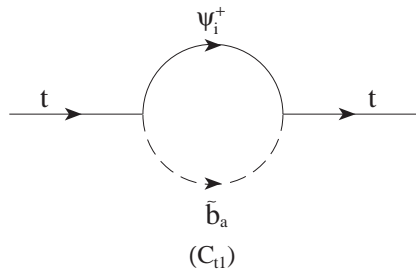
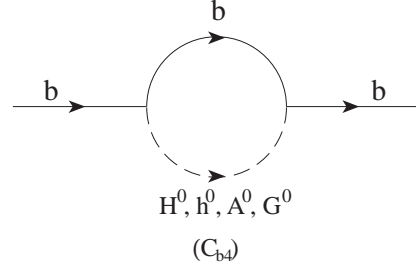
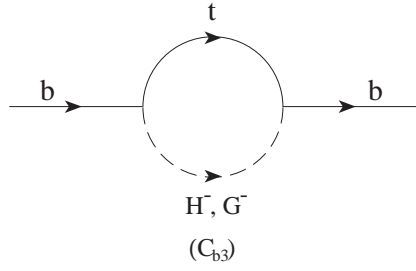
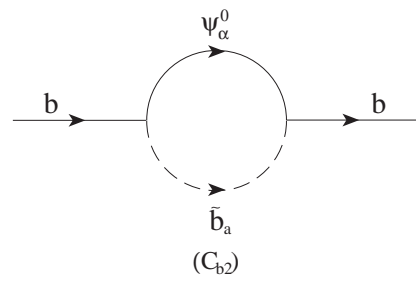
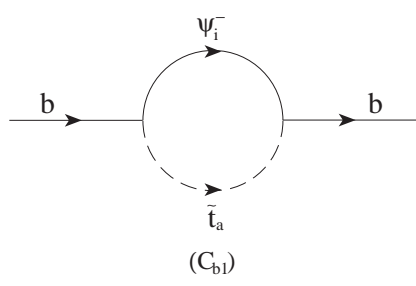


Fig.4

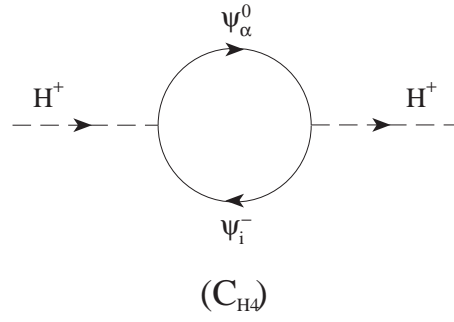
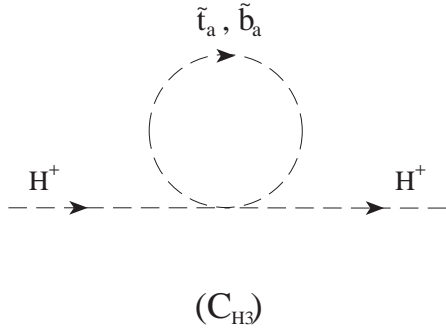
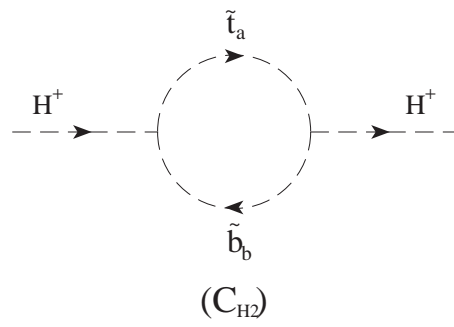
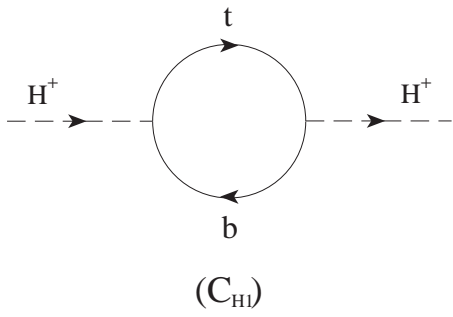


Fig.5

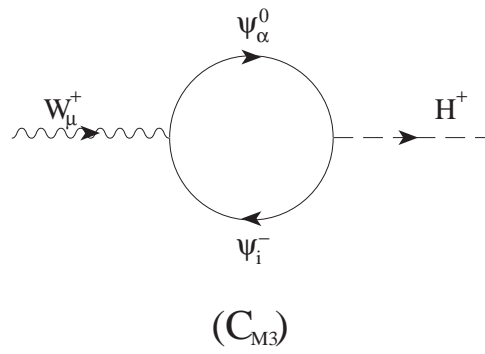
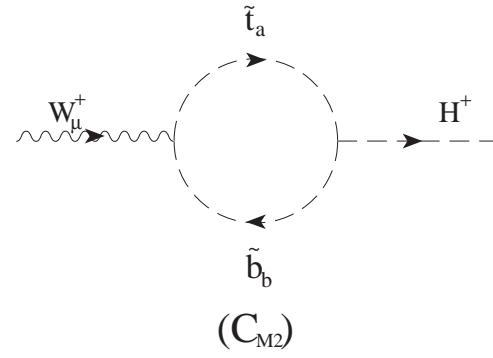
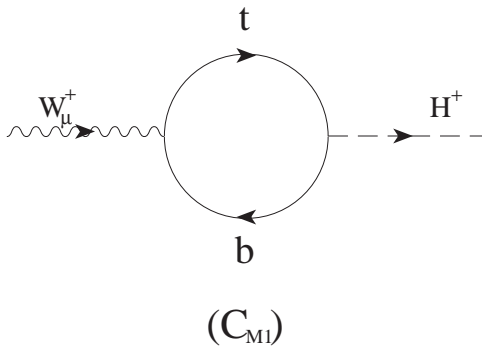


Fig.6

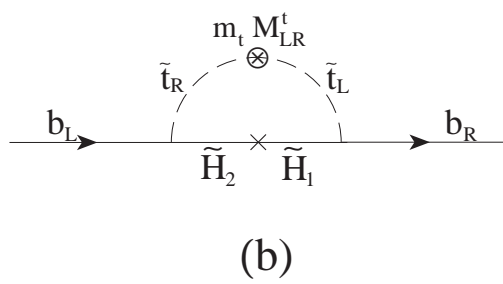
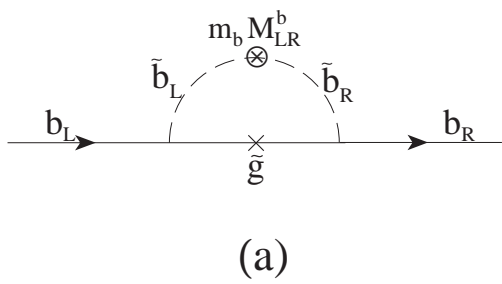


Fig.7

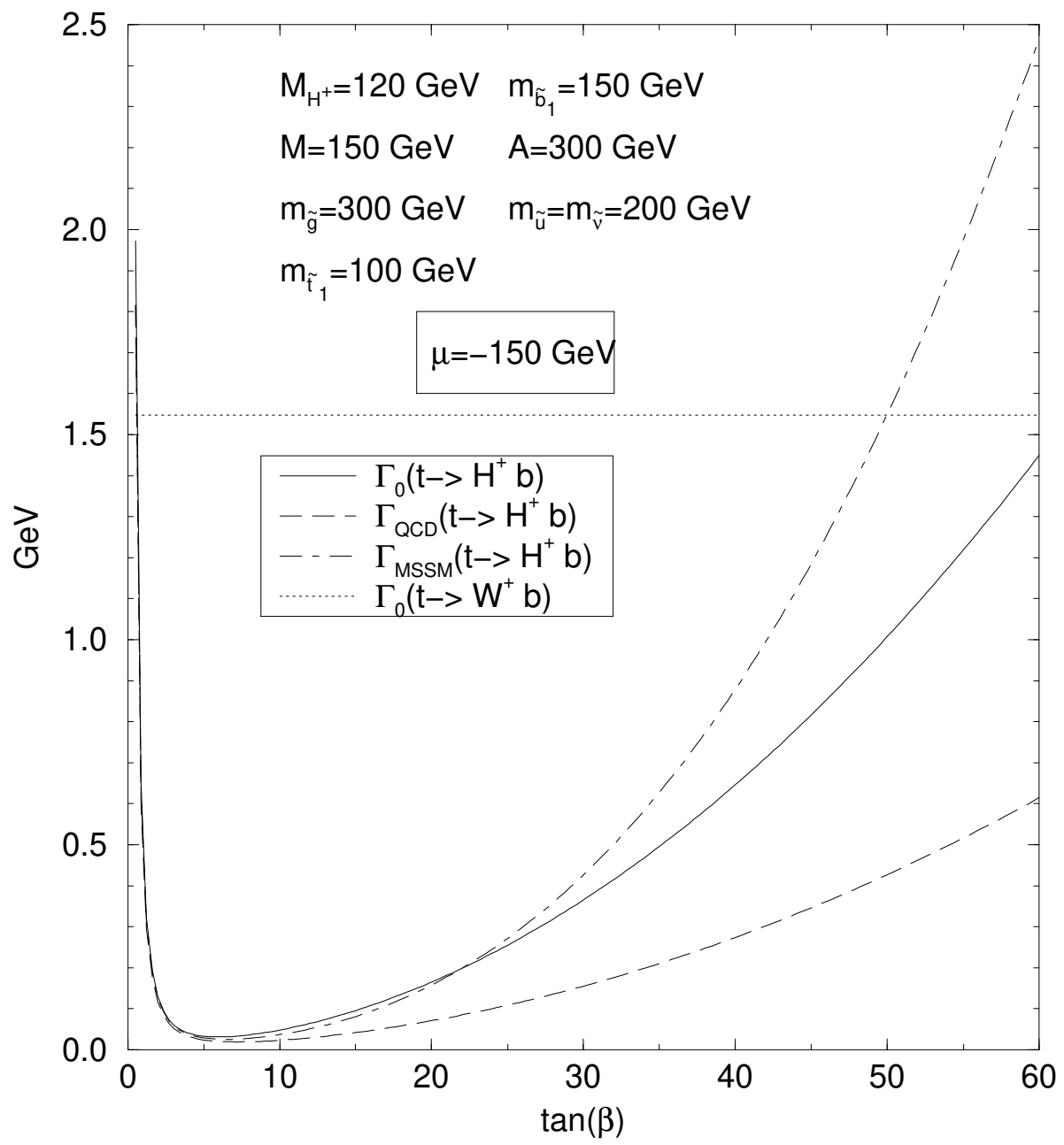


Fig.8

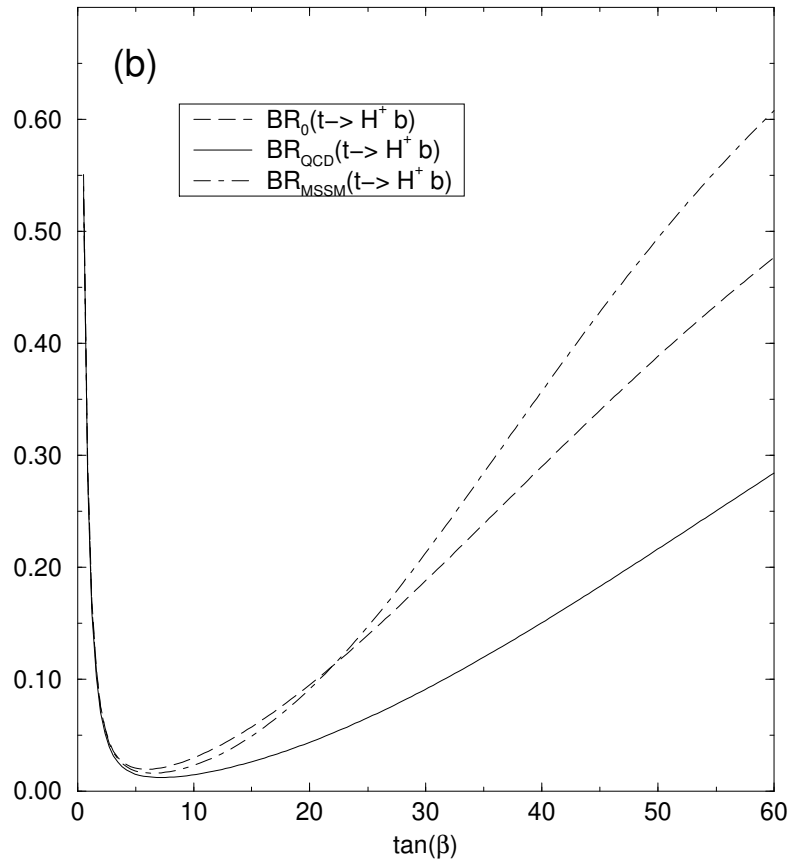
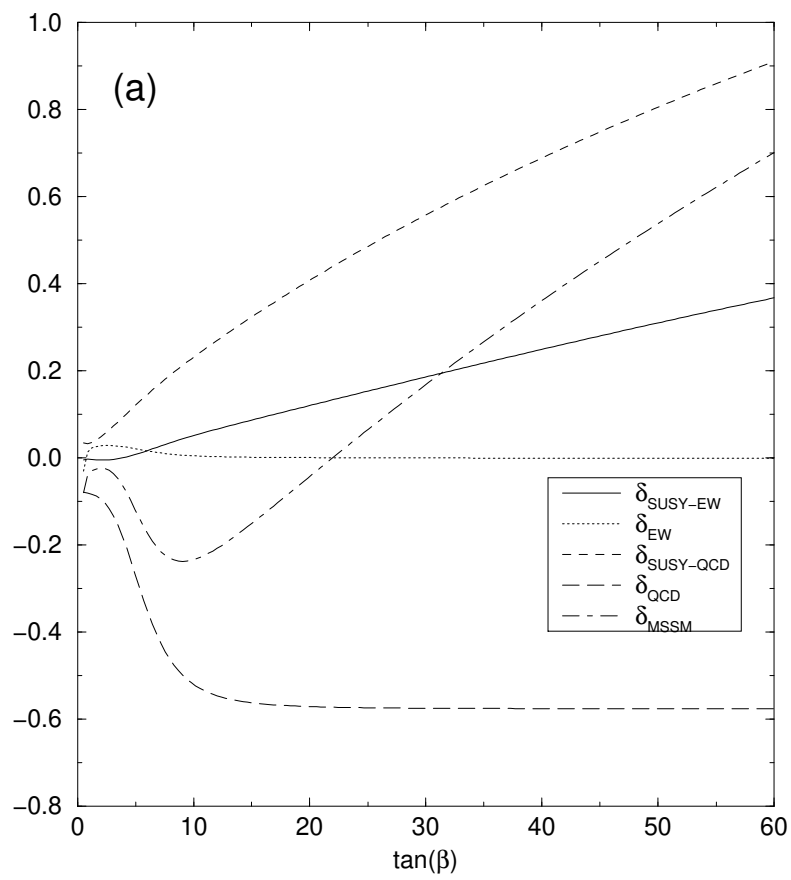


Fig.9

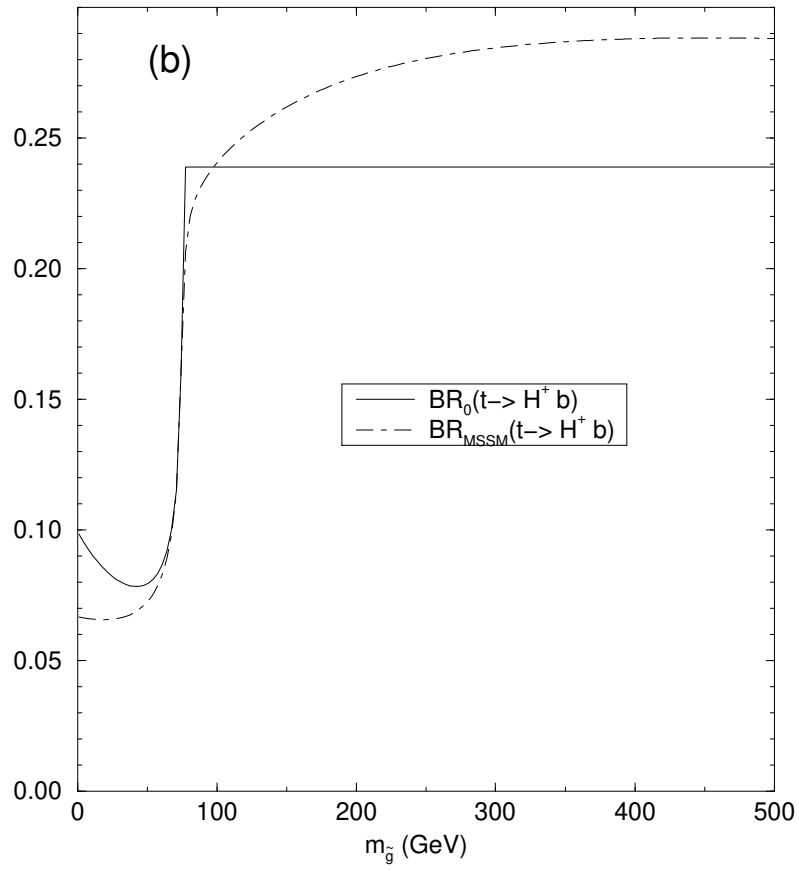
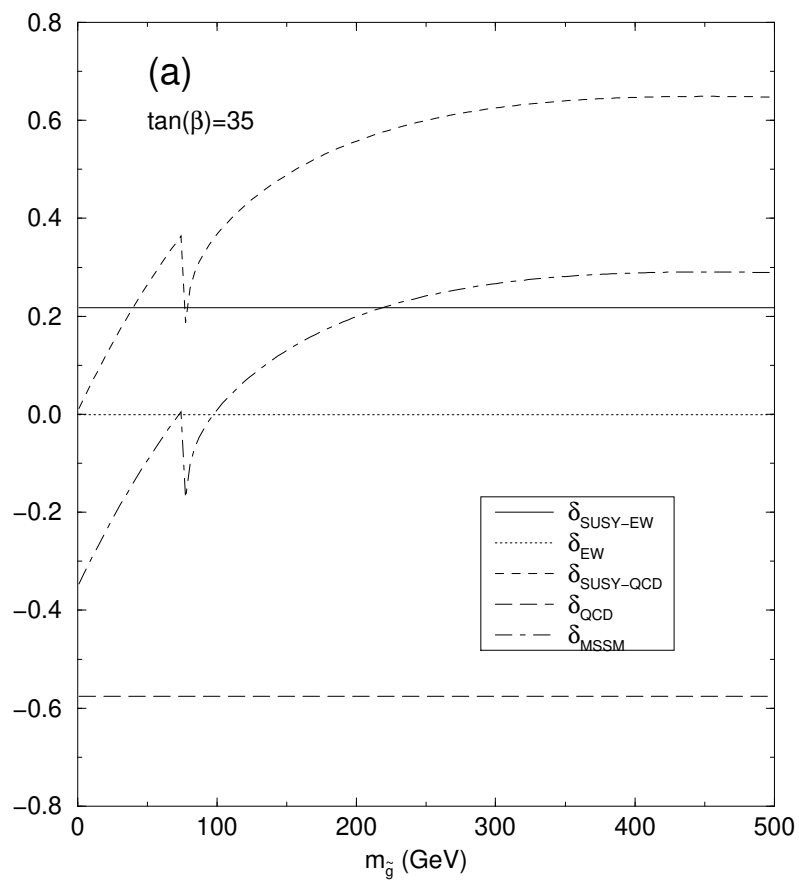


Fig.10

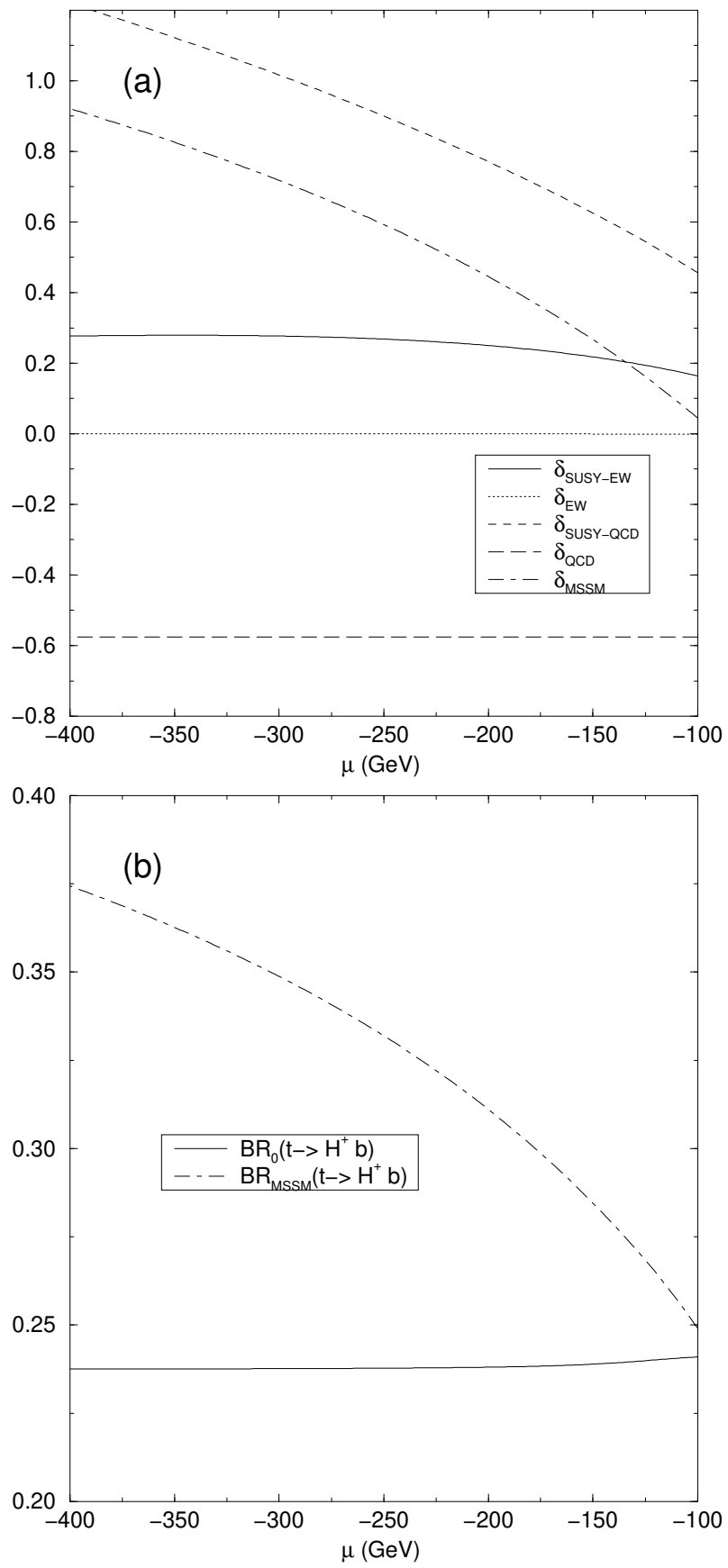


Fig.11

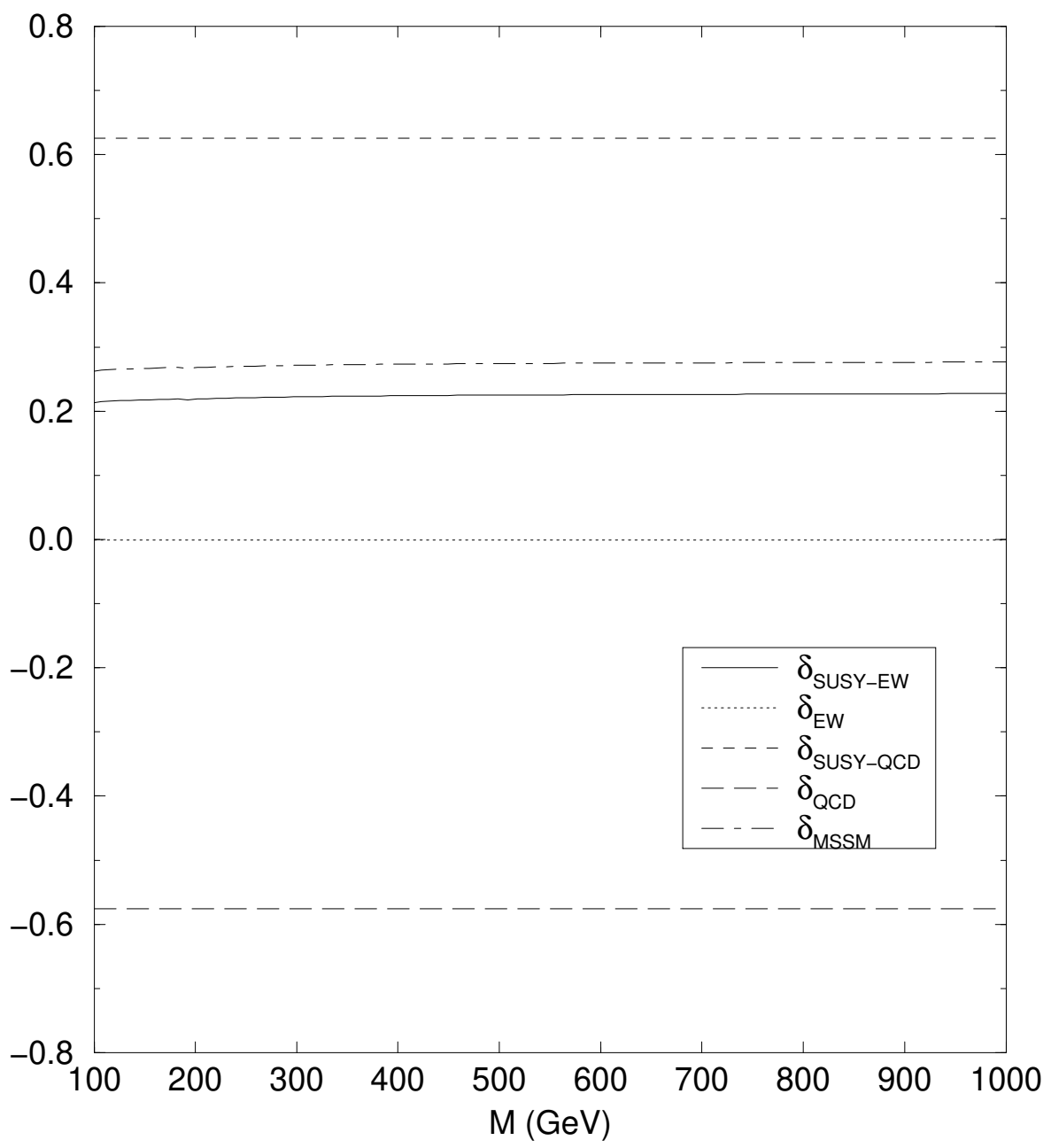


Fig.12

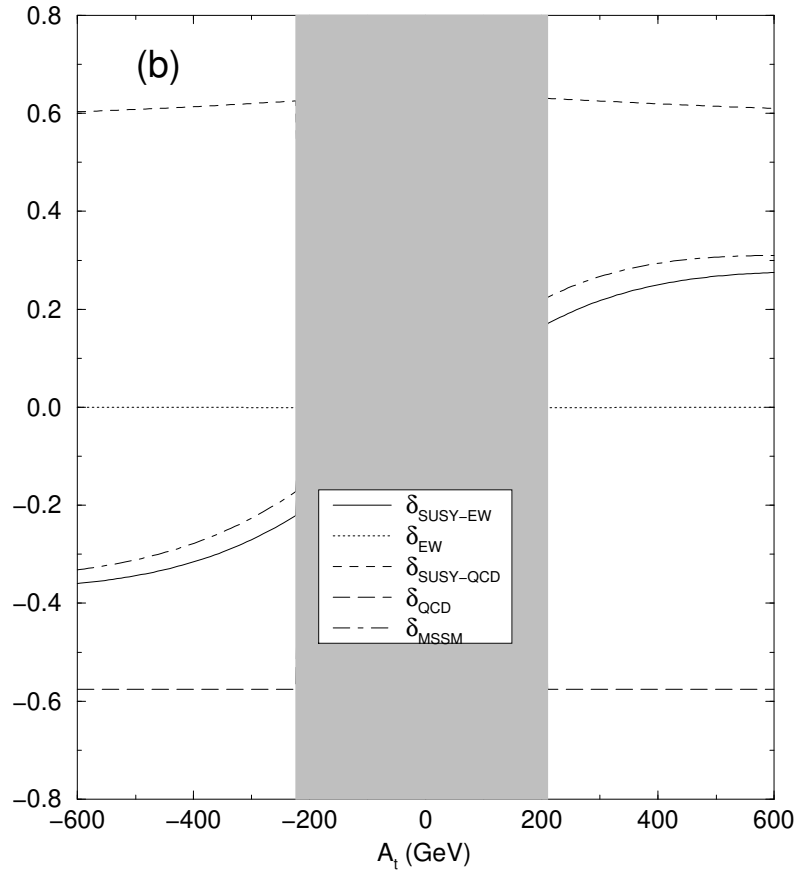
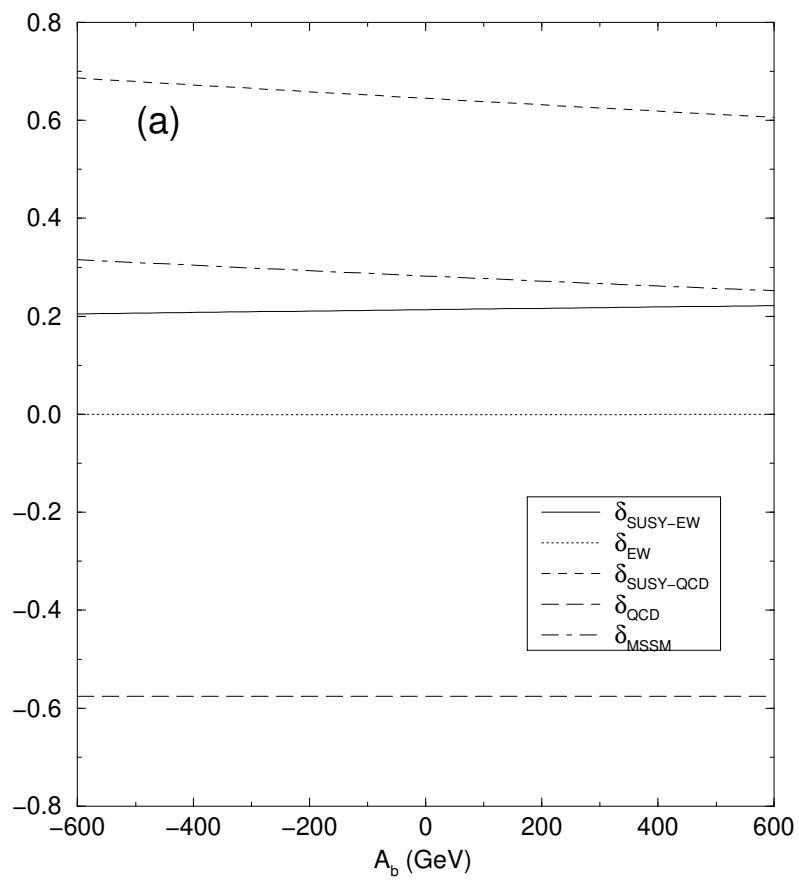


Fig.13

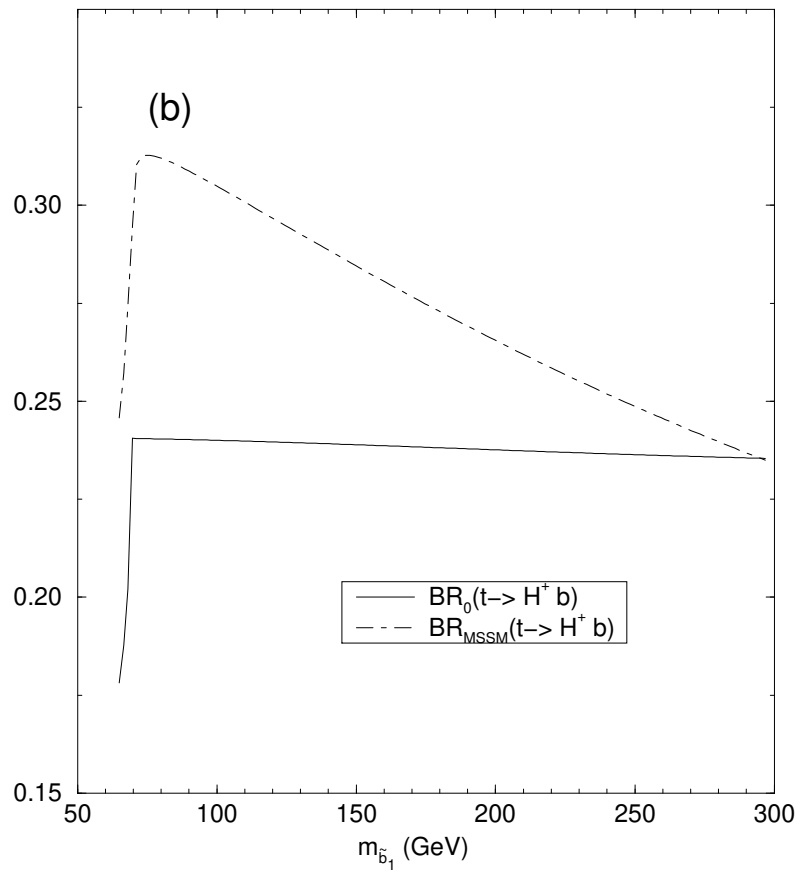
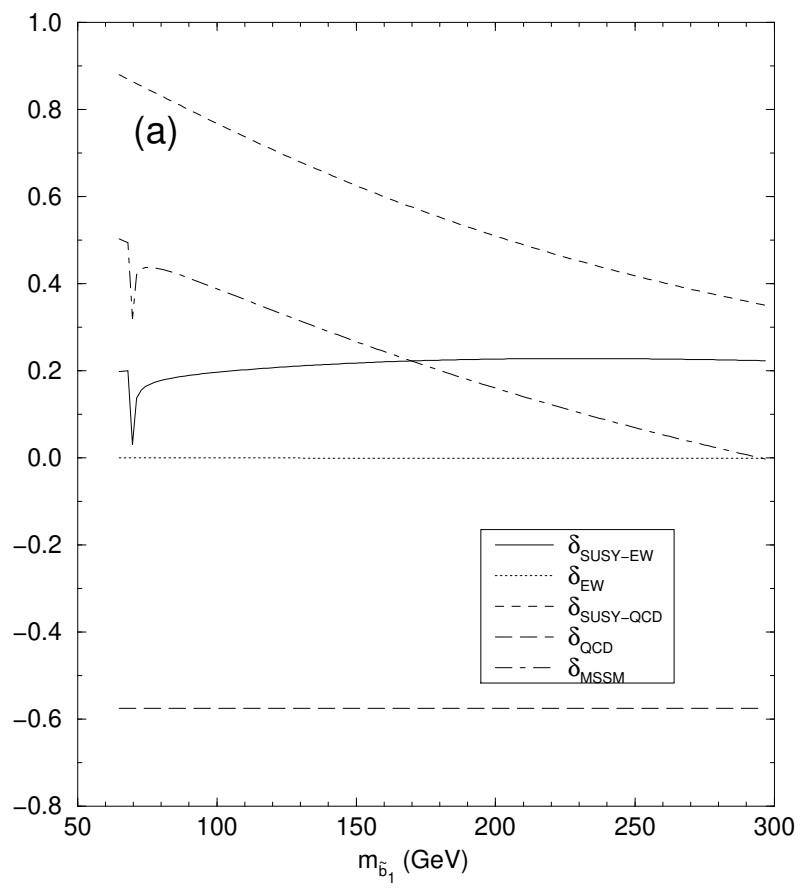


Fig.14

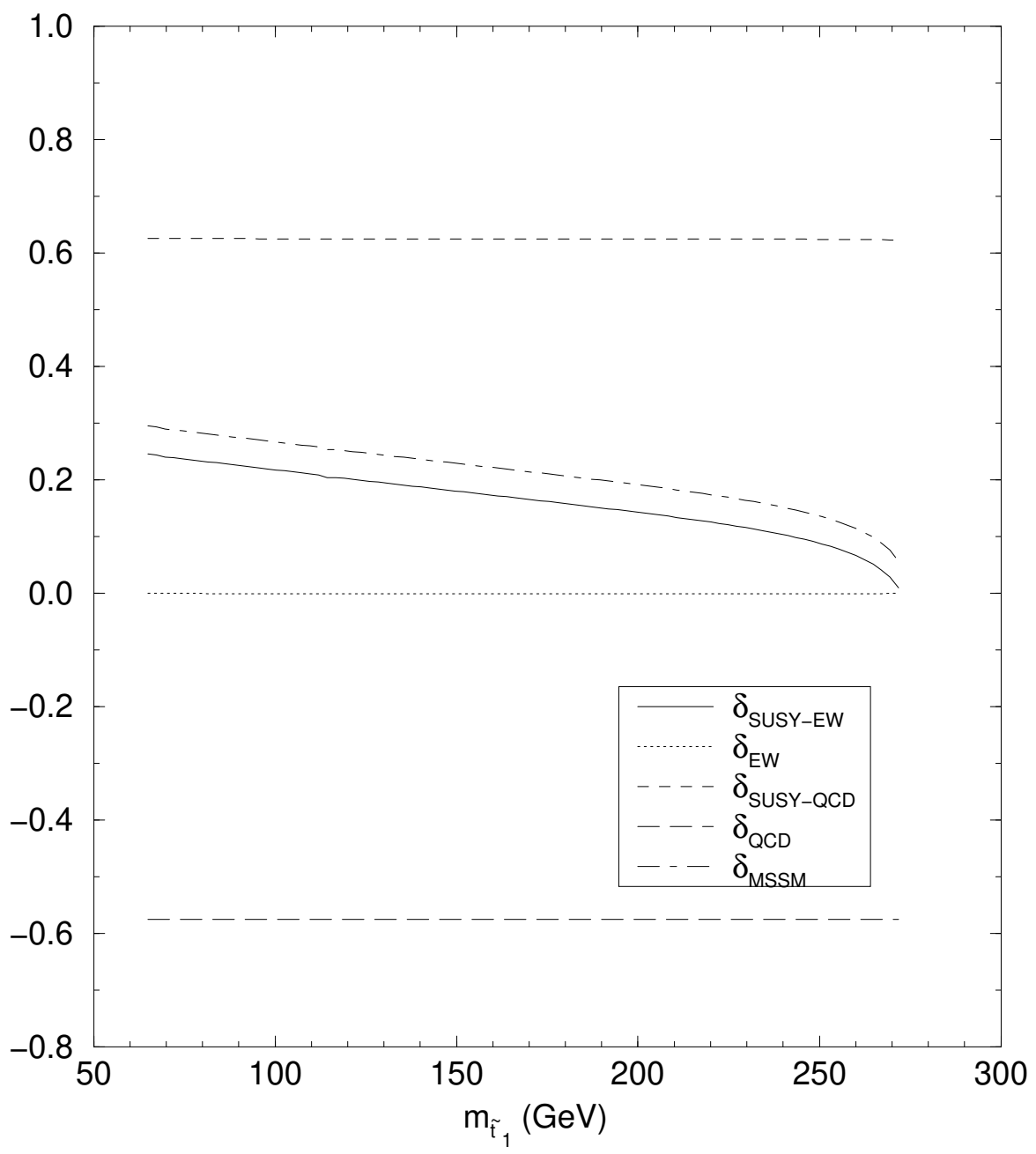


Fig.15

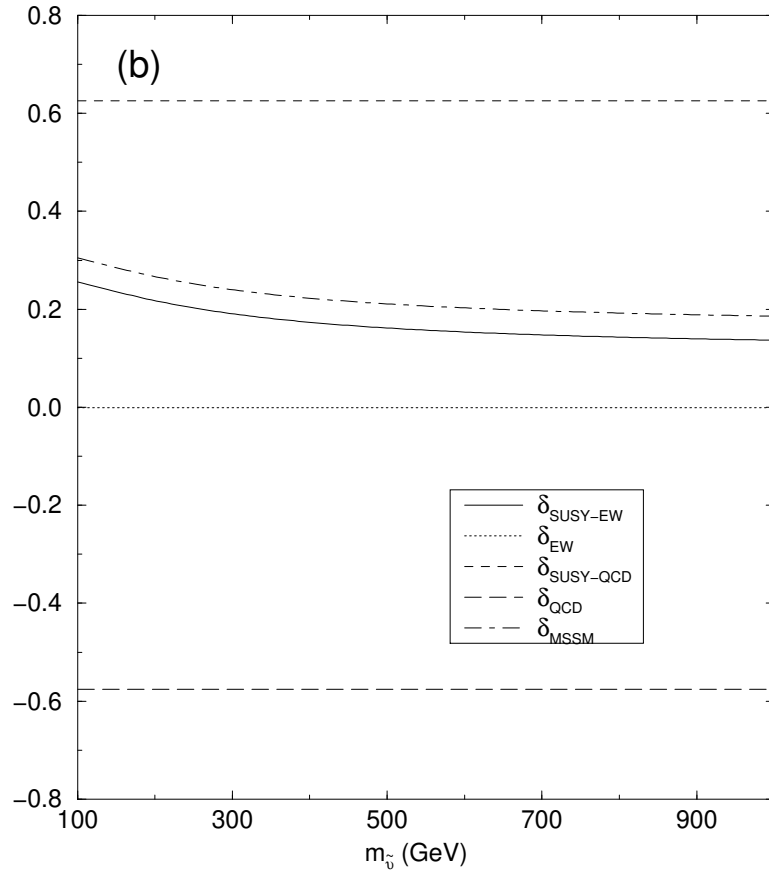
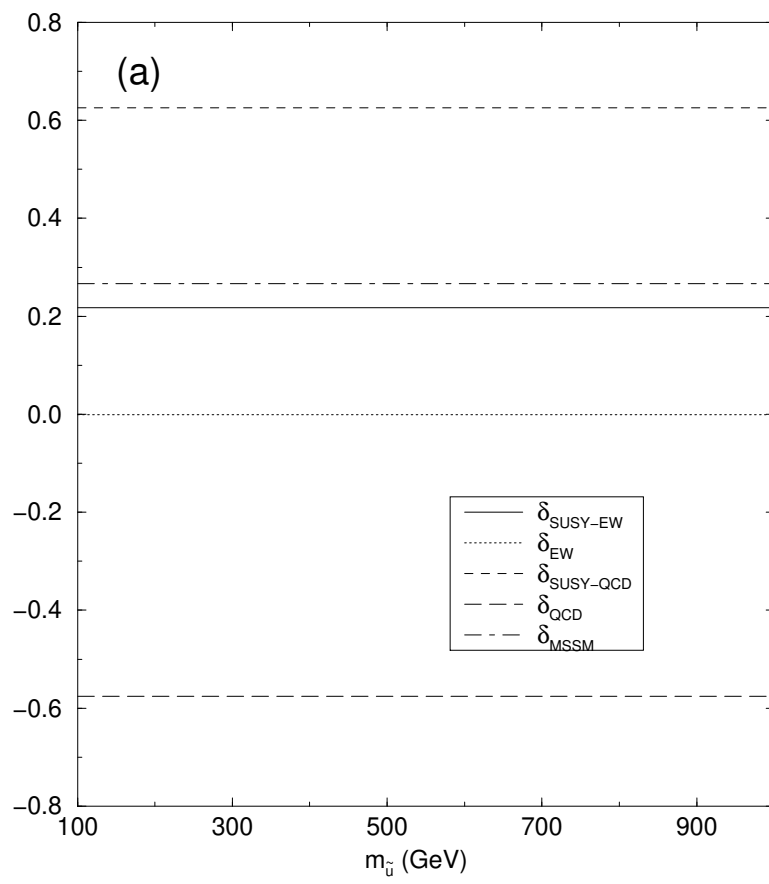


Fig.16

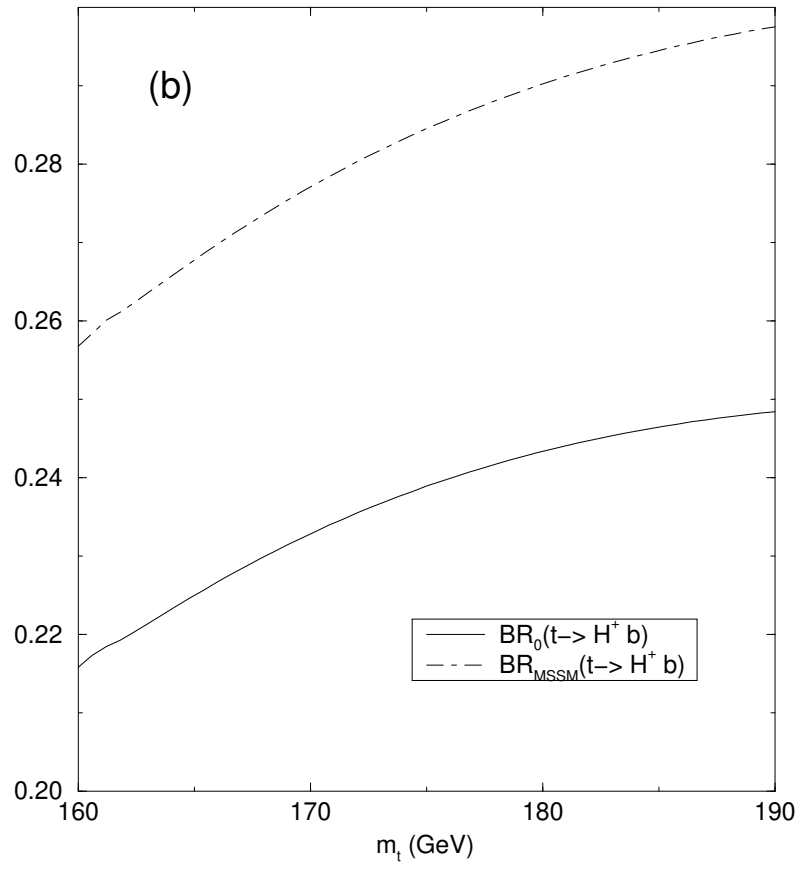
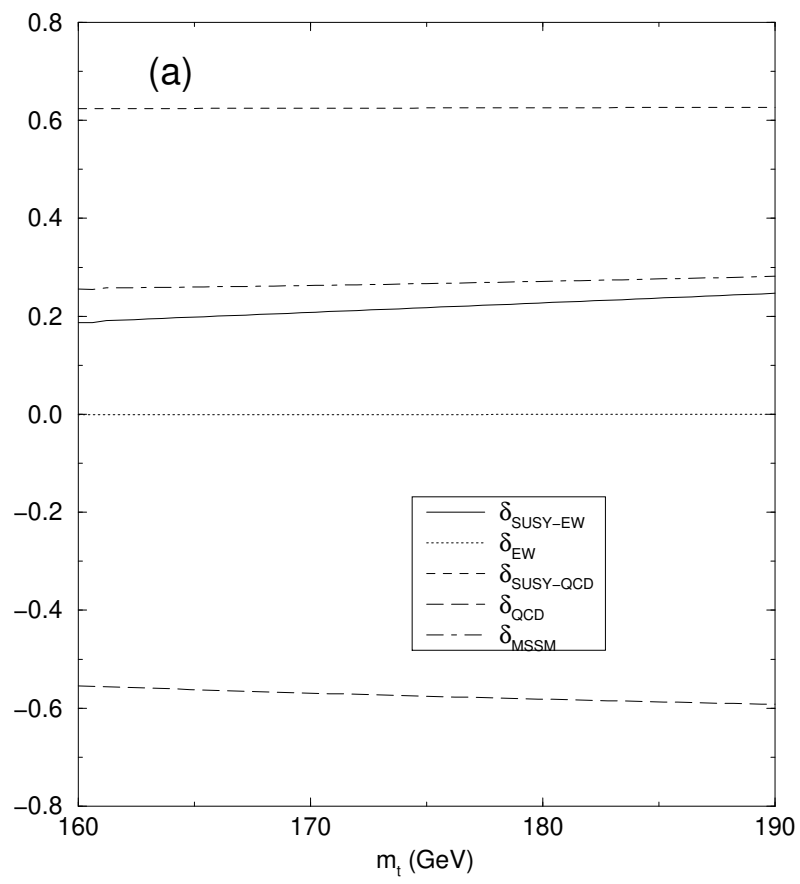


Fig.17

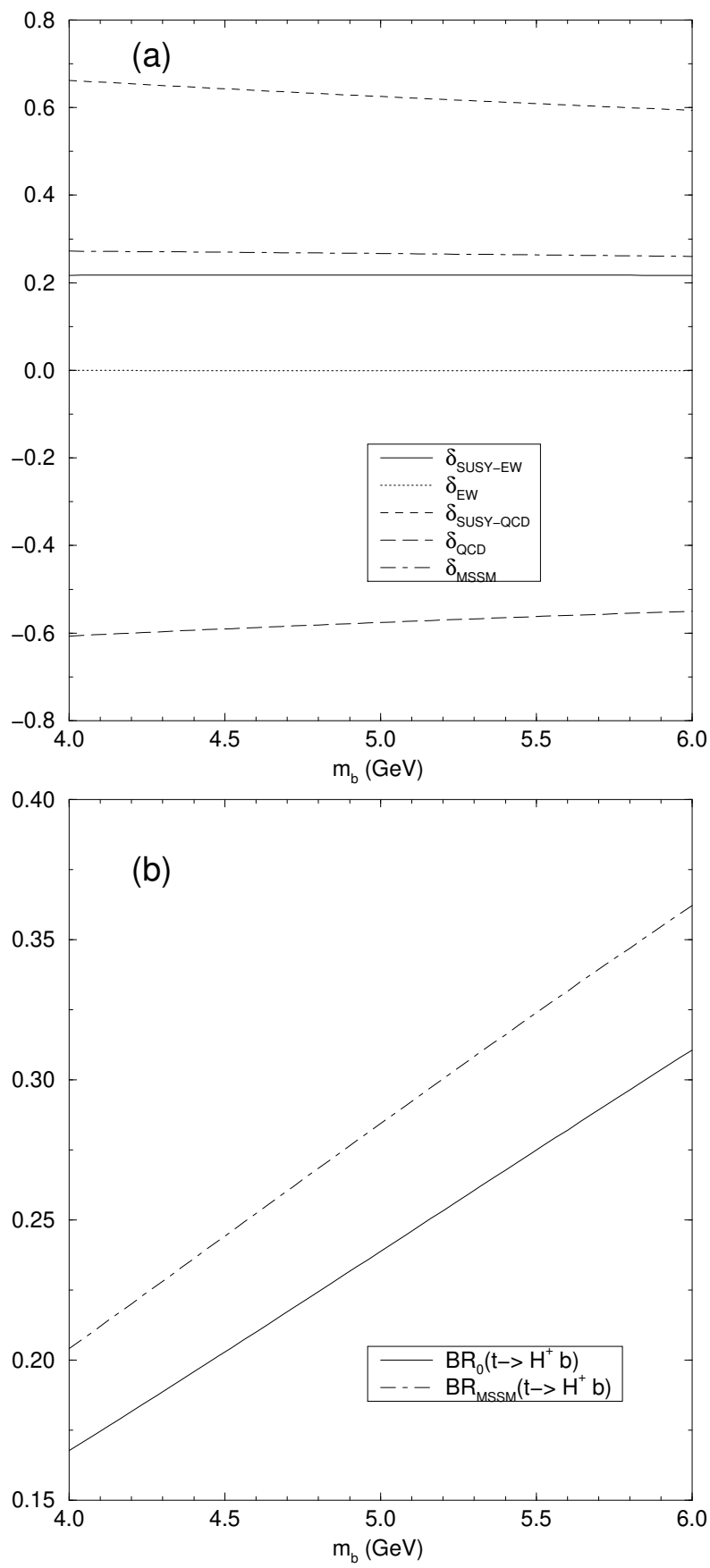


Fig.18

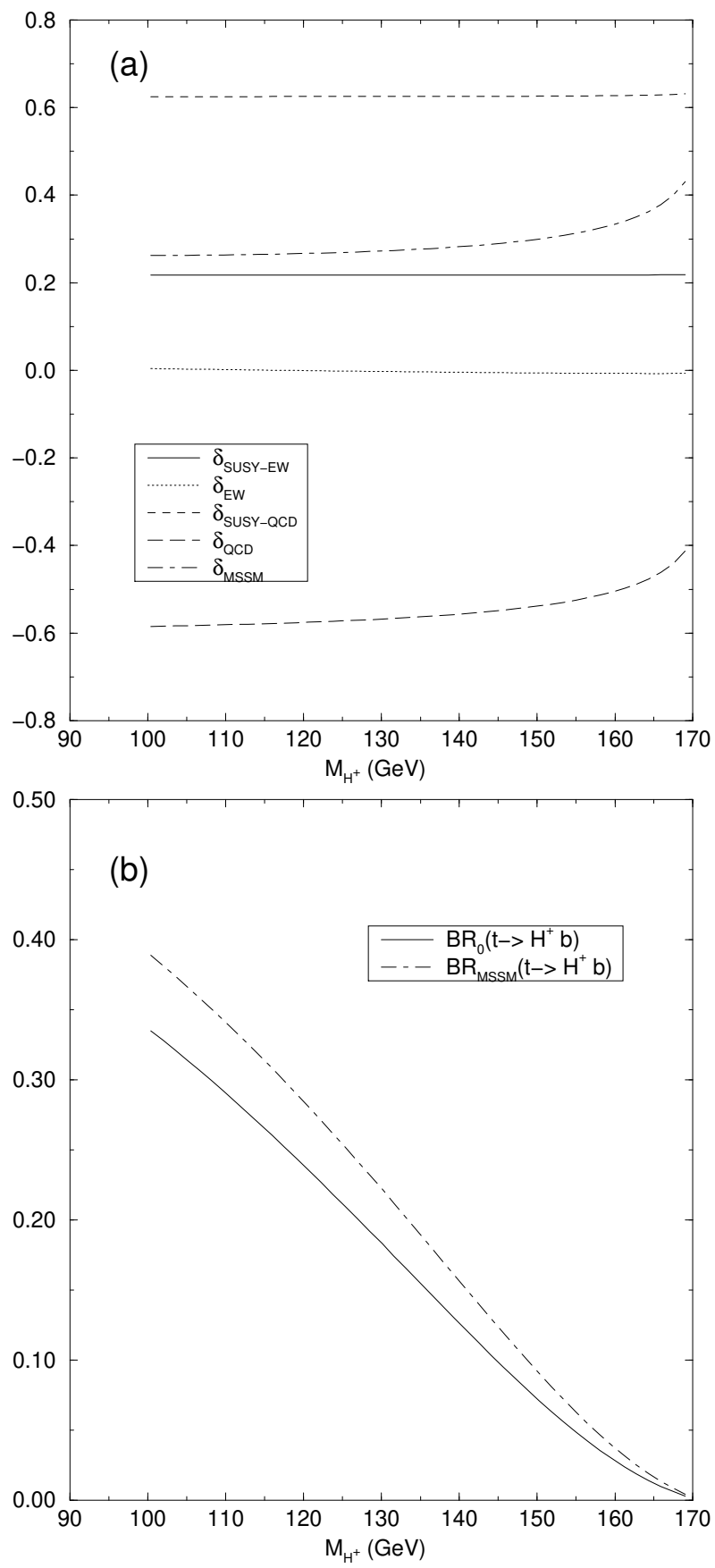


Fig.19

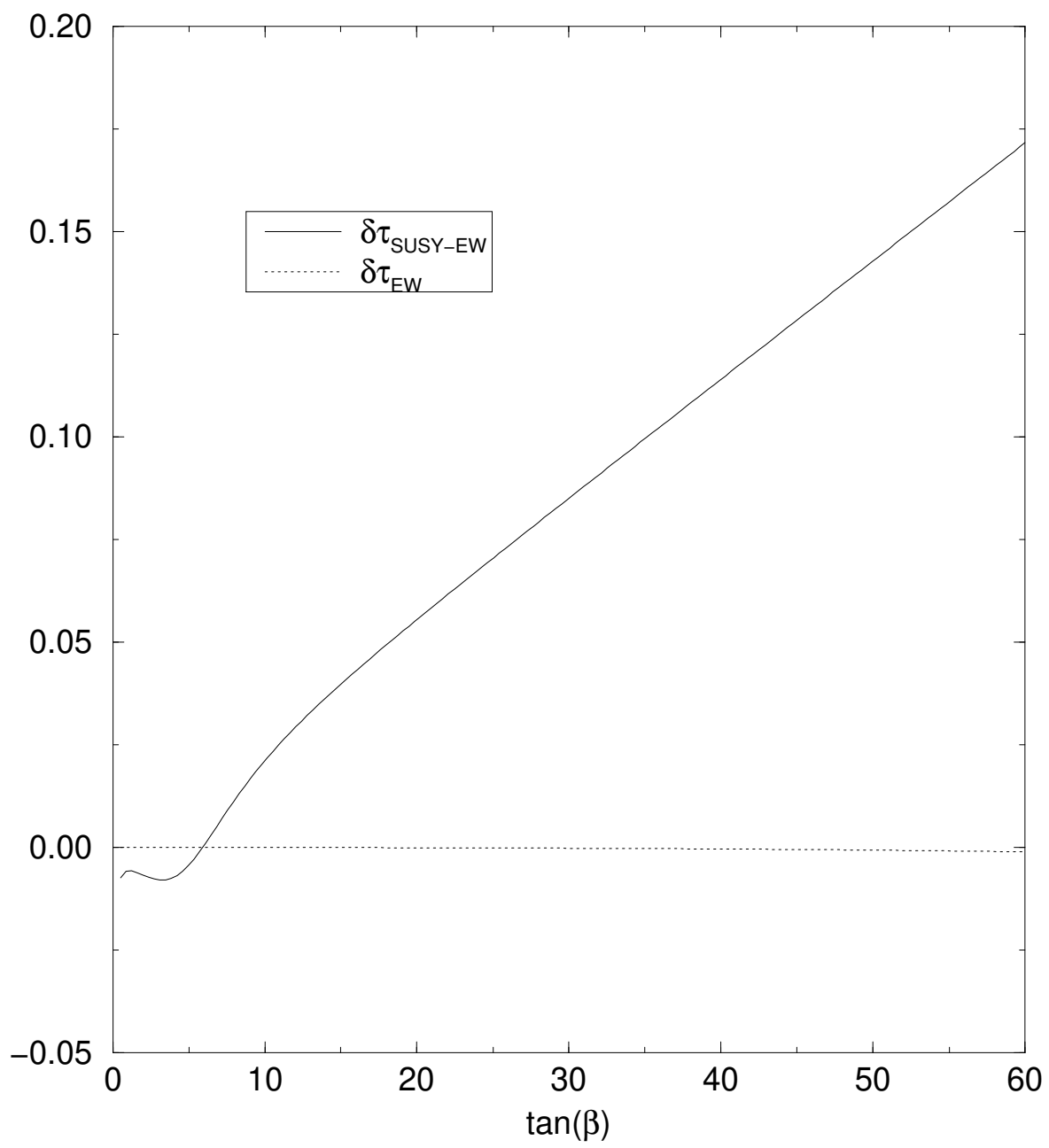
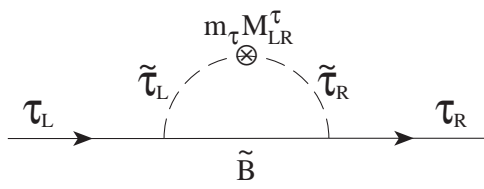
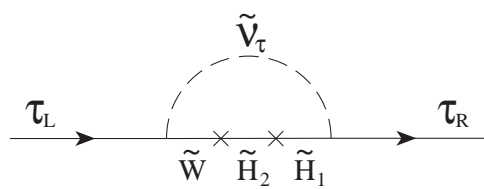


Fig.20



(a)



(b)

Fig.21

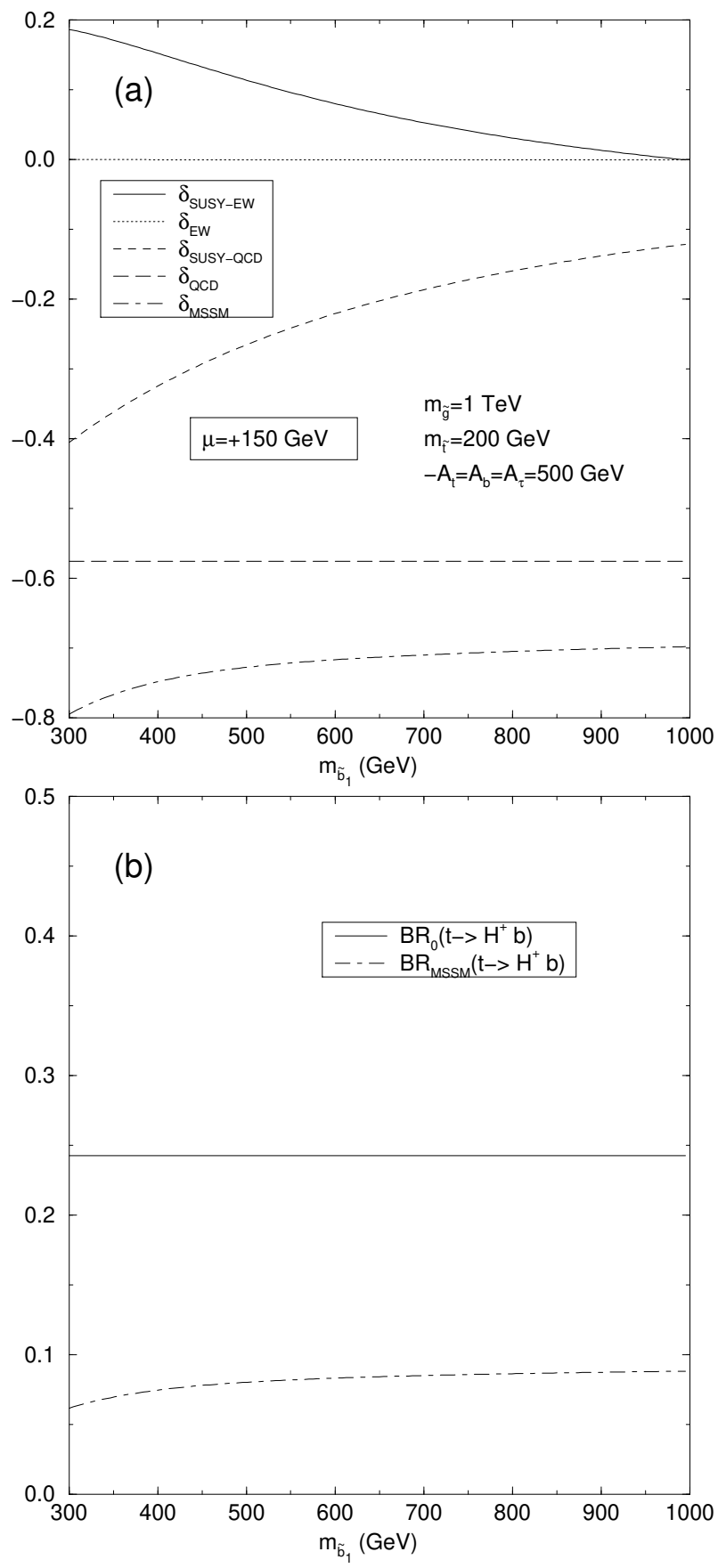


Fig.22

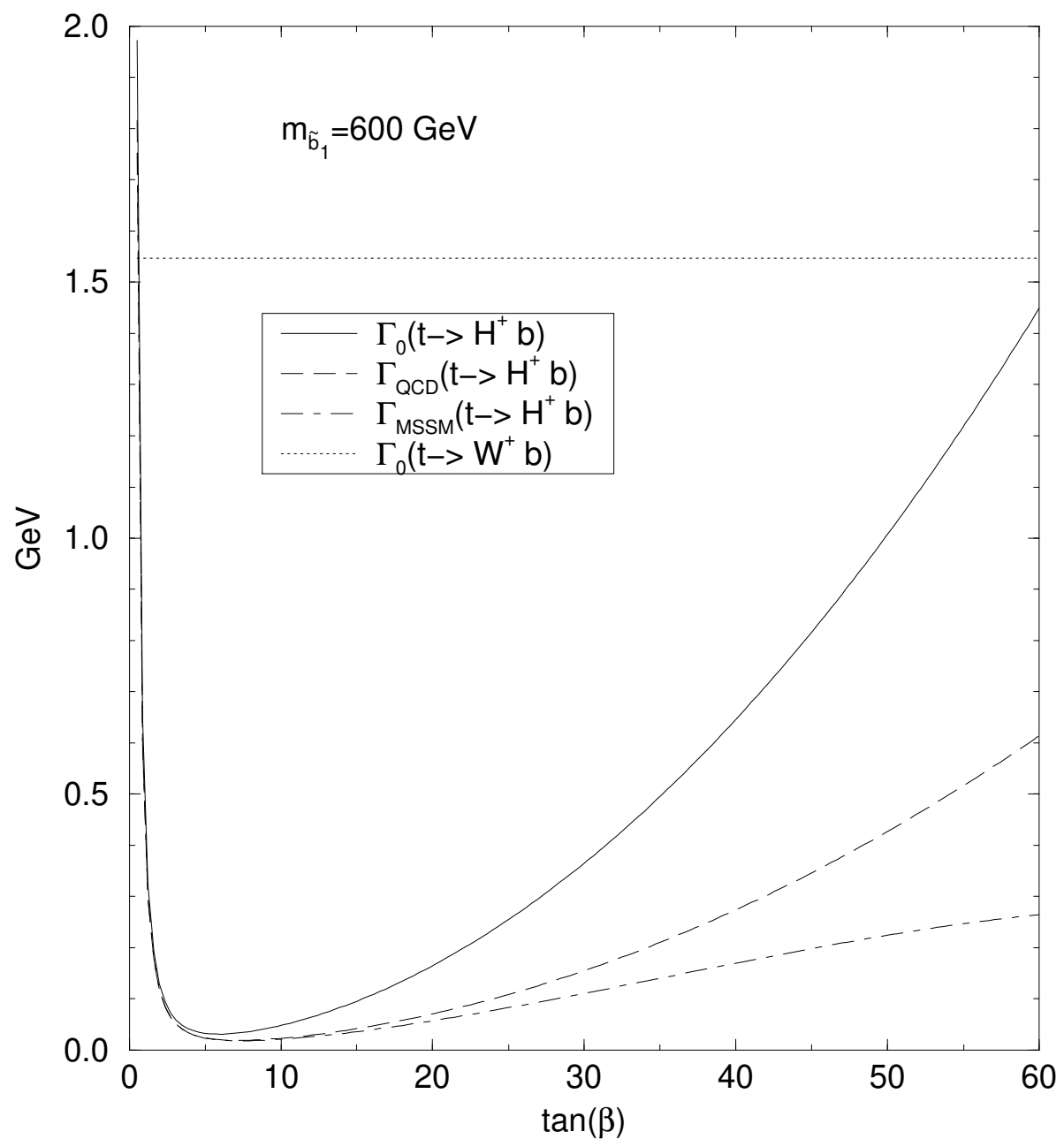


Fig.23

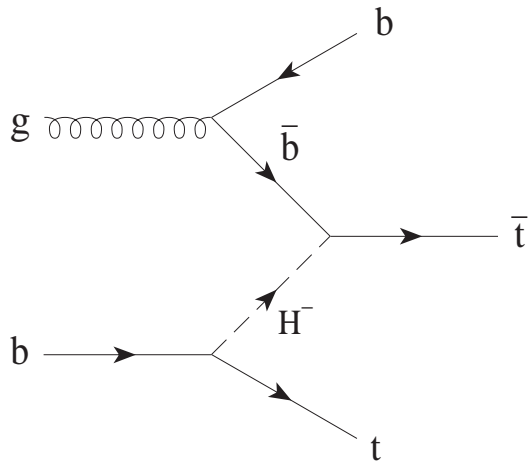
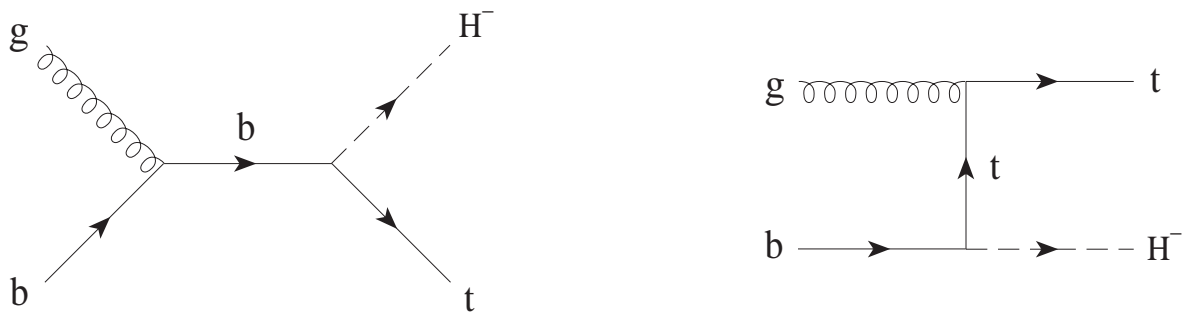


Fig.24

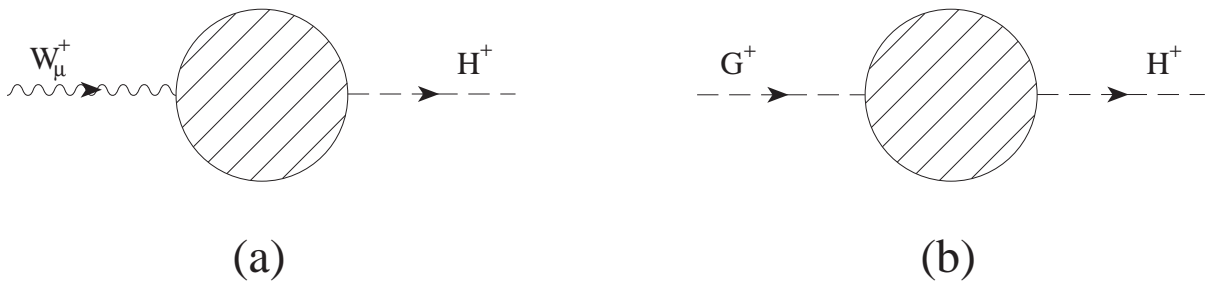


Fig.25